

*Doctoral thesis*

**Study on Geopolymer Materials Using Coal Ashes and Technology to  
Improve their Resistance to Carbonation**

**(石炭灰を用いたジオポリマー材料とその中性化抵抗性の向上技術  
に関する研究)**

**March, 2025**

**Li Xuezhong**

**Graduate School of Sciences and Technology for Innovation**

**Yamaguchi University**



## Acknowledgements

I would like to express my thanks to my supervisor, Professor Zhuguo Li at the Graduate School of Science and Technology for Innovation, Yamaguchi University, for his invaluable support, guidance, and constructive advice throughout this research.

My sincere appreciation also goes to K. Makihara, technical staff at the Integrated Technical Support Division of Yamaguchi University, for his valuable assistance.

I am grateful to the Japan Testing Center for Construction Materials Test Laboratory in West Japan and the Yamaguchi Prefectural Industrial Technology Institute for providing the equipment and support needed in the experiments of this study.

I extend my gratitude to my senior, Zhisong Xu, and my fellow lab members at Yamaguchi University for their invaluable support throughout my research and personal life over the years.

I am also thankful for the scholarship support from Yamaguchi University, which allowed me to focus on my research.

Finally, I am deeply grateful to my family for their constant encouragement and support, both mentally and physically, throughout these years.



## Abstract

Fly ash (FA) and clinker ash (CA) are the two major solid wastes discharged from thermal power plants. FA has been widely recycled in the production of Portland cement (PC) and PC-based concrete. Recently, FA has been used as an amorphous precursor of geopolymer (GP) that is a kind of low-carbon binder made of aluminosilicate precursors and alkali-activator solution. The GP has high strength, excellent acid and fire resistances, etc., providing an eco-friendly alternative to PC, but GP-based concrete has a lower carbonation resistance, compared to PC-based concrete, which may hinder the use of fly ash-based GP as a binder of reinforced concrete. On the other hand, the CA, which is highly porous and granular waste, is mainly used as road material or disposed in landfills at present. However, the CA has some amorphous components similar to FA, which may allow CA to easily be recycled as a fine aggregate in GP materials, but CA's porous structure may present challenges in the strength and durability of GP materials such as carbonation resistance.

In this study, in order to enable FA-based GP to be used as a binder for reinforced concrete, and to develop a technology for the effective recycling of CA as a fine aggregate in mortar or concrete, we first investigated the potential of CA recycling in GP materials, and then developed a surface modifying technology by using sodium aluminate solution (AN) to improve the carbonation resistance of GP materials blended with FA or/and CA.

This doctoral thesis consists of five chapters, each of which is summarized as follows:

Chapter 1 introduces the environmental benefits of using industrial wastes or by-products like FA and CA and the discharging situation of FA and CA. As the global construction industry focuses on reducing carbon emissions, the geopolymers using FA and ground granulated blast furnace slag (BFS) as precursors have been emerging as suitable alternatives to Portland cement (PC) due to its low carbon footprint. This chapter introduces also outlines the challenges of durability, especially carbonation resistance, of GP materials, and the recycling of CA in concrete. On the basis of this background, the purpose and contents of this study were presented.

In Chapter 2, past studies were reviewed in detail on the geopolymers mixed with FA or/and CA, examining their material properties, and the potential of GP and CA as PC substitute or natural sand was mentioned. FA-based GP has demonstrated low carbon footprints, but the past studies found that FA-based or blended GPs generally exhibit lower carbonation resistance than PC, especially when they are cured in the ambient air. Though the past studies proposed some measures to improve the carbonation resistance of GPs, the effectiveness is in doubt or lack of practical use. This chapter also identifies CA's potential as fine aggregate, since its aluminosilicate contents and reactivity in the alkaline solution may improve its internal structure and the interface between CA particles and GP

paste. Based on the review of previous studies, the issues that need to be addressed for the utilization of FA and CA in geopolymer materials have been summarized.

Chapter 3 describes the investigation on the use of sodium aluminate (AN) surface treatment to improve carbonation resistance of FA/BFS-based GP materials. For the heat (80°C)-cured, FA/BFS-based GP mortars using sea sand as fine aggregate, the AN surface treatment delayed the onset of carbonation of GP mortar and reduced the carbonation rate by over 70%. The effects of GP formulation on the AN surface treatment to improve the carbonation resistance of GP mortar were also discussed. The AN surface treatment also reduced the carbonation rate of the ambient (20°C)-cured, FA/BFS-based GP mortars for 23.9%, while this improvement is less than in the case of the heat-curing mortars. Also, the experimental results show that multiple treatment of AN at different ages can further improve the carbonation resistance. These results indicate that the AN surface treatment is an effective method to improve the durability of GP materials using FA as a precursor.

Chapter 4 describes the performances of FA/BFS-based GP concretes and mortars using CA as one of precursors or part of fine aggregate, including fluidity, setting time or/and working time, compressive and flexural strengths, and frost resistance, etc. The effects of different blending ratio of CA were investigated on the performances, and optimal blending ratio were discussed. In addition, as a porous fine aggregate, the effect of CA blend on the carbonation resistance of GP mortar was examined in detail. The AN surface treatment experiments for the GP mortars with different alkali-activator solutions and different CA blending ratios were also conducted. The results indicate that the use of CA as a precursor of GP will reduce the strength of GP, but when CA is used as fine aggregate in place of 20% or less of natural sand, the properties of GP mortar such as fluidity and strength will not be significantly reduced. Meanwhile, the improved AN surface treatment method, which dries mortars after they were ambient-cured and then applies the AN on their surfaces, can significantly increase the carbonation resistance of CA-blended, ambient-cured GP, which was superior to that of GP without using CA. The decrease of carbonation rate of ambient-cured GP mortar for 78.1%. Moreover, the reactivity of CA in alkali-activator solution, along with the AN surface treatment, can effectively enhance the interfacial transition zone (ITZ) between CA particles and the GP matrix.

In Chapter 5, the conclusions of this study were summarized and the future works were described.

# Contents

<b>Abstract.....</b>	<b>i</b>
<b>List of terms and abbreviations .....</b>	<b>vii</b>
<b>List of Figures.....</b>	<b>ix</b>
<b>List of Tables .....</b>	<b>xi</b>
<b>Chapter 1 Introduction.....</b>	<b>1</b>
1.1 Background of Research .....	1
<i>1.1.1 Fly ash and geopolymer .....</i>	<i>1</i>
<i>1.1.2 Clinker Ash.....</i>	<i>2</i>
1.2 Objectives of Research.....	4
1.3 Highlights of Research .....	5
1.4 Flowchart of Research.....	6
References .....	7
<b>Chapter 2 Review of Previous Researches.....</b>	<b>11</b>
2.1 Coal Ashes from Thermal Power Plants .....	11
2.2 Geopolymer and Carbonation Resistance Using Fly Ash.....	14
2.3 Recycling of Clinker Ash .....	17
2.4 Summary .....	19
References .....	20
<b>Chapter 3 Improvement of Carbonation Resistance of Geopolymers using Fly Ash as Active Filler .....</b>	<b>27</b>
3.1 Introduction .....	27
3.2 Experimental Program .....	30
<i>3.2.1 Raw Materials.....</i>	<i>30</i>
<i>3.2.2 Mix proportions of GP mortars.....</i>	<i>31</i>
<i>3.2.3 Specimens preparation .....</i>	<i>31</i>
<i>3.2.4 Property test, chemical and microstructure analysis .....</i>	<i>33</i>
3.3 Test Results and Discussion.....	35

3.3.1 <i>The effects of mix proportions on the effectiveness of AN surface treatment</i>	35
3.3.2 <i>The effects of treatment conditions on the effectiveness of AN surface treatment</i>	42
3.3.3 <i>Air permeability and strength of surface-modified GP mortars</i>	48
3.4 <b>Microstructure and Chemical Analysis of GP Mortars</b>	50
3.4.1 <i>SEM-EDS analysis of surface-modified GP mortar</i>	50
3.4.2 <i>XRD results of surface-modified GP mortar</i>	53
3.5 <b>Conclusions</b>	56
References	57
<b>Chapter 4 Geopolymer Materials Using Clinker Ash as Active Filler or Fine Aggregate</b>	<b>65</b>
4.1 <b>Introduction</b>	65
4.2 <b>Experimental Program</b>	68
4.2.1 <i>Raw materials</i>	68
4.2.2 <i>Mix proportions of GP materials</i>	68
4.2.3 <i>Specimen preparation</i>	69
4.2.4 <i>Surface treatment</i>	70
4.2.5 <i>Property test</i>	71
4.3. <b>Test Results and Discussion</b>	73
4.3.1 <i>Flesh properties of GP materials with CA</i>	73
4.3.2 <i>Mechanical properties of GP materials with CA</i>	74
4.3.3 <i>Frost resistance of GP concrete with CA</i>	77
4.3.4 <i>The effectiveness of AN treatment on GP mortars with CA</i>	80
4.4 <b>Microstructure and Chemical Analysis of GP Mortar with CA</b>	84
4.4.1 <i>SEM-EDS analysis of GP mortar with AN treatment</i>	84
4.4.2 <i>XRD analysis of GP mortar with Clinker Ash</i>	86
4.5 <b>Conclusions</b>	88
References	89
<b>Chapter 5 Conclusions and Future Works</b>	<b>95</b>
5.1 <b>Conclusions</b>	95
5.2 <b>Future Works</b>	97

**Paper List.....99**



## List of terms and abbreviations

Terms / Abbreviations	Meaning
AAS	Alkali activated slag
AF	Active filler
AN	Sodium aluminate solution
AS	Alkali activator solution
BFS	Ground granulated blast furnace slag
CA	Clinker ash
CAM	Geopolymer mortar with clinker ash
Cd	Carbonation depth
EDS	Energy dispersive X-ray spectroscopy
FA	Fly ash
G	Coarse aggregate
GP	Geopolymer
ITZ	Interfacial transition zone
JIS	Japanese Industrial Standards
NH	Sodium hydroxide solution
OPC	Ordinary Portland cement
PC	Portland cement
PSD	Particle size distribution
R.H.	Relative humidity
S	Fine aggregate
SEM	Scanning electron microscopy
WG	Water glass
XRD	X-ray diffraction
XRF	X-ray fluorescence



## List of Figures

- Fig. 2.1 Pile image of (a) CA
- Fig. 2.2 Raw materials of geopolymer mortar
- Fig. 3.1 Experimental process
- Fig. 3.2 The surfaces of geopolymer mortar specimens (40×40×160mm): (a) before treatment, (b) AN surface treatment by brush, (c) right after AN treatment, and (d) AN-treated specimen at 28-day age
- Fig. 3.3 Carbonation depth of GP mortars with different FA/BFS ratios
- Fig. 3.4 Carbonation depth of GP mortars with different WG/NH ratios
- Fig. 3.5 Carbonation depth of GP mortars with different AS/AF ratios
- Fig. 3.6 Schematic description of the carbonation of mortar
- Fig. 3.7 Carbonation depth of GP mortars with AN treatment at different ages
- Fig. 3.8 Carbonation depth of GP mortars with different concentrations of AN application
- Fig. 3.9 Viscosities of AN solutions with different concentrations
- Fig. 3.10 The changes of the a, b-values with frequency of AN treatment
- Fig. 3.11 Influences of sealed curing on the a, b-values
- Fig. 3.12 Air-permeability of GP mortars with and without AN surface treatment
- Fig. 3.13 Comparison of strengths of GP mortars with and without AN surface treatment
- Fig. 3.14 SEM images of FA-based GP mortars.
- Fig. 3.15 SEM images of BFS-based GP mortars
- Fig. 3.16 SEM images of FA&BFS blend-based GP mortars
- Fig. 3.17 XRD pattern of FA/BFS-blended GP mortars
- Fig. 4.1 Particle size distribution curves of fine aggregates
- Fig. 4.2 The surfaces of CA-blended geopolymer mortar specimens (40×40×160mm): (a) before treatment, (b) AN surface treatment by brush, (c) right after AN treatment, and (d) AN-treated specimen before accelerated carbonation test
- Fig. 4.3 Slump of fresh GP concrete: a) Replacing for FA; b) Replacing for sea sand
- Fig. 4.4 Flow table test results of GP mortars
- Fig. 4.5 Working times of GP concrete: a) Replacing for FA; b) Replacing for sea sand
- Fig. 4.6 Flexural strength of GP mortars with CA cured at 20 °C, and 80 °C
- Fig. 4.7 Compressive strength of GP concrete: a) Replacing for FA; b) Replacing for sea sand
- Fig. 4.8 Compressive strength of GP mortars with CA cured at 20 °C, and 80 °C

- Fig. 4.9 Relationship between the number of freeze-thaw cycles and relative dynamic modulus of elasticity of GP concretes
- Fig. 4.10 Relationship between the number of freeze-thaw cycles and mass change of GP concretes
- Fig. 4.11 Surfaces of GP concretes before and after the frost resistance test: a) Before 300 freeze-thaw recycles; b) After 300 freeze-thaw recycles
- Fig. 4.12 Carbonation depths of GP mortars with 20% CA in place of sea sand but with different WG/NH ratios
- Fig. 4.13 Carbonation depths of GP mortars with different replacing ratios of CA
- Fig. 4.14 Surface of CA particle before (a) and after (b) immersed with AS
- Fig. 4.15 CA particle bonded with GP matrix
- Fig. 4.16 The cracks between CA particle and OPC matrix
- Fig. 4.17 XRD pattern of CA and GP mortars

## List of Tables

- Table 3.1 Physical properties of raw materials used
- Table 3.2 Chemical compositions of FA and BFS (XRF analysis)
- Table 3.3 Alkali activator solution's components and density
- Table 3.4 Mix proportions of heat/ambient-cured GP mortars
- Table 3.5 Conditions of AN surface treatment for heat-cured GP
- Table 3.6 Comparison of average mole ratios of oxides of FA-based GP mortars with and without AN treatment
- Table 3.7 Comparison of average mole ratios of oxides of BFS-based GP mortars with and without AN treatment
- Table 3.8 Comparison of average mole ratios of oxides of FA&BFS blended-based GP mortars with and without AN treatment
- Table 4.1 Physical properties of raw materials used
- Table 4.2 Chemical compositions of raw materials (XRF analysis)
- Table 4.3 Components and densities of AS
- Table 4.4 Mix proportions of GP mortars (by mass)
- Table 4.5 Mix proportions of GP concretes mixed with CA



## **Chapter 1 Introduction**

**1.1 Background of Research**

**1.2 Objectives of Research**

**1.3 Highlights of Research**

**1.4 Frame of Research**



# Chapter 1

## Introduction

### 1.1 Background of Research

#### *1.1.1 Fly ash and geopolymer*

The construction industry, a major contributor to global CO<sub>2</sub> emissions, has increasingly turned its focus toward sustainable alternatives to ordinary Portland cement (OPC). The production of OPC is responsible for significant carbon emissions due to the calcination of limestone and the energy-intensive processes involved. This environmental burden is pressing as global urbanization and infrastructure demands grow, highlighting the urgent need for materials that can maintain or exceed the performance of traditional concrete while reducing environmental impact. Geopolymers (GPs), a class of materials synthesized from industrial by-products such as fly ash (FA) and ground granulated blast furnace slag (BFS), offer a promising, eco-friendly solution. Unlike conventional cement, the production of GPs does not involve high-temperature calcination of limestone and clay, etc., significantly lowering their carbon footprint.

GP is produced through the activation of aluminosilicates using alkaline solution[1], which creates a three-dimensional network that imparts unique properties[2], including high resistance to chemicals, fire, and heating, etc.[3–5]. These advantages make GP suitable for various structural applications, particularly in environments where traditional concrete may easily degrade. Despite their environmental benefits, GP face challenges in carbonation resistance, a crucial factor for the durability of reinforced concrete structures. Carbonation, a process where atmospheric CO<sub>2</sub> reacts with concrete, lowers alkalinity, increasing the risk of steel reinforcement corrosion. Thus, enhancing the carbonation resistance of GPs is essential for their viability as a long-term replacement for conventional concrete.

The increasing interest in sustainable construction materials has driven research on geopolymers, especially those incorporating FA and BFS as primary precursors[6]. FA, a by-product of coal combustion, and BFS, a waste product from iron manufacturing, are both abundant and suitable for geopolymer production, reducing waste and offering high mechanical strength and durability. However, carbonation remains a challenge, particularly in ambient-cured geopolymer concrete, which often exhibits lower carbonation resistance than traditional PC concrete. Researches on improving carbonation resistance in geopolymers have focused on various strategies, including optimizing mixture compositions, adjusting curing methods, and exploring surface treatments.

FA & BFS-based geopolymers have shown potential to enhance carbonation resistance, an essential attribute for concrete structures exposed to CO<sub>2</sub>. However, ambient-cured FA/BFS geopolymers typically have higher carbonation rates than PC concrete, requiring advanced approaches to improve durability. Heat-curing, usually at around 80°C, accelerates the geopolymerization process, leading to a denser microstructure and enhanced early strength. However, heat-curing can also lead to shrinkage cracks and internal pores due to rapid moisture loss, which facilitates CO<sub>2</sub> diffusion. Additionally, residual alkali activators in GP materials are more soluble than calcium hydroxide in PC concrete, making them more susceptible to carbonation under fluctuating moisture conditions.

Surface treatments and additives have shown promise in enhancing carbonation resistance in geopolymer materials. For instance, adding magnesium oxide (MgO) to silicate-activated slags forms hydrotalcite[7], a compound that can capture CO<sub>2</sub> and improve carbonation resistance. However, these improvements are limited, and further research is needed to optimize these mixtures for practical use. Organic coatings, such as waterborne epoxy resin, have demonstrated some success in reducing shrinkage and chloride ion diffusion, though their effectiveness in preventing carbonation is limited. A study by Kitasato and Li[8] showed that an organic coating made from hydrocarbon esters and silane compounds could significantly improve carbonation resistance, although concerns about long-term durability and water resistance remain.

Ambient-cured geopolymers, typically cured at around 20°C, present different challenges than heat-cured varieties[9]. While geopolymers cured at ambient temperatures can achieve acceptable mechanical properties, they generally have a lower carbonation resistance than PC concrete. The slower geopolymerization process at room temperature results in a less dense microstructure with larger pores and cracks, allowing CO<sub>2</sub> to penetrate more easily. Reducing the liquid-filler ratio in the GP mix has been suggested as a method to decrease porosity and improve carbonation resistance. However, the carbonation resistance of ambient-cured GPs remains heavily dependent on residual alkali content and environmental conditions.

Inorganic surface treatments are being explored as a more durable alternative for improving the carbonation resistance of ambient-cured GPs. These treatments aim to enhance the material's resistance to environmental exposure and maintain the alkalinity necessary for protecting steel reinforcement from corrosion. While organic coatings, such as waterborne epoxy, have shown promise in improving shrinkage resistance and reducing chloride ion diffusion, their performance in carbonation resistance has been limited. Some studies have indicated that hydrocarbon ester and silane-based coatings could offer better protection against carbonation, but there are still concerns about the coatings' long-term durability and water resistance.

### ***1.1.2 Clinker Ash***

Incorporating industrial by-products as aggregates in GP materials offers both environmental and economic advantages. However, such materials often increase the porosity and permeability of the

cement matrix, which can adversely impact carbonation resistance. For example, FA/BFS-based GP concrete with partial replacement of fine aggregates by CA has shown increased carbonation depth due to the higher permeability and porosity associated with the porous nature of CA.

Steel reinforcement is widely used in concrete structures to enhance structural strength and durability. Maintaining a high carbonation resistance is crucial to protect steel reinforcement from corrosion, a significant durability concern for reinforced concrete structures exposed to atmospheric CO<sub>2</sub>. However, compared to PC concrete, GP materials often exhibit lower carbonation resistance due to their different chemical composition and higher porosity. Residual sodium or potassium in the geopolymer matrix reacts more readily with CO<sub>2</sub> than the calcium hydroxide in PC concrete. Consequently, as internal pore-rich materials, the use of CA for partial or total replacement of sand as fine aggregates can further increase porosity, potentially compromising carbonation resistance.

In summary, geopolymers represent a sustainable and promising alternative to conventional Portland cement as construction materials. By utilizing industrial by-products such as FA and BFS, GPs can reduce carbon emissions, meanwhile achieving mechanical properties suitable for structural applications. Nevertheless, challenges remain, particularly in improving carbonation resistance, a critical factor for durability in reinforced concrete structures. Future research into optimized mix designs, alternative additives, and effective surface treatments is essential to enhance the carbonation resistance of both heat-cured and ambient-cured GP materials, paving the way for their broader adoption in sustainable construction practices.

## **1.2 Objectives of Research**

The primary objective of this research is to evaluate the potential of geopolymers made from fly ash (FA), as sustainable binder of reinforced concrete with enhanced carbonation resistance. The study aims to optimize geopolymer formulations and to develop a surface treatment technology to improve durability under both ambient and heat-curing conditions, and to develop the technology of using CA as fine aggregate in GP materials.

The main objectives of the present research are as follows:

1. Examine the effects of curing methods, comparing ambient and heat curing, on the carbonation resistance and overall performance of FA/BFS-based geopolymers.
2. Explore the incorporation of alternative recycled aggregates: clinker ash, and assess their impact on the mechanical properties and durability of geopolymers.
3. Evaluate the efficacy of surface treatments, particularly using sodium aluminate (AN), in enhancing carbonation resistance and longevity.
4. Analyze the microstructural changes in geopolymer materials resulting from different mixture compositions, CA, curing and AN treatment conditions.

This research provides comprehensive insights into optimizing geopolymer materials using FA or/and CA for sustainable construction, with a focus on durability and resilience in modern infrastructure applications.

### 1.3 Highlights of Research

1. The study explores various mix proportions of GPs using FA and BFS , incorporating alternative aggregates (clinker ash) to improve the mechanical properties and carbonation resistance of geopolymer materials under both ambient and heat-curing conditions.

2. Aqueous sodium aluminate solution was applied as a surface modifier to enhance carbonation resistance, aiming to make geopolymers more suitable for structural applications in harsh environments. This AN surface treatment was evaluated for its effectiveness in maintaining the alkalinity needed to protect steel reinforcement from corrosion in concrete.

3. By examining both ambient and heat-curing, the study identifies best practices for enhancing the carbonation resistance of FA/BFS-based geopolymers, highlighting energy-efficient ambient-curing methods for practical applications.

4. Using the SEM-EDS and XRD analyses, the author examines how different mixture compositions, curing methods, and surface treatments influence the microstructure of geopolymers, providing insight into the mechanisms that affect durability and carbonation resistance.

## **1.4 Flowchart of Research**

This thesis is organized into 6 chapters. The main content of every chapter is summarized here.

Chapter 1 provides an overview of the research background and objectives, as well as the environmental significance of using FA and BFS in building materials, aiming to highlight the impact of sustainable geopolymer alternatives.

Chapter 2 explores previous studies on geopolymer technology, focusing on factors influencing carbonation resistance and durability. This chapter lays groundwork for enhancing durability as a key experimental focus.

Chapter 3 provides a detailed account of the research methodology, including material selection, mix design, and data analysis of carbonation resistance improvement using sodium aluminate solution for different geopolymer formulations under thermal curing conditions.

Chapter 4 describes the research methods in detail, covering material selection, mix design, and data analysis of carbonation resistance improvement using sodium aluminate solution for different geopolymer formulations under ambient curing conditions, compared to GP materials cured under thermal conditions.

Chapter 5 investigates case studies on the use of alternative aggregates in GP materials from both macro and micro perspectives, evaluating the effects of various surface treatments (such as sodium aluminate) on durability. These findings aim to identify optimal approaches for practical applications.

Finally, chapter 6 relates the conclusions of this research and the further works.

## References

- [1] Z. Li, K. Ikeda, Compositions and Microstructures of Carbonated Geopolymers with Different Precursors, *Materials* (Basel). 17 (2024) 1491.
- [2] J. Tailby, K.J.D. MacKenzie, Structure and mechanical properties of aluminosilicate geopolymer composites with Portland cement and its constituent minerals, *Cem. Concr. Res.* 40 (2010) 787–794.
- [3] M. Lahoti, K.H. Tan, E.-H. Yang, A critical review of geopolymer properties for structural fire-resistance applications, *Constr. Build. Mater.* 221 (2019) 514–526.
- [4] S. Luhar, D. Nicolaidis, I. Luhar, Fire Resistance Behaviour of Geopolymer Concrete: An Overview, *Buildings*. 11 (2021).
- [5] A. Hassan, M. Arif, M. Shariq, T. Alomayri, S. Pereira, Fire resistance characteristics of geopolymer concrete for environmental sustainability: a review of thermal, mechanical and microstructure properties, *Environ. Dev. Sustain.* 25 (2023) 8975–9010.
- [6] Z. Li, S. Li, Carbonation resistance of fly ash and blast furnace slag based geopolymer concrete, *Constr. Build. Mater.* 163 (2018) 668–680.
- [7] S.A. Bernal, R. San Nicolas, R.J. Myers, R.M. de Gutiérrez, F. Puertas, J.S.J. van Deventer, J.L. Provis, MgO content of slag controls phase evolution and structural changes induced by accelerated carbonation in alkali-activated binders, *Cem. Concr. Res.* 57 (2014) 33–43.
- [8] Z. Li, S. Li, Experimental Study on the Properties of Geopolymer Concrete Using Fly Ash and Ground Granulated Blast Furnace Slag (Part 5: Neutralization Resistance), *Constr. Mater.* (2016) 1491–1492.
- [9] A. Gholampour, V.D. Ho, T. Ozbakkaloglu, Ambient-cured geopolymer mortars prepared with waste-based sands: Mechanical and durability-related properties and microstructure, *Compos. Part B Eng.* 160 (2019) 519–534.
- [10] M.M. Haque, N. Ankur, A. Meena, N. Singh, Carbonation and permeation behaviour of geopolymer concrete containing copper slag and coal ashes, *Dev. Built Environ.* 16 (2023) 100276.



## **Chapter 2 Review of Previous Researches**

### **2.1 Coal Ashes from Thermal Power Plants**

### **2.2 Geopolymer and Carbonation Resistance Using Fly Ash**

### **2.3 Recycling of Clinker Ash**

### **2.4 Summary**



# Chapter 2

## Review of Previous Researches

### 2.1 Coal Ashes from Thermal Power Plants

The by-products of coal combustion in thermal power plants, particularly coal ash, represent a significant source of industrial waste with extensive environmental and practical implications. Coal ash is primarily composed of fly ash (FA) and bottom ash, with FA being particularly valuable in construction due to its high silica and alumina content, making it an ideal precursor for geopolymer technology. The recycling and repurposing of FA and bottom ash, including clinker ash (CA), offer a sustainable pathway for construction materials, helping to reduce dependency on natural resources like river sand and alleviate waste disposal concerns. This review explores the characteristics, potential applications, and challenges associated with coal ash, emphasizing its role in construction and its impact on carbonation resistance, mechanical properties, and environmental sustainability.

FA is a fine, powdery material composed primarily of aluminosilicate glass and smaller amounts of crystalline phases like quartz and mullite. Generated as a by-product of coal combustion in power plants, FA contains essential compounds, such as silica ( $\text{SiO}_2$ ) and alumina ( $\text{Al}_2\text{O}_3$ ), which are critical for cementitious reactions. FA's chemical composition and pozzolanic activity make it highly suitable for use as a precursor in geopolymer binders[1] and a replacement for Portland cement (PC) in traditional concrete. The incorporation of FA in construction not only diverts substantial waste from landfills but also significantly reduces the carbon footprint associated with PC production.

The sustainable utilization of FA in geopolymer technology presents several environmental advantages, including reduced  $\text{CO}_2$  emissions and minimized consumption of virgin materials[2]. GPs formed from FA display notable properties, including high resistance to chemicals, fire, and thermal degradation, making them suitable for various structural applications, particularly in environments where conventional concrete may deteriorate. However, one of the challenges associated with FA-based GPs is their relatively low carbonation resistance compared to PC concrete[1,3,4]. This issue is critical in reinforced concrete structures, where carbonation can reduce the alkalinity needed to protect steel reinforcements from corrosion. Consequently, ongoing research seeks to improve the carbonation resistance of FA-based GPs through optimized curing methods, mix designs, and the addition of supplementary materials.

In terms of environmental impact, FA use in construction conserves landfill space and prevents potential leaching of harmful elements, such as heavy metals, into the soil and groundwater[5]. Moreover, studies demonstrate that FA-based GPs exhibit a reduced carbon footprint[6] compared to conventional cement, as they require no high-temperature calcination during production. Despite these advantages, the lower carbonation resistance of FA-based GPs remains a barrier, particularly in ambient-cured conditions, which typically result in higher porosity[7]. As research progresses, optimizing FA-based geopolymer formulations to enhance carbonation resistance is vital for achieving both sustainability and durability in modern construction applications.

Clinker ash, as shown in **Fig. 2.1(a)**, a type of bottom ash, is formed when unburned coal particles reach high temperatures in thermal power plants, melting and then cooling into a solidified, glassy substance[8–10]. The resulting ash is granular, porous, and irregularly shaped, resembling sand in texture. Although CA is often considered a waste product, it possesses unique properties that make it suitable for use as an aggregate in concrete. With growing restrictions on natural aggregate mining and an increased focus on environmental conservation, CA is emerging as a viable alternative to natural sand in construction applications.

The physical properties of CA, such as its porosity and particle size distribution, vary widely depending on the source and combustion process. Generally, CA has a lower density and higher porosity than natural sand, which affects its role in concrete mixtures[10]. Studies show that partial replacement of natural sand with CA in concrete and geopolymer formulations can reduce the environmental impact by recycling a significant amount of industrial waste. However, CA's porous nature can also increase water absorption, shrinkage, and permeability, which may negatively impact the mechanical performance and durability of concrete, especially in carbonation-prone environments.

Despite its benefits as a sustainable aggregate alternative, the carbonation resistance of CA-containing materials presents a significant challenge. Increased porosity from CA incorporation tends to raise carbonation rates, allowing CO<sub>2</sub> to penetrate more easily and react with the cementitious



**Fig. 2.1** Pile image of CA

matrix. This process reduces the alkalinity required to protect embedded steel reinforcements, making enhanced carbonation resistance a critical goal for CA-based applications. Furthermore, the compatibility of CA with other by-products like FA and BFS in geopolymer formulations is being explored to improve durability and sustainability. Overall, while CA shows promise as an alternative aggregate, optimizing mixture designs and evaluating long-term durability under various curing conditions are necessary steps to ensure its successful implementation.

However, the inclusion of alternative aggregates, such as CA introduces variability in carbonation resistance and durability. FA-based GPs typically exhibit lower carbonation resistance than PC concrete, a factor compounded by the higher porosity of materials of CA. Ambient curing, which is more energy-efficient than heat curing[1,7,23], further exacerbates carbonation issues by resulting in slower geopolymerization and greater pore formation.[24–28] In contrast, heat curing at elevated temperatures accelerates the geopolymerization process, leading to denser microstructures with improved early strength. However, this approach may also lead to shrinkage cracks and a subsequent increase in carbonation susceptibility.

Despite these challenges, research continues to refine the use of FA and CA in GPs, focusing on optimizing mixture compositions and curing conditions to enhance durability. For instance, adding supplementary materials like MgO in FA-based GPs has shown promise in improving carbonation resistance by forming hydrotalcite, which captures CO<sub>2</sub>. Similarly, studies are investigating whether combining FA with other aluminosilicate-rich by-products like BFS can enhance the mechanical properties and carbonation resistance of GPs, even under ambient curing conditions[1,3,29,30].

Coal ash, particularly FA, holds significant promise as a sustainable precursor for geopolymer technology. Its aluminosilicate-rich composition supports strong chemical bonds within the geopolymer matrix[31–33], resulting in high compressive strength and resistance to various environmental factors. clinker ash serves as alternative aggregates, contributing to sustainability by reducing the demand for natural sand. However, the porous nature of CA raises carbonation resistance challenges, necessitating continued research into optimized formulations and treatment methods.

Recycled fine aggregates, while environmentally advantageous, introduce additional porosity and microcracks, potentially compromising mechanical performance and carbonation resistance. As such, in GPs must be carefully managed to balance environmental benefits with durability requirements.

Overall, the integration of FA, CA into geopolymer technology reflects the construction industry's shift toward sustainability. Continued advancements in mixture optimization, alternative aggregates, and curing techniques will play a vital role in overcoming carbonation resistance challenges and unlocking the full potential of these by-products as key components in sustainable construction materials.

## 2.2 Geopolymer and Carbonation Resistance Using Fly Ash

The term “geopolymer (GP)” is proposed in 1978 by Davidovits. Geopolymers are polymers, a type of amorphous three-dimensional materials with complex composition, which is different to the crystal of  $\text{Ca}(\text{OH})_2$  and calcium silicate hydrate in OPC. Geopolymers based on fly ash can be produced by activation of water glass and sodium hydroxide solution, as shown in Fig. 2.2. GP have emerged as a sustainable alternative to Portland cement due to their lower carbon footprint and effective use of industrial by-products[34–36]. However, the carbonation resistance of FA-based geopolymers remains a critical factor in determining their suitability for long-term structural applications, particularly in reinforced concrete where maintaining alkalinity is essential to protect steel reinforcements from corrosion. Previous studies have investigated various aspects of carbonation in FA-based geopolymers, examining factors such as pH changes, carbonation depth, curing methods, and the impact of different activators on carbonation resistance.

Adam et al.[37] investigated the carbonation resistance of alkali-activated slag (AAS) and FA-based geopolymer concrete, specifically with heat curing. Notably, while AAS-based samples demonstrated typical carbonation-induced color changes with phenolphthalein solution, FA-based geopolymers did not display such changes, suggesting that the carbonation products in FA-based geopolymers might retain higher pH levels. This observation led to the hypothesis that carbonation products in FA-based geopolymers include compounds with high pH, which could explain the absence of color change, as expressed in the reactions:

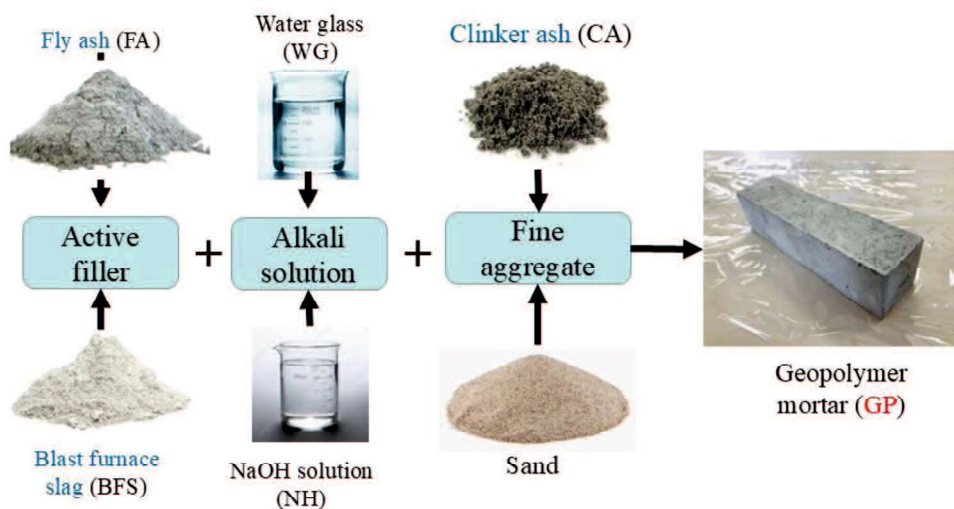
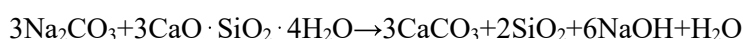
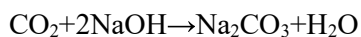


Fig. 2.2 Raw materials of geopolymer mortar

Further exploring this phenomenon, Law et al.[38] measured pH levels in FA-based geopolymer mortars over time and found that pH values remained above 10 throughout carbonation exposure. These results suggest that the unique carbonation process of FA-based geopolymers could preserve a sufficiently high pH, which may reduce the risk of steel corrosion even in the absence of traditional protective measures. Benal et al.[39] confirmed this hypothesis, revealing that carbonation in FA-based geopolymers primarily results in the formation of alkali bicarbonate salts within the pore solution, while the core binder gel structure (N-A-S-H) remains largely unaffected. This distinct carbonation mechanism, which contrasts with that of conventional Portland cement, underscores the potential for FA-based geopolymers to maintain a stable internal environment even under carbonation conditions.

Other researchers reported that heat-cured FA-based geopolymers exhibit low volume of permeable voids[25]. This is attributed to their denser microstructure and reduced pore interconnectivity, factors that are favorable for reducing water ingress and improving durability. The researchers also proposed that FA-based geopolymers form a protective oxide film on their surface, further enhancing resistance to permeation, oxidation, and carbonation.

Despite these benefits, FA-based geopolymers still face challenges with carbonation resistance, particularly under ambient curing conditions, which typically produce more porous materials. Studies continue to seek methods to improve the carbonation resistance of these materials, particularly in contexts where high durability and low permeability are essential.

Research into low-calcium FA and BFS combinations has expanded to understand their effects on carbonation resistance. Benal et al.[39] conducted in-depth studies on the microstructural effects of carbonation in FA and BFS-based geopolymers. By comparing FA-based, AAS-based, and mixed FA/BFS geopolymers, they highlighted differences in carbonation products and microstructural stability. Their findings indicated that in mixed FA/BFS geopolymers, carbonation primarily impacts the C-A-S-H gel formed by BFS activation, while the N-A-S-H gel structure from FA activation remains relatively stable. This stability of the N-A-S-H phase could provide FA/BFS-based geopolymers with unique durability characteristics.

Curing methods play a significant role in determining the carbonation resistance of FA-based geopolymers. Khan et al.[40] investigated the carbonation resistance of FA-based geopolymers with a 10% BFS blend and low-calcium FA (90%) under both natural and accelerated carbonation conditions. Their study measured carbonation depth and pH changes under CO<sub>2</sub> concentrations of 1% and 3%, with observed carbonation depths of 2.57 mm/year, 6.3 mm/year, and 55.6 mm/year, respectively, under natural, 1%, and 3% CO<sub>2</sub> conditions. These findings provide a quantitative basis for assessing the carbonation-induced corrosion risks for reinforcement in FA-based geopolymers, although they do not yet offer a precise model for predicting carbonation progression over time.

Pasupathy et al.[4] extended this investigation by examining FA/BFS-based geopolymer concretes exposed to air for over eight years. They proposed a root function relationship between carbonation depth and time, concluding that carbonation rates are influenced by factors such as permeability, porosity, and pore size. According to their model, the carbonation coefficient ( $K$ , mm/year) correlates positively with these microstructural properties. Additionally, they noted that phenolphthalein sometimes provides unclear carbonation front identification due to the differing carbonate products of calcium (from BFS) and sodium (from FA). This differentiation also influenced carbonation resistance, as mixes activated solely with NaOH or KOH exhibited greater resistance than those using a combination of these activators with sodium silicate. Their long-term study provides one of the most realistic approximations of carbonation resistance in FA/BFS-based geopolymers, approximating real-world conditions.

The unique carbonation mechanisms in FA-based geopolymers, particularly when combined with BFS, present both opportunities and challenges for durable construction applications. FA-based geopolymers maintain high pH levels upon carbonation due to the formation of alkali bicarbonates, which differ from the calcium carbonates prevalent in Portland cement. This distinction suggests that FA-based geopolymers may be less susceptible to steel corrosion, even with partial carbonation. However, the microstructural characteristics of FA and FA/BFS-based geopolymers, such as porosity, curing conditions, and activator selection are critical in determining overall carbonation resistance.

The combination of FA and BFS in geopolymer formulations offers potential improvements in strength and durability[41–43] but may require specific adjustments to optimize carbonation resistance[1,3]. Researches show that heat curing tends to produce denser, less permeable structures, beneficial for FA-based geopolymers[25]. However, these benefits can be offset by shrinkage and cracking[44–46], which may enhance carbonation susceptibility. Consequently, further research into balanced curing methods, alternative activators, and optimized mixture designs is necessary to achieve the desired balance of mechanical performance and carbonation resistance.

In summary, FA-based geopolymers show promise as a low-carbon, durable alternative to traditional cementitious materials. However, advancements in understanding their carbonation behavior, particularly in mixed FA/BFS geopolymers, are essential to unlocking their full potential in structural applications. Continued exploration of curing methods, activator compositions, and mix designs will be key to achieving both environmental and durability goals in future FA-based geopolymer applications.

## 2.3 Recycling of Clinker Ash

The substantial production of industrial waste from thermal power plants, steel manufacturing, and municipal waste incineration has created a pressing need for sustainable recycling methods, especially in the construction industry. Among these by-products, clinker ash, generated in large quantities from coal-fired power plants, offers significant potential as a substitute for traditional sand aggregates in concrete. Clinker ash[47–51] has become the focus of recent research as a means to reduce dependency on natural aggregates and alleviate environmental burdens. This section explores the properties, potential applications, and challenges associated with these materials, focusing particularly on clinker ash in the context of sustainable construction.

Clinker ash is a form of bottom ash produced when coal is combusted in thermal power plants. During high-temperature combustion (approximately 1500°C), unburned coal particles melt and solidify into a glassy, granular material upon cooling. The resulting clinker ash consists of porous, irregularly shaped particles with a sand-like texture. The clinker ash is making up around 5–15% of generated coal ash, is still not being recycled effectively. Disposal of unused clinker ash as pond and landfill gives rise to significant socio-economic and environmental problems. This by-product is typically disposed of in landfills, posing environmental and land-use concerns. The significant quantities of CA produced annually highlight the need to explore its potential as a replacement for natural aggregates in concrete, especially in regions facing restrictions on sand mining due to environmental conservation efforts.

Physically, CA is lighter and more porous than natural aggregates, with high water absorption capacity[52,53] due to its unique internal structure. This increased porosity can be a drawback in concrete applications, as it may lead to higher permeability, shrinkage, and carbonation susceptibility. Chemically, clinker ash contains a mix of oxides, including silica ( $\text{SiO}_2$ ), alumina ( $\text{Al}_2\text{O}_3$ ), and various metal oxides[54–56], which can contribute to the pozzolanic activity of concrete[57–59]. The presence of these oxides allows CA to partially react with cementitious materials[60–63], which can help enhance the mechanical properties of concrete when incorporated in appropriate proportions.

The environmental benefits of incorporating clinker ash in construction materials are substantial. Using CA as a partial or full replacement for natural aggregates reduces landfill waste, decreases the demand for sand mining, and conserves natural resources. Furthermore, the recycling of CA aligns with sustainability goals by diverting waste from landfills and promoting the circular economy in construction. However, the unique physical and chemical properties of CA present both benefits and limitations for its use in concrete.

By utilizing clinker ash as an aggregate, construction materials can achieve a lower environmental footprint, making them more sustainable. The recycling of CA not only diverts waste

from landfills but also conserves river sand, which is being depleted at an unsustainable rate due to the growing demand in the construction industry.

Clinker ash's high porosity, while useful for certain applications, can increase the permeability and shrinkage of concrete. The open structure of CA particles allows for greater water absorption, which may negatively affect concrete's resistance to freeze-thaw cycles and chemical ingress[64–66]. Increased permeability also allows carbon dioxide (CO<sub>2</sub>) to penetrate more easily, raising concerns about carbonation[23,67,68] and potential steel reinforcement corrosion. The high porosity of CA can accelerate carbonation rates, especially under ambient curing conditions. This poses a durability challenge for concrete structures exposed to aggressive environments. Research has shown that CA-based concrete exhibits a higher carbonation rate than traditional Portland cement concrete, highlighting the need for optimized mixture designs to enhance durability.

Concrete incorporating CA typically exhibits higher carbonation rates than traditional PC concrete. The increased porosity associated with these materials allows CO<sub>2</sub> to diffuse more easily into the matrix, thereby accelerating carbonation and reducing the alkalinity needed to protect steel reinforcements.

The integration of clinker ash in concrete formulations represents an essential step towards sustainable construction. However, their unique properties necessitate optimized mixture designs, specific curing methods, and potentially additional treatments to enhance durability and carbonation resistance. Future research should focus on refining mixture proportions, enhancing material compatibility, and exploring potential additives that could offset the increased carbonation rates associated with these recycled materials.

In conclusion, clinker ash offers promising alternatives to natural aggregates, aligning with the construction industry's shift toward sustainable materials. Their use reduces the environmental impact of concrete production and supports circular economy principles by repurposing industrial by-products. Nevertheless, overcoming the durability challenges associated with these materials—particularly in terms of carbonation resistance—will be crucial for their broader application in reinforced concrete structures.

## 2.4 Summary

In this chapter, the coal combustion by-products, specifically fly ash (FA) and clinker ash (CA), were highlighted as sustainable construction materials. These materials, rich in silica and alumina, are promising alternatives to Portland cement and natural aggregates, helping to lower carbon emissions, reduce landfill waste, and conserve natural resources like river sand.

FA is particularly suitable for geopolymer (GP) technology due to its pozzolanic properties, which improve concrete durability and resistance to chemical and thermal degradation. However, FA-based geopolymers generally exhibit lower carbonation resistance, especially under ambient curing, which may compromise steel reinforcement in concrete. Clinker ash, a granular by-product with high porosity, is also useful as a sand replacement in concrete, reducing environmental impact but raising concerns over carbonation due to its open structure.

The common challenge across CA is their high porosity, which accelerates carbonation, reducing durability in reinforced concrete. Despite these challenges, ongoing research aims to optimize mixture designs, improve curing methods, and explore additives to enhance the durability of these materials. Successfully integrating CA in construction could significantly advance sustainable practices in the construction industry, supporting a circular economy and reducing environmental impact.

## References

- [1] Z. Li, S. Li, Carbonation resistance of fly ash and blast furnace slag based geopolymer concrete, *Constr. Build. Mater.* 163 (2018) 668–680.
- [2] N. Shehata, O.A. Mohamed, E.T. Sayed, M.A. Abdelkareem, A.G. Olabi, Geopolymer concrete as green building materials: Recent applications, sustainable development and circular economy potentials, *Sci. Total Environ.* 836 (2022) 155577.
- [3] Z. Li, S. Li, Effects of wetting and drying on alkalinity and strength of fly ash/slag-activated materials, *Constr. Build. Mater.* 254 (2020) 119–069.
- [4] K. Pasupathy, M. Berndt, A. Castel, J. Sanjayan, R. Pathmanathan, Carbonation of a blended slag-fly ash geopolymer concrete in field conditions after 8 years, *Constr. Build. Mater.* 125 (2016) 661–669.
- [5] C. Wang, K. Liu, D. Huang, Q. Chen, M. Tu, K. Wu, Z. Shui, Utilization of fly ash as building material admixture: Basic properties and heavy metal leaching, *Case Stud. Constr. Mater.* 17 (2022) e01422.
- [6] J. Dong, M. Chen, J. Wang, Recycling and optimum utilization of GFRP waste into low-carbon geopolymer paste for sustainable development, *J. Build. Eng.* 97 (2024) 110867.
- [7] X. Li, Z. Li, Surface treatment of inorganic modifier for improving carbonation resistance of geopolymers, *Constr. Build. Mater.* 400 (2023) 132748.
- [8] R. Tagi, N. Yoshimoto, A. Nakashita, N. Ohmoto, Shear Properties of Clinker Ash and Construction Generated Soil Mixtures BT - Sustainable Construction Resources in Geotechnical Engineering, in: H. Hazarika, S.K. Haigh, B. Chaudhary, M. Murai, S. Manandhar (Eds.), Springer Nature Singapore, Singapore, 2024: pp. 463–472.
- [9] M. Suzuki, A. Nakashita, K. Tsukuda, Y. Wakatsuki, Applicability of clinker ash as fill material in steel strip-reinforced soil walls, *Soils Found.* 58 (2018) 16–33.
- [10] M.J. Winter, M. Hyodo, Y. Wu, N. Yoshimoto, M. Bin Hasan, K. Matsui, Influences of particle characteristic and compaction degree on the shear response of clinker ash, *Eng. Geol.* 230 (2017) 32–45.
- [11] Z. Li, R. Kondo, K. Ikeda, Recycling of waste Incineration bottom ash and heavy metal immobilization by geopolymer production, *J. Adv. Concr. Technol.* 19 (2021) 259–279.
- [12] X.-G. Li, Y. Lv, B.-G. Ma, Q.-B. Chen, X.-B. Yin, S.-W. Jian, Utilization of municipal solid waste incineration bottom ash in blended cement, *J. Clean. Prod.* 32 (2012) 96–100.
- [13] Z. Li, R. Kondo, K. Ikeda, Development of Foamed Geopolymer with Addition of Municipal Solid Waste Incineration Fly Ash, *J. Adv. Concr. Technol.* 19 (2021) 830–846.
- [14] A.T. Ahmed, H.A. Khalid, Effectiveness of novel and traditional treatments on the

performance of incinerator bottom ash waste, *Waste Manag.* 31 (2011) 2431–2439.

[15] S.K. Kirthika, S.K. Singh, Durability studies on recycled fine aggregate concrete, *Constr. Build. Mater.* 250 (2020) 118850.

[16] R. Martínez-García, M.I. Sánchez de Rojas, P. Jagadesh, F. López-Gayarre, J.M. Morán-del-Pozo, A. Juan-Valdes, Effect of pores on the mechanical and durability properties on high strength recycled fine aggregate mortar, *Case Stud. Constr. Mater.* 16 (2022) e01050.

[17] Z. Li, J. Liu, J. Xiao, P. Zhong, A method to determine water absorption of recycled fine aggregate in paste for design and quality control of fresh mortar, *Constr. Build. Mater.* 197 (2019) 30–41.

[18] J. Geng, J. Sun, Characteristics of the carbonation resistance of recycled fine aggregate concrete, *Constr. Build. Mater.* 49 (2013) 814–820.

[19] J. Sim, C. Park, Compressive strength and resistance to chloride ion penetration and carbonation of recycled aggregate concrete with varying amount of fly ash and fine recycled aggregate, *Waste Manag.* 31 (2011) 2352–2360.

[20] L. Li, J. Xiao, D. Xuan, C.S. Poon, Effect of carbonation of modeled recycled coarse aggregate on the mechanical properties of modeled recycled aggregate concrete, *Cem. Concr. Compos.* 89 (2018) 169–180.

[21] R. V Silva, R. Neves, J. de Brito, R.K. Dhir, Carbonation behaviour of recycled aggregate concrete, *Cem. Concr. Compos.* 62 (2015) 22–32.

[22] T. Zhang, M. Chen, Y. Wang, M. Zhang, Roles of carbonated recycled fines and aggregates in hydration, microstructure and mechanical properties of concrete: A critical review, *Cem. Concr. Compos.* 138 (2023) 104994.

[23] K. Pasupathy, J. Sanjayan, P. Rajeev, Evaluation of alkalinity changes and carbonation of geopolymer concrete exposed to wetting and drying, *J. Build. Eng.* 35 (2021) 102029.

[24] F.G.M. Aredes, T.M.B. Campos, J.P.B. Machado, K.K. Sakane, G.P. Thim, D.D. Brunelli, Effect of cure temperature on the formation of metakaolinite-based geopolymer, *Ceram. Int.* 41 (2015) 7302–7311.

[25] A. Noushini, A. Castel, The effect of heat-curing on transport properties of low-calcium fly ash-based geopolymer concrete, *Constr. Build. Mater.* 112 (2016) 464–477.

[26] N. Ranjbar, A. Kashefi, M.R. Maheri, Hot-pressed geopolymer: Dual effects of heat and curing time, *Cem. Concr. Compos.* 86 (2018) 1–8.

[27] C. Gunasekara, R. Dirgantara, D.W. Law, S. Setunge, Effect of Curing Conditions on Microstructure and Pore-Structure of Brown Coal Fly Ash Geopolymers, *Appl. Sci.* 9 (2019).

[28] H. Zhang, L. Li, C. Yuan, Q. Wang, P.K. Sarker, X. Shi, Deterioration of ambient-cured and heat-cured fly ash geopolymer concrete by high temperature exposure and prediction of

its residual compressive strength, *Constr. Build. Mater.* 262 (2020) 120924.

[29] J. Kim, S. Na, Y. Hama, Effect of Blast-Furnace Slag Replacement Ratio and Curing Method on Pore Structure Change after Carbonation on Cement Paste, *Materials (Basel)*. 13 (2020).

[30] S.S. Narani, S. Siddiqua, Accelerated carbonation of alkali-activated blended blast furnace slag and wood fly ash: Carbon capture kinetics, chemical and mechanical evolutions, *Constr. Build. Mater.* 411 (2024) 134570.

[31] E. Kamseu, C. Ponzoni, C. Tippayasam, R. Taurino, D. Chaysuwan, V.M. Sglavo, P. Thavorniti, C. Leonelli, Self-compacting geopolymer concretes: Effects of addition of aluminosilicate-rich fines, *J. Build. Eng.* 5 (2016) 211–221.

[32] B. Aouan, S. Alehyen, M. Fadil, M. El Alouani, H. Saufi, M. Taibi, Characteristics, microstructures, and optimization of the geopolymer paste based on three aluminosilicate materials using a mixture design methodology, *Constr. Build. Mater.* 384 (2023) 131475.

[33] C. Tennakoon, P. De Silva, K. Sagoe-Crentsil, J.G. Sanjayan, Influence and role of feedstock Si and Al content in Geopolymer synthesis, *J. Sustain. Cem. Mater.* 4 (2015) 129–139.

[34] S.A. Khan, N. Mir, A. Kul, O. Şahin, M. Şahmaran, M. Koç, Renewable energy for carbon footprint reduction of green geopolymers material's production for built-environment, *Energy Reports*. 8 (2022) 852–858.

[35] I. Luhar, S. Luhar, A Comprehensive Review on Fly Ash-Based Geopolymer, *J. Compos. Sci.* 6 (2022).

[36] C. Horan, M. Genedy, M. Juenger, E. van Oort, Fly Ash-Based Geopolymers as Lower Carbon Footprint Alternatives to Portland Cement for Well Cementing Applications, *Energies*. 15 (2022).

[37] A. Adam, Strength and durability properties of alkali activated slag and fly ash-based geopolymer concrete, 2009.

[38] D.W. Law, A.A. Adam, T.K. Molyneaux, I. Patnaikuni, A. Wardhono, Long term durability properties of class F fly ash geopolymer concrete, *Mater. Struct.* 48 (2015) 721–731.

[39] S.A. Bernal, J.L. Provis, B. Walkley, R. San Nicolas, J.D. Gehman, D.G. Brice, A.R. Kilcullen, P. Duxson, J.S.J. van Deventer, Gel nanostructure in alkali-activated binders based on slag and fly ash, and effects of accelerated carbonation, *Cem. Concr. Res.* 53 (2013) 127–144.

[40] M.S.H. Khan, A. Castel, A. Akbarnezhad, S.J. Foster, M. Smith, Utilisation of steel furnace slag coarse aggregate in a low calcium fly ash geopolymer concrete, *Cem. Concr. Res.* 89 (2016) 220–229.

[41] S. Sukprasert, M. Hoy, S. Horpibulsuk, A. Arulrajah, A.S.A. Rashid, R. Nazir, Fly ash based geopolymer stabilisation of silty clay/blast furnace slag for subgrade applications, *Road Mater. Pavement Des.* 22 (2021) 357–371.

[42] G. Kürklü, The effect of high temperature on the design of blast furnace slag and

coarse fly ash-based geopolymer mortar, *Compos. Part B Eng.* 92 (2016) 9–18.

[43] A. Wardhono, C. Gunasekara, D.W. Law, S. Setunge, Comparison of long term performance between alkali activated slag and fly ash geopolymer concretes, *Constr. Build. Mater.* 143 (2017) 272–279.

[44] I. Khan, T. Xu, A. Castel, R.I. Gilbert, M. Babae, Risk of early age cracking in geopolymer concrete due to restrained shrinkage, *Constr. Build. Mater.* 229 (2019) 116840.

[45] C. Kuenzel, L.J. Vandeperre, S. Donatello, A.R. Boccaccini, C. Cheeseman, Ambient temperature drying shrinkage and cracking in metakaolin-based geopolymers, *J. Am. Ceram. Soc.* 95 (2012) 3270–3277.

[46] D.S. Perera, O. Uchida, E.R. Vance, K.S. Finnie, Influence of curing schedule on the integrity of geopolymers, *J. Mater. Sci.* 42 (2007) 3099–3106.

[47] N. Singh, M. M., S. Arya, Influence of coal bottom ash as fine aggregates replacement on various properties of concretes: A review, *Resour. Conserv. Recycl.* 138 (2018) 257–271.

[48] M. Singh, R. Siddique, Properties of concrete containing high volumes of coal bottom ash as fine aggregate, *J. Clean. Prod.* 91 (2015) 269–278.

[49] L.B. Andrade, J.C. Rocha, M. Cheriaf, Influence of coal bottom ash as fine aggregate on fresh properties of concrete, *Constr. Build. Mater.* 23 (2009) 609–614.

[50] H. Hamada, A. Alattar, B. Tayeh, F. Yahaya, A. Adesina, Sustainable application of coal bottom ash as fine aggregates in concrete: A comprehensive review, *Case Stud. Constr. Mater.* 16 (2022) e01109.

[51] M. Singh, R. Siddique, Strength properties and micro-structural properties of concrete containing coal bottom ash as partial replacement of fine aggregate, *Constr. Build. Mater.* 50 (2014) 246–256.

[52] R. Siddique, Compressive strength, water absorption, sorptivity, abrasion resistance and permeability of self-compacting concrete containing coal bottom ash, *Constr. Build. Mater.* 47 (2013) 1444–1450.

[53] L.B. Andrade, J.C. Rocha, M. Cheriaf, Evaluation of concrete incorporating bottom ash as a natural aggregates replacement, *Waste Manag.* 27 (2007) 1190–1199.

[54] L.M. Deraman, M. Abdullah, L.Y. Ming, K. Hussin, Z. Yahya, A.A. Kadir, Utilization of bottom ash for alkali-activated (Si-Al) materials: A review, *J. Eng. Appl. Sci.* 10 (2006) 8351–8357.

[55] N.L. Rahim, S.A. Mohammed, R.C. Amat, N.M. Ibrahim, N. Hamzah, S. Samsudin, S. Salehuddin, M.A. Rahim, E. Holban, Waste to concrete material: Potential Study of Chemical Characterization of Coal Fly Ash and Bottom Ash, *IOP Conf. Ser. Earth Environ. Sci.* 1216 (2023) 12023.

[56] N.I.R. Ramzi, S. Shahidan, M.Z. Maarof, N. Ali, Physical and Chemical Properties

of Coal Bottom Ash (CBA) from Tanjung Bin Power Plant, IOP Conf. Ser. Mater. Sci. Eng. 160 (2016) 12056.

[57] P. Pormmoon, A. Abdulmatin, C. Charoenwaiyachet, W. Tangchirapat, C. Jaturapitakkul, Effect of cut-size particles on the pozzolanic property of bottom ash, J. Mater. Res. Technol. 10 (2021) 240–249.

[58] A. Abdulmatin, W. Tangchirapat, C. Jaturapitakkul, An investigation of bottom ash as a pozzolanic material, Constr. Build. Mater. 186 (2018) 155–162.

[59] M. Cheriaf, J.C. Rocha, J. Péra, Pozzolanic properties of pulverized coal combustion bottom ash, Cem. Concr. Res. 29 (1999) 1387–1391.

[60] İ.B. Topçu, M.U. Toprak, T. Uygunoğlu, Durability and microstructure characteristics of alkali activated coal bottom ash geopolymer cement, J. Clean. Prod. 81 (2014) 211–217.

[61] R.A. Antunes Boca Santa, A.M. Bernardin, H.G. Riella, N.C. Kuhnen, Geopolymer synthesized from bottom coal ash and calcined paper sludge, J. Clean. Prod. 57 (2013) 302–307.

[62] P. Choeycharoen, W. Sornlar, A. Wannagon, A sustainable bottom ash-based alkali-activated materials and geopolymers synthesized by using activator solutions from industrial wastes, J. Build. Eng. 54 (2022) 104659.

[63] İ.B. Topçu, M.U. Toprak, Properties of geopolymer from circulating fluidized bed combustion coal bottom ash, Mater. Sci. Eng. A. 528 (2011) 1472–1477.

[64] B. Zhang, Durability of low-carbon geopolymer concrete: A critical review, Sustain. Mater. Technol. 40 (2024) e00882.

[65] Y. Xie, X. Lin, T. Ji, Y. Liang, W. Pan, Comparison of corrosion resistance mechanism between ordinary Portland concrete and alkali-activated concrete subjected to biogenic sulfuric acid attack, Constr. Build. Mater. 228 (2019) 117071.

[66] L. Gu, P. Visintin, T. Bennett, Evaluation of accelerated degradation test methods for cementitious composites subject to sulfuric acid attack; application to conventional and alkali-activated concretes, Cem. Concr. Compos. 87 (2018) 187–204.

[67] R. Pouhet, M. Cyr, Carbonation in the pore solution of metakaolin-based geopolymer, Cem. Concr. Res. 88 (2016) 227–235.

[68] T.H. Vu, N. Gowripalan, P. De Silva, A. Paradowska, U. Garbe, P. Kidd, V. Sirivivatnanon, Assessing carbonation in one-part fly ash/slag geopolymer mortar: Change in pore characteristics using the state-of-the-art technique neutron tomography, Cem. Concr. Compos. 114 (2020) 103759.

## **Chapter 3 Improvement of Carbonation Resistance of Geopolymers using Fly Ash as Active Filler**

### **3.1 Introduction**

### **3.2 Experimental Program**

### **3.3 Test Results and Discussion**

### **3.4 Microstructure and Chemical Analysis of GP Mortars**

### **3.5 Conclusions**



# Chapter 3

## Improvement of Carbonation Resistance of Geopolymers using Fly Ash as Active Filler

### 3.1 Introduction

Industrial by-products such as fly ash (FA) from coal-fired power plants, blast furnace slag (BFS), and municipal solid waste incineration ash pose significant environmental challenges due to their disposal. Geopolymer (GP) technology offers an innovative and sustainable solution by converting these wastes into valuable construction materials, particularly as a substitute for ordinary Portland cement (OPC). The environmental advantages of geopolymer materials are substantial, particularly in reducing the carbon footprint of traditional cement production. By utilizing industrial by-products such as FA and BFS, geopolymer materials can achieve significant reductions in CO<sub>2</sub> emissions compared to OPC production[1,2]. Additionally, geopolymer concrete exhibits desirable properties, including high early strength, excellent bonding with reinforcement, and superior resistance to chemical corrosion and fire, making it an attractive option for sustainable infrastructure projects [3–7].

Heat-cured geopolymers, particularly those utilizing FA and BFS as precursors, offer notable mechanical and environmental benefits. Heat curing at elevated temperatures (typically around 80°C) accelerates the geopolymerization process, resulting in a denser microstructure and enhanced early strength[8]. These materials achieve up to 60% lower CO<sub>2</sub> emissions than OPC but require heat curing to maximize their strength and durability. The combination of FA and BFS further enhances mechanical performance, particularly in high-performance applications, due to the synergy between their chemical compositions during heat curing[9]. This makes FA/BFS-based geopolymers highly suitable for construction projects requiring robust mechanical properties.

Extensive research on heat-cured geopolymer materials has explored their compressive strength, resistance to chemical attack and fire, and microstructural evolution[10–13]. While these studies highlight the superior properties of heat-cured GPs, they also reveal challenges regarding carbonation resistance. Carbonation, which reduces the alkalinity of the concrete matrix, is a critical issue because it compromises the protection of steel reinforcement against corrosion. Studies have shown that heat-cured geopolymers, particularly those based on FA/BFS blends, exhibit faster carbonation rates

compared to OPC concrete with similar compressive strength[14,15]. This is attributed to the intrinsic properties of geopolymers, such as their rapid polymerization and residual alkali content, which are more susceptible to carbonation reactions.

The carbonation resistance of heat-cured geopolymers is influenced by factors such as curing conditions and precursor materials. While heat curing reduces porosity and enhances mechanical strength, it can also lead to shrinkage cracks and internal pores, facilitating CO<sub>2</sub> diffusion[16]. Additionally, the residual alkali activators in geopolymers, such as sodium and potassium, are more soluble than calcium hydroxide in OPC, making them more prone to carbonation reactions, particularly under wet-dry cycles. Addressing this challenge has become a key focus for researchers seeking to improve the durability of heat-cured GP materials.

Several strategies have been explored to enhance the carbonation resistance of geopolymers. Additives such as magnesium oxide (MgO) have been shown to improve carbonation resistance by forming hydrotalcite, a compound that can capture CO<sub>2</sub>. However, the improvement is limited, and further optimization is necessary for practical applications[17]. Surface treatments have also been investigated, with organic coatings like waterborne epoxy resin offering some success in reducing shrinkage and chloride ion diffusion, though their effectiveness in preventing carbonation remains limited[18]. Advanced inorganic surface treatments, such as aqueous sodium aluminate (AN) solutions, have demonstrated significant potential. For instance, AN treatment on heat-cured FA/BFS-based GP mortars resulted in a reduction in carbonation depth by over 70% under accelerated carbonation conditions[19,20].

Ambient-cured geopolymers, which are cured at room temperature (around 20°C), face different challenges compared to their heat-cured counterparts. While GP technology offers substantial environmental benefits by utilizing industrial by-products, ambient-cured GPs generally exhibit lower mechanical performance and carbonation resistance. FA/BFS-based GP concrete cured at ambient temperatures demonstrates faster carbonation rates than OPC concrete, particularly during the early stages of exposure to CO<sub>2</sub>[21]. This is a significant limitation for their use in reinforced concrete structures, where carbonation compromises the alkalinity needed to protect steel reinforcement from corrosion.

The slower geopolymerization process at ambient temperatures leads to a less dense microstructure in these materials, contributing to their lower mechanical strength and carbonation resistance[22,23]. Although FA/BFS-based GP concrete can achieve acceptable mechanical properties under ambient conditions, the carbonation rate remains a critical concern. Larger pores and cracks caused by drying shrinkage further exacerbate CO<sub>2</sub> penetration in ambient-cured GPs, making them less durable than heat-cured alternatives or OPC[24]. Additionally, the residual alkali content in ambient-cured GPs is highly vulnerable to carbonation and leaching during wet-dry cycles, further reducing their long-term durability[16].

Efforts to address the carbonation resistance of ambient-cured GPs have focused on optimizing mix designs and exploring surface treatments. Reducing the liquid-filler ratio in the geopolymer mix has been proposed to lower porosity and enhance carbonation resistance. However, this approach alone has not been sufficient to achieve durability comparable to OPC concrete[18]. Organic coatings, such as waterborne epoxy resin and hydrocarbon ester/silane-based materials, have shown limited success in improving carbonation resistance but raise concerns regarding long-term durability and water resistance[25]. These limitations highlight the need for more robust and sustainable surface treatment solutions.

Inorganic surface treatments have emerged as a promising alternative for enhancing the carbonation resistance of ambient-cured geopolymers. Inspired by the success of silicate-based treatments in OPC concrete, researchers have explored the use of AN solutions to improve the durability of GP materials. In accelerated carbonation tests, AN treatment on ambient-cured FA/BFS-based GP mortars significantly improved carbonation resistance, though the improvement was less pronounced than in heat-cured specimens[26]. The effectiveness of AN treatment depended on the initial porosity of the GP material, which was influenced by mix proportions and curing conditions.

This study contributes to the development of durable geopolymer technologies by investigating the mechanisms behind carbonation resistance in both heat-cured and ambient-cured GP materials. By examining the effects of surface treatments, mix designs, and curing methods, the findings offer valuable insights for optimizing GP materials for practical applications, particularly in environments where carbonation poses a significant durability challenge. These advancements hold promise for the widespread adoption of geopolymers as sustainable alternatives to conventional cement in construction.

## 3.2 Experimental Program

### 3.2.1 Raw Materials

The FA of JIS (Japanese Industrial Standards) grade II and the BFS of JIS 4000 class were used as active fillers (AF) of GP mortars, which physical properties and chemical compositions are shown in **Tables 3.1** and **3.2**, respectively. The metal oxide contents and density of AN with a concentration of 40 wt% are presented in **Table 3.1**, too. Other AN solutions with different concentrations were prepared by diluting 40 wt% AN solution with distilled water. Sea sand, washed in advance with tap water, was used as fine aggregate of the GP mortars.

Three kinds of alkali activator solution (AS), named AS01, AS11 and AS31, were used, which were sodium hydroxide solution (NH) with 10 moles or a mixture of water glass aqueous solution

Table 3.1 Physical properties of raw materials used

Raw material	Properties, etc.
FA	Specific gravity: 2.30, Blaine fineness: 4392 cm <sup>2</sup> /g
BFS	Specific gravity: 2.88, Blaine fineness: 4180 cm <sup>2</sup> /g
Sea sand	Oven-dry density: 2.51, surface-dry density: 2.56, specific water absorption: 1.81%, solid content: 66.7%, F.M. 2.87
Sodium aluminate solution	Compositions: Na <sub>2</sub> O 19%, Al <sub>2</sub> O <sub>3</sub> 20%, Molar ratio (Na <sub>2</sub> O/Al <sub>2</sub> O <sub>3</sub> ): 1.56, Specific gravity: 1.49 (40 wt% concentration)

Table 3.2 Chemical compositions of FA and BFS (XRF analysis)

Active filler	Chemical compositions (%)								
	SiO <sub>2</sub>	Al <sub>2</sub> O <sub>3</sub>	CaO	Fe <sub>2</sub> O <sub>3</sub>	MgO	Na <sub>2</sub> O	K <sub>2</sub> O	TiO <sub>2</sub>	Others
FA	59.10	23.91	3.48	7.37	1.06	1.07	1.68	1.27	1.06
BFS	34.67	14.46	43.13	0.34	5.50	0.25	0.25	0.55	0.85

Table 3.3 Alkali activator solution's components and density

Alkali activator solution	WG : NH, by volume	Specific gravity	Mole ratio of SiO <sub>2</sub> /Na <sub>2</sub> O	Molarity of Na <sub>2</sub> O (mole/L)
AS01	0:1	1.330	0	5.000
AS11	1:1	1.359	0.696	2.438
AS31	3:1	1.374	1.255	3.108

Table 3.4 Mix proportions of heat/ambient-cured GP mortars

Series No.	Parameters	WG: NH (WG/AS)	AS/AF	BFS: FA (BFS/AF)	S/AF
1	Control mix	3:1	0.5	3:7(0.3)	2.0
2	BFS blending ratio	(0.75)		0:1 (0)	
3				1:1 (0.5)	
4				1:0 (1)	
5				3:7	
6	WG/NH ratio	0:1 (0)		0.3)	
7	AS/AF	0.75	0.45		
8			0.55		

Notes: 25 wt.% AN solution was applied twice at 3 days old, and the specimens were sealed as cured till 28 days after the treatment.

(WG) and the NH according to the volume ratio of WG: NH = 1:1 or 3:1, as shown in **Table 3.3**. The WG was prepared by diluting JIS No.1 grade sodium silicate ( $\text{Na}_2\text{SiO}_3$ ) with distilled water by a volume ratio of 1:1.

### 3.2.2 Mix proportions of GP mortars

The mix proportions of GP mortars used in this study are shown in **Table 3.4**. Based on the preliminary investigation, we found that series No.1 had adequate fluidity for specimen production, thus, it was used as the control mixture. Then, the other GP mortars were designed by adjusting the BFS blending ratio, WG/NH ratio by volume, and liquid-fillers ratio by mass, as shown in **Table 3.4**, on the basis of series No.1. In this experiment, the ratio of fine aggregates (S) to AF was 2.0 throughout by mass.

Also, for clarifying appropriate AN treatment conditions, the effects of the AN solution concentration, AN surface treatment frequency within 3 days, the age of mortar specimen when the AN surface treatment, whether the mortar specimens were sealed after the AN surface treatment during curing, and curing temperatures were investigated, as summarised **Table 3.5**. The GP specimens with the same mix proportion were tested and the effects of different conditions of AN treatment were reflected on the carbonation degree of GP mortars.

### 3.2.3 Specimens preparation

The experimental process is shown in **Fig. 3.1**. A Hobart planetary mortar mixer was used to mix the GP mortars. The active fillers and sea sand were first put into the mixer and mixed for 1 minute. Then, the alkali activator was added and mixed for 2 min. to get GP mortar. Finally, freshly mixed GP

Table 3.5 Conditions of AN surface treatment for heat-cured GP

Series No.	Factors	Mortar Age, frequency of AN application	AN concentration by mass (%)	State during curing
9	Control	No-AN application		Sealed
10	Age when the AN was applied	7 days, twice	25	Sealed
11		20 days, twice		
12	Concentrations of AN	3 days, twice	10	
13			20	
14			30	
15			40	
16			AN treatment frequency	
17	Sealing state during curing	3 days, twice		Not sealed

Notes: Mix proportions of GP mortar of series 9-17 were the same as those of series No.1 shown in Table 3.4.

mortar was used to produce the prism specimens with a 4 cm side length of square section and 16 cm length, which were used for the accelerated carbonation test. Each of the mortar specimens was compacted by a table vibrator for 1 minute, followed by levelling the top surface with a metal spatula. After being sealed with water-retention tape, half of the specimens were first cured in the air at 80 °C for 8 hours, then stored in a 20 °C temperature and 60% R.H. curing chamber till 28-day age (hereafter referred to as heat-curing). The other half specimens were demoulded after one day and then moved into the curing chamber with 20°C temperature and 60% relative humidity for 28 days in until reaching a 28-day age (hereafter referred to as ambient-curing). The temperature and time conditions set for heat-curing methods are commonly used in the field of geopolymer research. The specimens were demoulded at 1 day age.

The six surfaces of half of the prismatic specimens were applied with AN solution at the ages of 3, 7 and 28 days, respectively, according to the treatment conditions shown in **Tables 3.4** and **3.5**. Although the application was conducted by a brush according to the number of AN application determined in advance, the amount of AN solution applied was uncertain, depending on the surface conditions of specimen such as denseness and moisture content. **Fig. 3.2** shows the appearance of 80 °C-cured GP mortars before and after AN surface treatment. After AN treatment, surfaces of GP mortar becomes slightly white.

### 3.2.4 Property test, chemical and microstructure analysis

#### (1) Accelerated carbonation test

After 28 days of curing, four surfaces (two ends, top and bottom surfaces) of mortar specimens were sealed with an airtight sealing tape to ensure that CO<sub>2</sub> diffuses into the specimens only through the two side surfaces. Then, the specimens were placed into a carbonation test chamber with 5% of CO<sub>2</sub> concentration, 20 °C, and R.H. 60%. At an interval of two weeks, the mortar specimen was cut at about 10 mm interval to measure carbonation depth. It should be noted that during the cutting, to

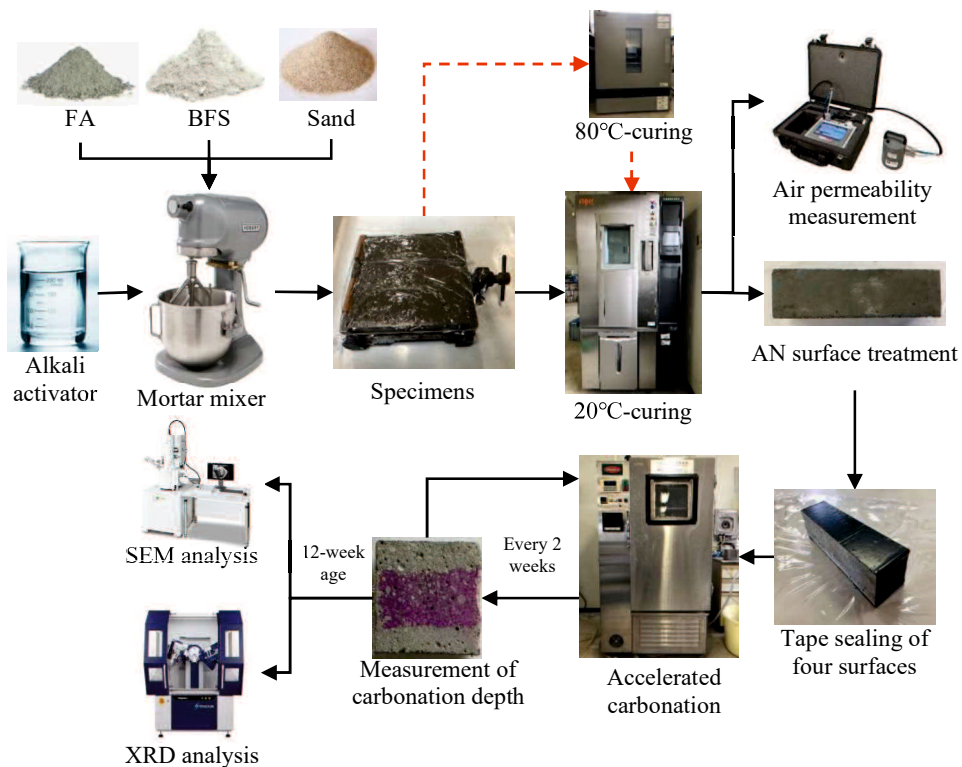


Fig. 3.1 Experimental process

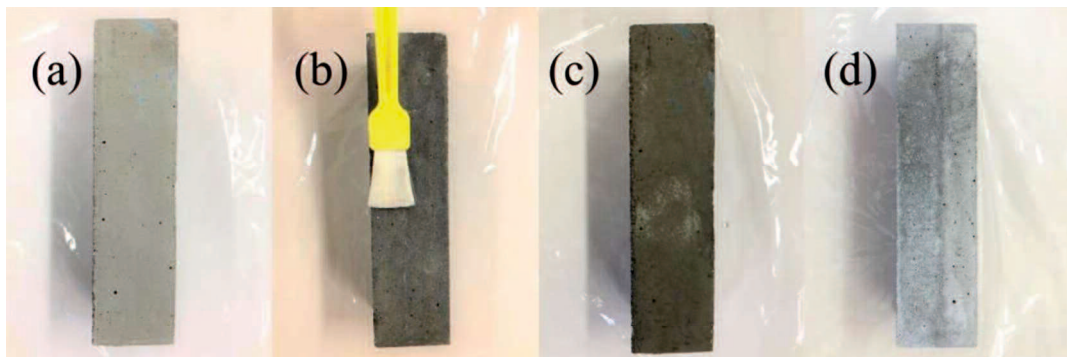


Fig. 3.2 The surfaces of geopolymer mortar specimens (40 × 40 × 160mm): (a) before treatment, (b) AN surface treatment by brush, (c) right after AN treatment, and (d) AN-treated specimen at 28-day age

ensure that the alkali matters were not washed away, spraying water was not used as a dust countermeasure.

The depth of the colorless region from the surface of the prism specimen was measured at 3 min. strictly after spraying the 1% phenolphthalein solution. The average value of six depths, three values on one side and 1 cm interval respectively, was recorded as carbonation depth. After the measurement of carbonation depth, the cut sections were sealed with airtight tape, and the remained GP mortar samples were returned to the CO<sub>2</sub> chamber to continue the carbonation test. The accelerated carbonation test lasted 18 weeks.

### *(2) Strength measurement*

For clarifying the effect of the AN-surface treatment on the strength of BFS/FA blend-based GP, we measured the flexural and compressive strengths of mortars of series No.1 and No.3, with and without the AN treatment, using a universal testing machine on 28-day age. The specimens were prisms with dimensions of 40 mm×40 mm×160 mm, which were cured by the 80 °C-curing method. The flexural strength was an average of three prismatic specimens for each mixture, while the compressive strength was an average of six fractured prismatic pieces after the flexural test.

### *(3) SEM-EDS and XRD analysis*

To investigate the microstructural change and reaction products of surface-modified GPs, XRD (X-ray diffraction) and SEM-EDS (scanning electron microscopy) analyses of GP mortars with and without AN surface treatment at 3-day age were conducted. The specimens analysed were sampled from GP mortars which were FA-based (series No. 2), BFS-based (series No. 4), and FA/BFS-based (series No. 1), respectively, which were cured at 80 °C for 8 hours and then 20 °C for 27 days.

The SEM-EDS and XRD analyses were collected from the surface layer with 1 mm depth, where it was believed that the AN solution diffused from colour change. The samples of the SEM-EDS analysis were pre-treated by embedding in resin and then polishing. The SEM-EDS analysis was taken under 15 kV accelerating voltage. ZAF corrections were automatically done for point analysis data. The XRD analysis used a CuK $\alpha$  source, 40 kV-120 mA power supply, 1° -1° -1°-0.3 mm slit method, scanning speed 4°/min, and 0.02° step scans in the 2 $\theta$  range of 5-60°.

### 3.3 Test Results and Discussion

#### 3.3.1 The effects of mix proportions on the effectiveness of AN surface treatment

The diffusion of carbon dioxide and the carbonation are greatly influenced by the features of matrix mortar such as denseness and chemical compositions[21], and the presence of coarse aggregate greatly affects the measurement accuracy of carbonation depth because coarse aggregate particles make the front line of carbonation into a jagged curve. Thus, in this study, we used GP mortars instead of concrete to discuss the effect of AN surface treatment on the carbonation resistance of GP materials.

The effects of AN treatment on the carbonation resistance of GP mortar with different mix proportions and with the different treatment conditions were discussed on the basis of regression analysis of carbonation depth - carbonation time relationship for different mortars and treatment conditions. As described later, due to the AN surface treatment, the carbonation depth of part of the specimens could be detected only after a period, so we used Eq. (1) for the regression analysis.

$$C_d = a \cdot \sqrt{\text{CO}_2\% / 5.0} \cdot \sqrt{t - b} \quad (1)$$

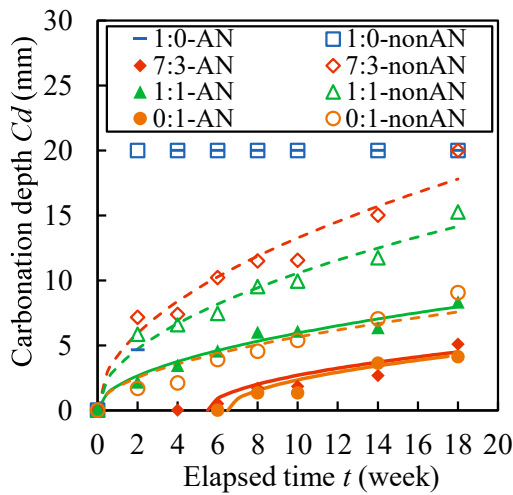
where  $C_d$  is carbonation depth (mm),  $t$  is carbonation period (week),  $\text{CO}_2\%$  represents  $\text{CO}_2$  concentration (%),  $a$  is proportional coefficient (mm/ $\sqrt{\text{week}}$ ), and  $b$  is elapsed time until the depth of carbonation can be detected, i.e., onset time of neutralization (week,  $\geq 0$ ).

In Eq. (1), the proportional coefficient  $a$  implies the rate of increase of the carbonation depth with elapsed time and therefore is called carbonation rate coefficient. The smaller the  $a$ , the higher the carbonation resistance of GP mortar. And the larger the  $b$ , the later the onset of neutralization, and therefore the higher the initial carbonation resistance.

In Fig. 3.3, Fig. 3.4, Fig. 3.5 and Fig. 3.8, The equations in the table of right part of the figure are the relationships of carbonation depths with elapsed times of accelerated time of different GP mortars with and without AN treatment and the corresponding goodness of fits ( $R^2$ ) are under the equations. In addition, the variations of coefficients of  $a$  and  $b$  are also listed in the right column in the table. With the comparison of the carbonation equations of GP mortars with different mix proportions before and after AN treatment, we can clearly observe the differences in the effectiveness of AN treatment on various GP mortars of mix proportions.

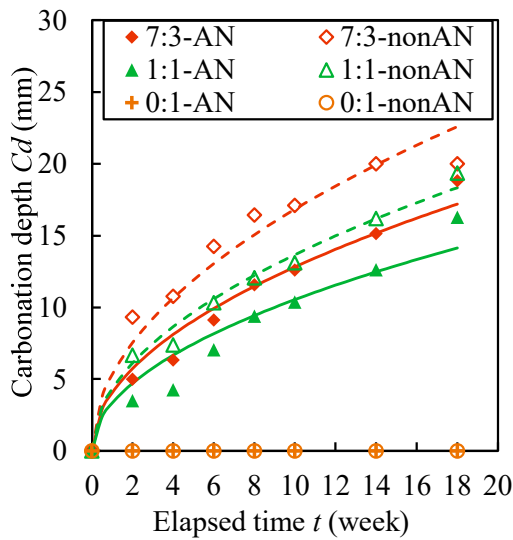
##### (1) Effect of FA/BFS ratio

Fig. 3.3 (a) and (b) show the test results of the relationship between the carbonation depth and the elapsed time for the GP mortars with different FA/BFS blending ratios by mass. The heat-cured BFS/FA blend-based mortars had smaller carbonation depths for the same elapsed time. This is because heat-curing promotes the reaction of FA and BFS, especially FA, with more products leading to a denser microstructure at 28-day age [27,28]. However, the carbonation resistance of the BFS sole-based GP mortar cured by the heating method was lower compared with the BFS sole-based GP mortar



FA/ BFS	AN treatment	Non-AN treatment	Decrease of $a$ (%)	$b$ (week)
1:0	-	-	-	-
7:3	$C_d = 1.27\sqrt{t-5.5}$ $R^2 = 0.876$	$C_d = 4.19\sqrt{t}$ $R^2 = 0.990$	69.73	5.5
1:1	$C_d = 1.88\sqrt{t}$ $R^2 = 0.993$	$C_d = 3.33\sqrt{t}$ $R^2 = 0.994$	43.54	0
0:1	$C_d = 1.25\sqrt{t-7}$ $R^2 = 0.934$	$C_d = 1.78\sqrt{t}$ $R^2 = 0.971$	29.77	7

(a) Heat-cured GP mortars



FA/ BFS	AN treatment	Non-AN treatment	Decrease of $a$ (%)	$b$ (week)
7:3	$C_d = 4.05\sqrt{t}$ $R^2 = 0.932$	$C_d = 5.32\sqrt{t}$ $R^2 = 0.924$	23.87	0
1:1	$C_d = 3.33\sqrt{t}$ $R^2 = 0.981$	$C_d = 4.32\sqrt{t}$ $R^2 = 0.997$	22.89	0
0:1	-	-	-	-

(b) Ambient-cured GP mortars

Fig. 3.3 Carbonation depth of GP mortars with different FA/BFS ratios (Series No. 1, 2, 3, 4)

cured in the ambient air. This is because the dry shrinkage and moisture escape arising from the heat-curing resulted in more porosity and larger cracks in the BFS-based GP mortar [29,30]. FA-based GP mortar without BFS addition was easy to carbonate, the carbonation reached the center of the 80 °C-cured prism specimen with 40 mm side length at two weeks, but the AN surface treatment delayed the complete carbonation time from two weeks to one month. On the other hand, the BFS-based GP mortar cured in the ambient air had no detectable carbonation depth within 18 weeks, regardless of the AN surface treatment, and thus the benefit of the AN surface treatment was not confirmed. This is because the reaction products are few in the FA sole-based GP, which leads to a high porosity of GP [31].

As shown in Fig. 3.3 (a), For the 80 °C-cured mortar specimens with AN surface treatment, the time to detect the depth of carbonation was delayed by 2-4 weeks. Therefore, we used the two parameters  $a$ ,  $b$  in Eq. 3 to characterize the carbonation resistance of the surface-treated GPs, of which

$b$  represents delayed time, and  $a$  is the carbonation rate coefficient as usual. The regression equations for the relationship between carbonation depth and time, and the obtained  $a$ ,  $b$  values are shown under each graph. The smaller the  $a$ -value or the larger the  $b$ -value, the higher the carbonation resistance. Under the heat-curing method, the AN surface treatment had an obvious effect on the carbonation resistance improvement. That is, due to the surface treatment, the  $a$  value was decreased or/and the  $b$  value is larger than zero.

It is obvious from **Fig. 3.3 (a)** that the lower the blending ratio of BFS, the larger the carbonation rate coefficient of the non AN-treated mortar. However, the mortar with a larger carbonation rate coefficient attained a better improvement from the viewpoint of the decrease of  $a$  value. In the case of 30% of the BFS blending ratio, the AN treatment yielded the highest decrease in the carbonation rate coefficient  $a$ . Therefore, it is concluded that the AN surface modifier is more suitable for BFS/FA blend-based GP with a low BFS blending ratio. Considering that the carbonation resistance is mainly dependent on the porosity of GP [32,33], a smaller BFS blending ratio leads to large porosity and large pore size [34,35], which makes the AN solution penetration easier and thus brings better modification.

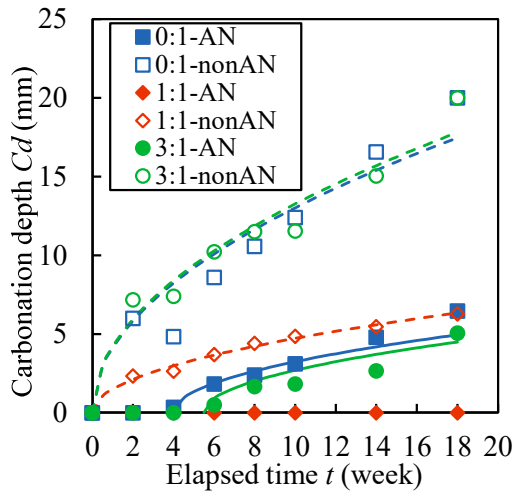
**Fig. 3.3 (b)** illustrate the test results on the relationship between carbonation depth and elapsed time for ambient-cured geopolymer (GP) mortars with different FA/BFS blending ratios. For mortars cured at 20°C, the carbonation depth was greater compared to those cured at 80°C, given the same elapsed time. This difference arises because ambient curing results in a slower reaction between FA and BFS, leading to a less dense microstructure.

The BFS-based GP mortar cured in ambient air exhibited strong carbonation resistance, with no detectable carbonation depth within 18 weeks, regardless of AN surface treatment. In contrast, FA-based GP mortars without BFS showed rapid carbonation, reaching the center of the specimen within two weeks, although the AN surface treatment extended this period to one month. However, the benefit of AN surface treatment was not significant for the BFS-based GP mortar, likely due to the lower porosity formed under ambient conditions.

The relationship between carbonation depth and time was characterized by two parameters,  $a$  and  $b$ , where  $a$  represents the carbonation rate and  $b$  the delayed time. For ambient-cured mortars, AN surface treatment lowered the carbonation rate coefficient, though the improvement was less pronounced compared to heat-cured samples. Mortars with lower BFS content saw more significant improvements in carbonation resistance after AN treatment, as their higher porosity allowed better penetration of the AN solution.

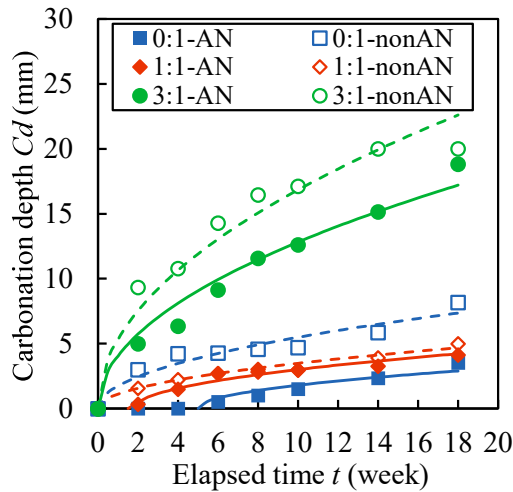
#### (2) *Effect of WG/NH ratio*

**Fig. 3.4 (a)** show the relationship between the carbonation depth and the elapsed time for the 30% BFS/70% FA blend-based GP mortars produced by different AS solutions and cured at 80°C. The AN surface treatment yielded a significant enhancement in carbonation resistance for GP mortars, regardless of the curing method. Furthermore, even though the AS solution used in GP mortar was



WG /NH	SiO <sub>2</sub> /Na <sub>2</sub> O	AN treatment	Non-AN treatment	Decrease of <i>a</i> (%)
0:1	0.00	$C_d = 1.32\sqrt{t-4}$ $R^2 = 0.918$	$C_d = 4.11\sqrt{t}$ $R^2 = 0.978$	67.86
1:1	0.69	$b > 18$	$C_d = 1.49\sqrt{t}$ $R^2 = 0.998$	-
3:1	1.25	$C_d = 1.27\sqrt{t-5.5}$ $R^2 = 0.876$	$C_d = 4.19\sqrt{t}$ $R^2 = 0.990$	69.68

(a) Heat-cured GP mortars



WG/ NH	SiO <sub>2</sub> / Na <sub>2</sub> O	AN treatment	NonAN treatment	Decrease of <i>a</i> (%)
0:1	0.00	$C_d = 0.80\sqrt{t-4}$ $R^2 = 0.909$	$C_d = 1.73\sqrt{t}$ $R^2 = 0.985$	53.74
1:1	0.69	$C_d = 1.04\sqrt{t-1.8}$ $R^2 = 0.882$	$C_d = 1.10\sqrt{t}$ $R^2 = 0.958$	4.96
3:1	1.25	$C_d = 4.05\sqrt{t}$ $R^2 = 0.993$	$C_d = 5.32\sqrt{t}$ $R^2 = 0.992$	23.87

(b) Ambient-cured GP mortars

Fig. 3.4 Carbonation depth of GP mortars with different WG/NH ratios (Series No. 1, 5, 6)

changed, the AN surface treatment was still more effective for the 80 °C-cured specimens in reducing the *a* value and increasing the *b* value, i.e. the improvement of carbonation resistance was greater for the 80 °C-cured GPs. When treated with the AN solution, the 80 °C-cured GP mortar with a WG/NH volumetric ratio of 1:1 was not carbonated during the accelerated carbonation period of 18 weeks. The continuous dissolution of silicate from the precursors due to the activation of alkali forms many free Si-O-Si tetrahedral monomers, which contribute to the SiO<sub>4</sub> and AlO<sub>4</sub> linking. The increase of SiO<sub>2</sub>/Na<sub>2</sub>O mole ratio is reported to promote the formation of N-A-S-H gels in GPs [36]. However, the apparent porosity of GP would increase when the mole ratio of SiO<sub>2</sub>/Na<sub>2</sub>O exceeds 0.806 [37]. This can explain why the carbonation depths of the GP mortar specimens with a WG/NH ratio of 3:1 (SiO<sub>2</sub>/Na<sub>2</sub>O = 1.25) were greater than those with a WG/NH ratio of 1:1 (SiO<sub>2</sub>/Na<sub>2</sub>O = 0.69). More residual Na<sup>+</sup> present in pores is another reason why the GP mortar specimens with a WG/NH ratio of

1:1 had smaller carbonation depths. That is, an appropriate  $\text{SiO}_2/\text{Na}_2\text{O}$  molar ratio is essential to achieve high carbonation resistance of GP. We found that in the case of 80 °C-curing, the specimen with WG/NH=0:1 had a lower improvement degree of carbonation resistance than the specimen with WG/NH=3:1. At present we are not clear about the reasons. The AN surface treatment effectiveness is estimated to be influenced by a combination of factors such as drying shrinkage cracks, residual  $\text{Si}^{4+}$ ,  $\text{Na}^+$  content, and the porosity of GP.

**Fig. 3.4** (b) show the relationship between carbonation depth and elapsed time for 30% BFS/70% FA blend-based geopolymer (GP) mortars produced using different AS solutions and cured at 20°C. The AN surface treatment significantly enhanced carbonation resistance across all GP mortars, regardless of the AS solution used.

Before AN surface treatment, the GP mortar with a WG/NH ratio of 3:1 exhibited the highest carbonation rate, followed by the 0:1 ratio, and the lowest carbonation rate was observed for the 1:1 ratio. This indicates that the  $\text{SiO}_2/\text{Na}_2\text{O}$  molar ratio plays a critical role in carbonation resistance, with the WG/NH ratio of 1:1 ( $\text{SiO}_2/\text{Na}_2\text{O} = 0.69$ ) being the most effective in reducing carbonation depth.

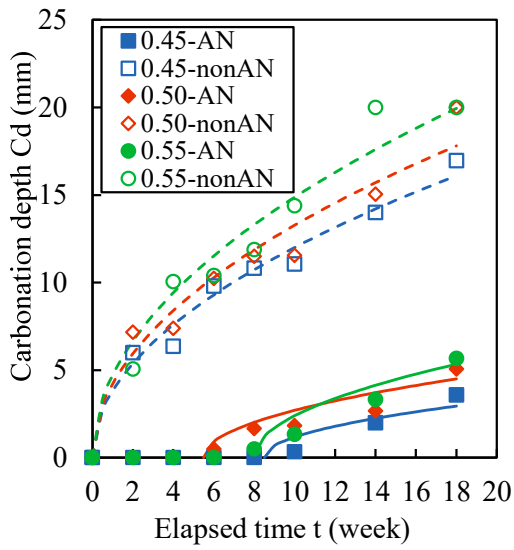
After AN surface treatment, the GP mortar with a WG/NH ratio of 3:1 still had the highest carbonation rate, followed by the 1:1 ratio, and the 0:1 ratio exhibited the lowest carbonation rate. This change is likely due to the higher porosity of the GP mortar with a WG/NH ratio of 3:1, which allows better penetration of the AN solution, thereby leading to improved modification and better carbonation resistance. This is also the reason why the GP mortar with WG/NH ratio of 3:1 experienced the greatest reduction in carbonation rate with AN treatment. Conversely, the GP mortar with a WG/NH ratio of 0:1, which has lower initial carbonation resistance, benefitted the most from the AN treatment due to its relatively low porosity, which allowed for more effective surface sealing.

In summary, the AN surface treatment was more effective in reducing carbonation for ambient-cured GP mortars with a higher initial carbonation rate, particularly those with higher porosity. The porosity and chemical composition, particularly the  $\text{SiO}_2/\text{Na}_2\text{O}$  molar ratio, are significant factors in determining the carbonation resistance of GP mortars after treatment.

### (3) AS/AF ratio

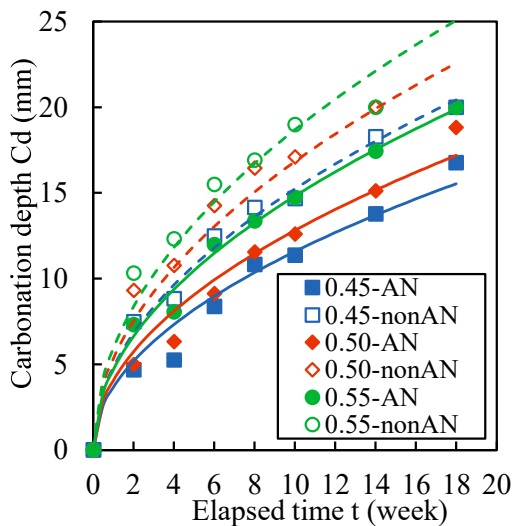
**Fig. 3.5** (a) and (b) show the experimental results of the relationship between the carbonation depths and the elapsed time for the 30% BFS/70% FA blend-based GP mortars with different liquid-active filler (AS/AF) ratios. Regardless of curing method, the smaller the AS/AF ratio, the smaller carbonation depth for the same elapsed time. As reported in other studies, a lower AS/AF ratio leads to finer pores and lower porosity [38], less drying shrinkage [39], and thus contributes to a higher carbonation resistance of GP materials [21,40].

It is clearly observed that the surface treatment of AN solution improved the carbonation resistance of the GP mortars from **Fig. 3.5** (a), though the 80 °C-cured GP mortars got a much reduction in the carbonation depth. And the AN surface treatment greatly delays the beginning time



AS/AF	AN treatment	Non-AN treatment	Decrease of a (%)	b (week)
0.45	$C_d = 0.95\sqrt{t-8.5}$ $R^2 = 0.963$	$C_d = 3.79\sqrt{t}$ $R^2 = 0.995$	74.87	8.5
0.50	$C_d = 1.27\sqrt{t-5.5}$ $R^2 = 0.876$	$C_d = 4.19\sqrt{t}$ $R^2 = 0.990$	69.73	5.5
0.55	$C_d = 1.37\sqrt{t-8}$ $R^2 = 0.839$	$C_d = 4.70\sqrt{t}$ $R^2 = 0.991$	64.14	8

(a) Heat-cured GP mortars



AS/AF	AN treatment	Non-AN treatment	Decrease of a (%)	b (week)
0.45	$C_d = 3.66\sqrt{t}$ $R^2 = 0.992$	$C_d = 4.81\sqrt{t}$ $R^2 = 0.998$	23.97	0
0.5	$C_d = 4.05\sqrt{t}$ $R^2 = 0.993$	$C_d = 5.32\sqrt{t}$ $R^2 = 0.992$	23.87	0
0.55	$C_d = 4.68\sqrt{t}$ $R^2 = 0.998$	$C_d = 5.91\sqrt{t}$ $R^2 = 0.993$	20.71	0

(b) Ambient-cured GP mortars

Fig. 3.5 Carbonation depth of GP mortars with different AS/AF ratios (Series No. 1, 7, 8)

of carbonation of the 80 °C-cured GP mortars, as shown in **Fig. 3.5** (a), thus the *b* value is 4~8 weeks. That is to say, in the general range of AS/AF ratio, regardless of AS/AF ratio, the carbonation resistance of BFS/FA blend-based GP can be expected to be improved by the AN surface treatment. In the case of heat-curing, the decrease of *a* value can be reduced by more than 70%. And it can be concluded that the smaller the AS/AF ratio, the higher the improvement effectiveness from the decreasing degree of the *a* value. When the AS/AF ratio was 0.45, the starting point of carbonation was delayed to 8 weeks. However, the specimen with an AS/AF ratio of 0.55 had a longer delaying time of carbonation (*b* value) than the specimen with an AS/AF ratio of 0.50, which suggests that the

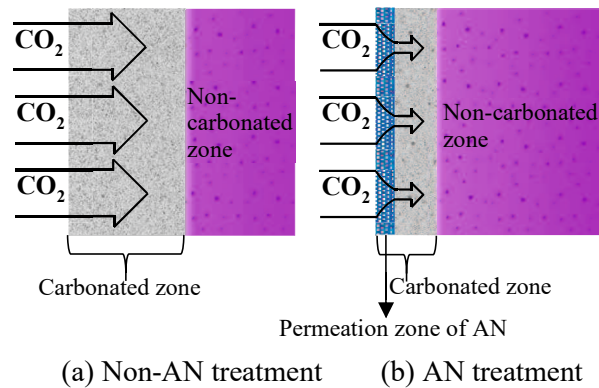


Fig. 3.6 Schematic description of the carbonation of mortar

$b$  value depends on the AN's permeation ability, that is, the initial porosity of GP that is influenced by the AS/AF ratio. If the AN solution forms a dense layer in the surface layer of GP, this dense layer would delay the start of carbonation. The  $b$  value depends on the thickness and denseness of this dense layer, as shown in **Fig. 3.6**. Once the carbonation starts behind this dense layer, the rate of carbonation will depend on the degree of denseness and alkalinity inside the GP. High water content reduces the AN's inside permeation ability, which correspondingly reduces the effectiveness of AN surface treatment.

**Fig. 3.5 (b)** illustrate the relationship between carbonation depth and elapsed time for 30% BFS/70% FA blend-based geopolymer (GP) mortars with different AS/AF ratios, which were all 20°C-cured specimens. Regardless of the AS/AF ratio, the carbonation resistance of ambient-cured GP mortars was lower, as the onset of carbonation occurred at the first week for all AS/AF ratios.

Before the AN surface treatment, the carbonation rate was highest for the GP mortar with an AS/AF ratio of 0.55, followed by 0.50, and lowest for 0.45, suggesting that a smaller AS/AF ratio leads to finer pores, lower porosity, and higher carbonation resistance. This trend can be attributed to the fact that a lower AS/AF ratio results in less drying shrinkage and a denser microstructure, as supported by previous studies.

After AN surface treatment, the carbonation resistance of the ambient-cured mortars improved, though the effect was less pronounced compared to heat-cured specimens. The AN treatment helped reduce the carbonation rate, but due to the relatively higher water content in the 20°C-cured GP mortars, AN's permeation ability was limited, reducing its effectiveness. Unlike heat-cured mortars, where the AN treatment significantly delayed carbonation, the ambient-cured specimens did not experience a noticeable delay in the onset of carbonation.

In conclusion, the AN surface treatment was effective in enhancing the carbonation resistance of ambient-cured GP mortars, though its improvement was less substantial compared to heat-cured

counterparts. The effectiveness of the AN treatment was also influenced by the initial porosity of the GP mortar, which was determined by the AS/AF ratio.

### ***3.3.2 The effects of treatment conditions on the effectiveness of AN surface treatment***

#### *(1) Time points of AN treatment*

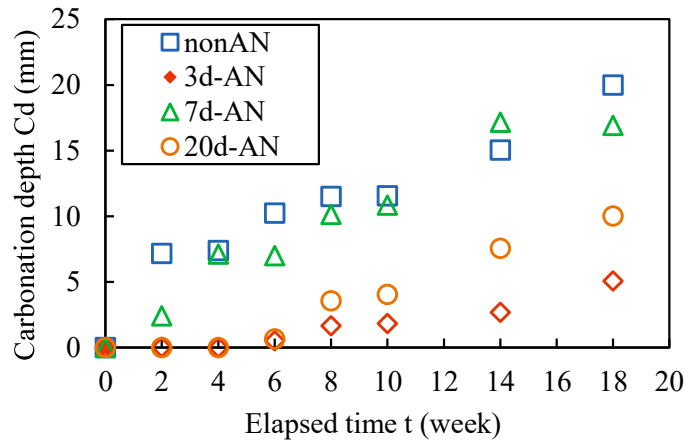
**Fig. 3.7** presents the carbonation depths of the 70% FA/30% BFS blend-based GP mortars, which were cured in a sealed state and treated with the 25 wt% AN solution on the surfaces at different material ages. As shown in **Fig. 3.7** (a), the AN surface treatment at 3-day age led to the maximum decreases in the carbonation depth of the 80 °C-cured specimen, compared to the treatment at 7 days and 20 days, though the two later treatments also reduced the carbonation depth.

Although the curing of the specimens was performed in a sealed state with plastic tape, the sealing with plastic tape or film does not strictly prevent the loss of moisture from the specimen. Thus, for the heat-cured specimens, after the 8-hour 80 °C curing, the water content should decrease greatly [39], benefiting the internal diffusion of the AN solution. It is reported that no matter whether sodium silicate or sodium hydroxide is used as an alkaline activator, the compressive strength reaches its ultimate strength at 7 days if heat-curing [41]. Accordingly, after 7 days, GP has considerable strength and denseness. Although the increase of denseness is favourable to carbonation resistance, it makes the internal diffusion of AN solution difficult. Therefore, the AN solution gained the best diffusion when the surface treatment was performed at 3 days, leading to the largest decrease of carbonation depth.

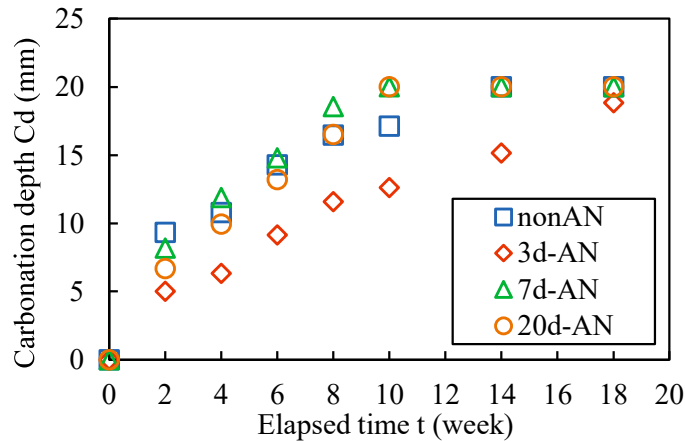
Dry shrinkage crack growth with age increased the internal diffusion of AN solution may be the reason for this experimental result. Additional experiments will be conducted to confirm this experimental phenomenon.

**Fig. 3.7** (b) presents the carbonation depths of the 70% FA/30% BFS blend-based ambient-cured GP mortars, which were cured in a sealed state and treated with the 25 wt% AN solution on the surfaces at different material ages. As shown in **Fig. 3.7** (b), for the 20 °C-cured specimen, the AN surface treatment at 3-day age also greatly reduced the carbonation depth, while the treatment at 7-day and 20-day ages had almost no reduction effect. The reasons for these results are not entirely clear to us, but are discussed below.

However, for the 20 °C-cured specimens, since they were cured in a sealed state with plastic tape for 28 days, we believe that they had high moisture during the curing. The reaction products undoubtedly increased with age, i.e. the denseness of the specimen increased with age [26,31,42]. The high water content and the increase in denseness added difficulties to the internal diffusion of the AN solution. Therefore, the AN surface treatment at the 7 or 20-day age for the 20 °C-cured specimens had almost no effect on the improvement of carbonation resistance. However, at the 3-day age, although the water content was high, the reaction products were few and the specimen is not yet dense,



(a) Heat-cured GP mortars



(b) Ambient-cured GP mortars

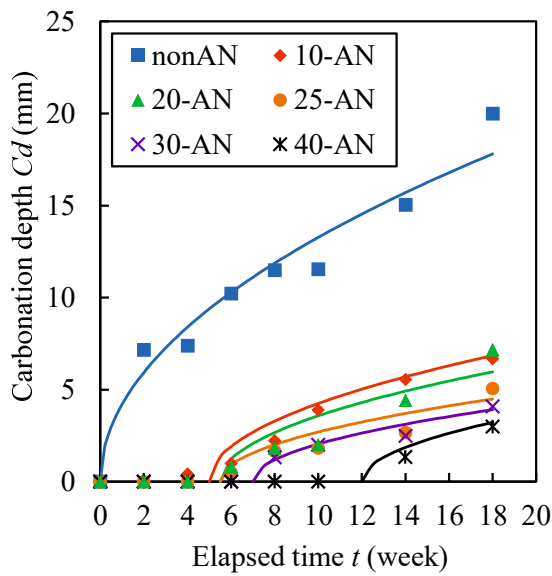
Fig. 3.7 Carbonation depth of GP mortars with AN treatment at different ages (Series No. 1, 9, 10, 11)

thus, the AN solution could have a certain degree of internal diffusion. Therefore, for the specimen sealed and cured at room temperature, a certain improvement effect was observed for the treatment at 3-day age.

We found that the AN surface treatment at the 20-day age was better than that at the 7-day age, even for the 20 °C-cured specimens. Dry shrinkage crack growth with age increased the internal diffusion of AN solution may be the reason for this experimental result. Additional experiments will be conducted to confirm this experimental phenomenon.

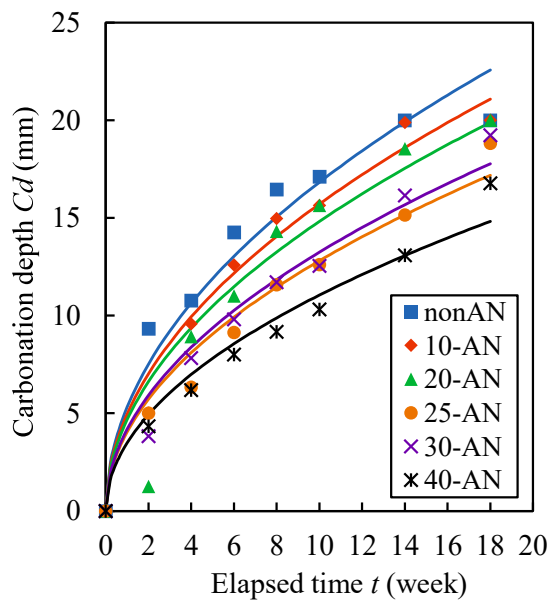
#### (2) Concentration of AN solution

**Fig. 3.8** demonstrates the experimental results of the 70% FA/30% BFS blend-based GP mortars, which were modified on surfaces by different AN solutions with 10-40 wt% concentrations. And **Fig. 3.9** shows the viscosity of each AN solution at 20 °C, which was measured with a B-type viscometer.



Conc. of AN	Regressive equation and R <sup>2</sup>	Decrease of a (%)	Increase of b (week)
Non-AN	$C_d = 4.19\sqrt{t}$ R <sup>2</sup> = 0.990	-	-
10%	$C_d = 1.40\sqrt{t-5}$ R <sup>2</sup> = 0.892	54.75	3.5
20%	$C_d = 1.88\sqrt{t-5.5}$ R <sup>2</sup> = 0.907	59.81	5.5
25%	$C_d = 1.27\sqrt{t-5.5}$ R <sup>2</sup> = 0.876	69.73	5.5
30%	$C_d = 1.17\sqrt{t-7}$ R <sup>2</sup> = 0.966	71.91	7
40%	$C_d = 1.31\sqrt{t-12}$ R <sup>2</sup> = 0.961	68.68	12

(a) Heat-cured GP mortars



Conc. of AN	Regressive equation and R <sup>2</sup>	Decrease of a (%)	Increase of b (week)
Non-AN	$C_d = 5.32\sqrt{t}$ R <sup>2</sup> = 0.992	-	-
10%	$C_d = 4.97\sqrt{t}$ R <sup>2</sup> = 0.994	6.62	0
20%	$C_d = 4.68\sqrt{t}$ R <sup>2</sup> = 0.976	11.91	0
25%	$C_d = 4.05\sqrt{t}$ R <sup>2</sup> = 0.993	23.88	0
30%	$C_d = 4.19\sqrt{t}$ R <sup>2</sup> = 0.992	21.27	0
40%	$C_d = 3.49\sqrt{t}$ R <sup>2</sup> = 0.992	33.32	0

(b) Ambient-cured GP mortars

Fig. 3.8 Carbonation depth of GP mortars with different concentrations of AN application (Series No. 1, 9, 12, 13, 14, 15)

The viscosity of AN solution increases with its concentration, but from 30% to 40%, the viscosity sharply increases. In general, solutions with low viscosity have high permeability into GP materials [43].

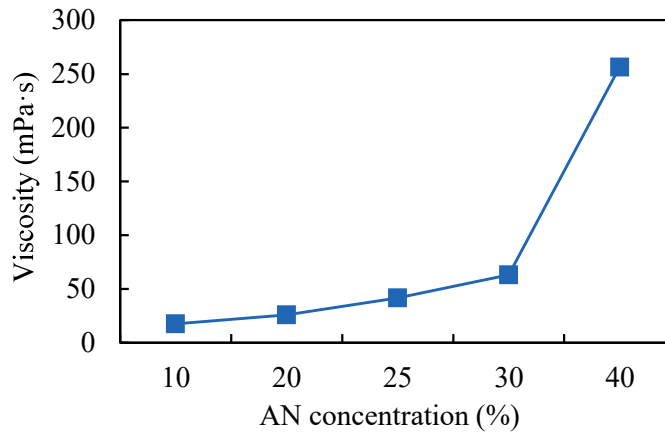


Fig. 3.9 Viscosities of AN solutions with different concentrations

From the experimental results of the 80 °C -cured specimens, we found that when the concentration of AN solution was below 25%, the decreasing rate of  $a$  value was low, but when the concentration exceeded 25%, the decreasing rates of  $a$  value were very close for 25-40% concentration, but the  $b$  value showed a tendency to increase with increasing the AN concentration. This result can be explained by the following analysis: AN solution makes the surface layer of GP mortar dense through the generation of N-A-S-H gels and the filling effect after drying, thus delaying the onset of carbonation of GP. Therefore, although a highly concentrated AN solution does not tend to permeate much into the inside and increase the internal denseness, it greatly increases the denseness of the surface layer, resulting in an increase in the  $b$ -value. In contrast, a low concentration of AN solution cannot greatly increase the denseness of the surface layer due to the small amount of effective ingredients, but it can increase the denseness of the inside due to its high diffusion ability, thus reducing the carbonation rate coefficient  $a$ . However, if the concentration of AN solution is too small and thus its effective ingredients are few, even if it can diffuse to the inside of GP, the decrease of the carbonation rate coefficient  $a$  is limited.

Therefore, the 40% AN solution is recommended as a surface modifier for GP, regardless of whether the GP is cured at room temperature or high temperature. The surface treatment of 40% AN solution would reduce the carbonation rate coefficient of heat-cured GP mortar by about 70%, i.e. double the carbonation resistance. It also reduces the carbonation rate coefficient of ambient-cured GP mortar by more than 30% simultaneously. In combination with the AN surface treatment and the increase of GP compactness by optimising the use of raw materials and their proportions, it becomes easy to make the GP concrete reach the carbonation resistance of PC concrete of the same strength.

**Fig. 3.8 (b)** demonstrates the experimental results of the 70% FA/30% BFS blend-based ambient-cured GP mortars, which were modified on surfaces by different AN solutions with 10-40 wt%

concentrations. As **Fig. 3.9** shows the viscosity of each AN solution at 20 °C, which was measured with a B-type viscometer. The viscosity of AN solution increases with its concentration, but from 30% to 40%, the viscosity sharply increases.

The improvement in carbonation resistance of the AN treatment was small for the ambient-cured specimens, i.e. the decreasing rate of  $a$  value is low. Based on the experimental results of the ambient-cured specimens, although the onset of carbonation of ambient-cured GP mortars occurred within the first week for all concentrations of AN, the rate of decrease in the  $a$  value was relatively low when the AN solution was below 20% concentration. However, when the concentration was between 25% and 30%, the decrease in the  $a$  value was over 20%. The greatest reduction in the carbonation rate was observed when using the undiluted 40% AN solution and reached over 30%. Overall, the improvement in carbonation resistance of GP mortars by the AN solution increased with the rising of concentration.

Same as concluded for heat-cured GP mortars, the observed results can be explained as follows: the AN solution enhances the density of the surface layer of the GP mortar through the formation of N-A-S-H gels and a filling effect after drying. Although the lower concentrations of AN solutions can penetrate into the interior of mortar, they can not effectively increase the surface layer density due to the limited presence of effective ingredients. Whereas the ambient-cured GP has a loose microstructure at an early age, such as 3 days, compared to the heat-cured GP[52]. Thus, it is thought that even highly concentrated AN solutions have the potential to penetrate the inside of GP due to the loose structure. In fact, as shown in **Fig. 3.8** (b), the greatest decrease in the  $a$ -value was observed when using the 40% AN solution.

Therefore, the 40% AN solution is recommended as a surface modifier for GP, regardless of whether the GP is cured at room temperature or high temperature. It also reduces the carbonation rate coefficient of ambient-cured GP mortar by more than 30% simultaneously. In combination with the AN surface treatment and the increase of GP compactness by optimising the use of raw materials and their proportions, it becomes easy to make the GP concrete reach the carbonation resistance of PC concrete of the same strength.

### *(3) Number of AN treatments and sealed curing after treatment*

It is clearly shown in **Fig. 3.10** (a) that for the 80 °C-cured GP mortars, increasing the number of AN treatments had almost no effect on the carbonation rate coefficient  $a$ , but the beginning of carbonation was delayed ( $b$  value increased), which indicates that the 2 treatments increased the denseness of the GP surface layer more than the one treatment.

For the 80 °C-cured specimens, the drying of specimens and the occurrence of drying shrinkage cracks make the penetration of AN solution easier, so a single treatment can largely reduce the  $a$  value, but the rapid internal penetration of AN solution with less surface stay requires twice treatment. Although the twice treatment delayed the onset of carbonation, they did not change the carbonation

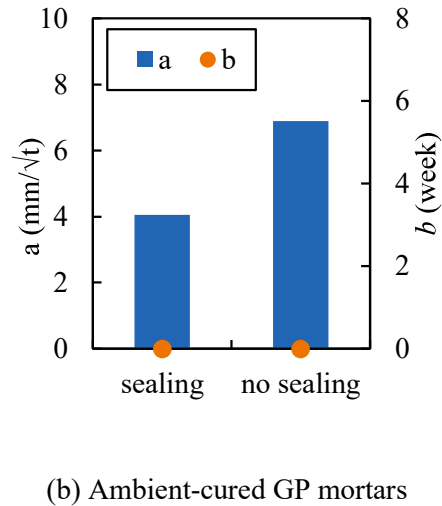
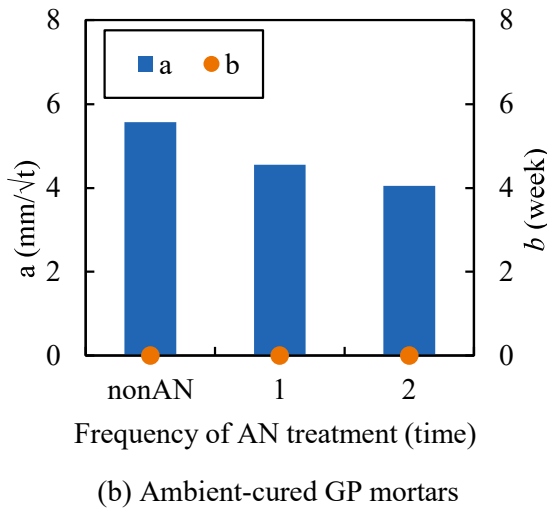
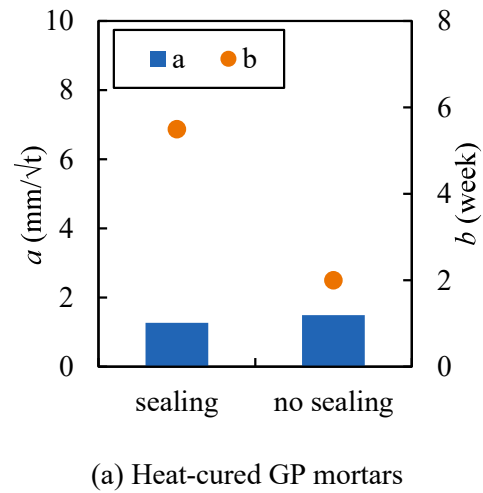
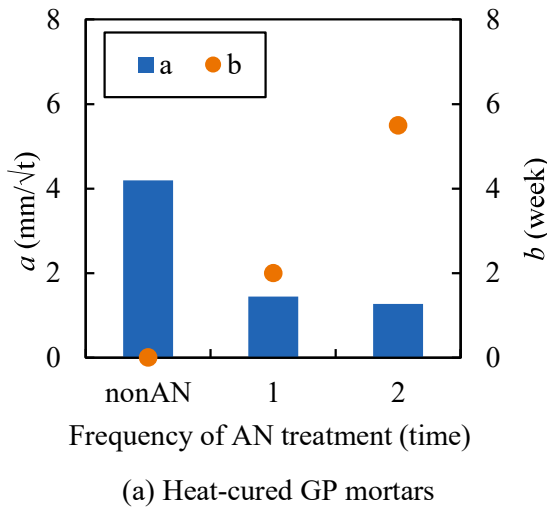


Fig. 3.10 The changes of  $a$ ,  $b$ -values of heat-cured GP mortars with frequency of AN treatment

Fig. 3.11 Influences of sealed curing on the  $a$ ,  $b$ -values for ambient-cured GP mortars

rate coefficient of the 80 °C-cured specimens. Therefore, from the perspective of long-term carbonation depth, once treatment is also an option for GPs cured at high temperatures.

**Fig. 3.10 (b)** clearly shows that for the ambient-cured GP mortars, as the number of AN surface treatments increased from one to two at 3 days of age, the carbonation rate coefficient  $a$  decreased. However, no delay in carbonation was observed, as indicated by a  $b$ -value of zero.

For the ambient-cured specimens, the high moisture content and limited crack formation hinder the penetration of the AN solution. Consequently, multiple treatments are necessary to enhance the density of the surface layer. Despite several treatments, achieving a dense surface layer remains challenging due to the moisture present during the treatment process. Although two treatments delayed the onset of carbonation, they did not alter the carbonation rate coefficient  $a$  for these specimens.

**Fig. 3.11** (a) demonstrates the influence of sealed curing after the AN surface treatment on the  $a$ ,  $b$  values. The sealing did not further contribute to much improvement in the carbonation resistance of the 80 °C-cured specimens, but the beginning of carbonation was delayed for two weeks. This means that the specimens without sealing were carbonated during the curing period. Therefore, from the perspective of long-term carbonation depth, unsealed curing after the AN treatment is an option for simplifying construction if GPs are cured at high temperatures.

**Fig. 3.11** (b) illustrates the impact of sealed curing after AN surface treatment on the  $a$  and  $b$  values. Sealing did not significantly enhance the carbonation resistance of the 20 °C-cured specimens, although it did lower the carbonation rate coefficient  $a$ . The onset of carbonation was not delayed. Therefore, for ambient-cured GP mortars, sealed curing is recommended, while unsealed curing may be a viable option for simplifying construction in high-temperature conditions.

### 3.3.3 Air permeability and strength of surface-modified GP mortars

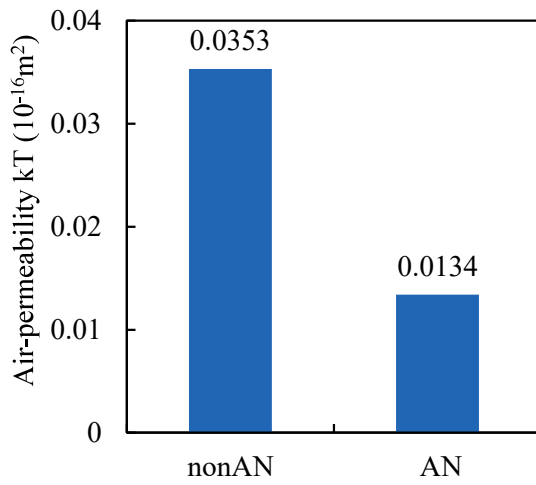
**Fig. 3.12** (a) illustrates the air permeability of the GP mortar specimens cured by the 80 °C-curing method. It shows that the AN surface treatment greatly reduced the air permeability of the GP mortar specimens, which suggests that the internal structure of GP can become dense if the GP surface is modified by the AN solution. As described later, the AN treatment at least decreased the cracks in the surface layer of GP mortar.

Due to dry shrinkage, the geopolymer experienced the 80 °C-curing has large cracks with sizes of 0.01 - 0.1  $\mu\text{m}$ . Large cracks result in higher air permeability. However, it is no doubt that heat-curing contributes to many formations of geopolymeric products and, thus a dense microstructure [27,28], which makes  $\text{CO}_2$  diffusion difficult into the geopolymeric matrix between large cracks.

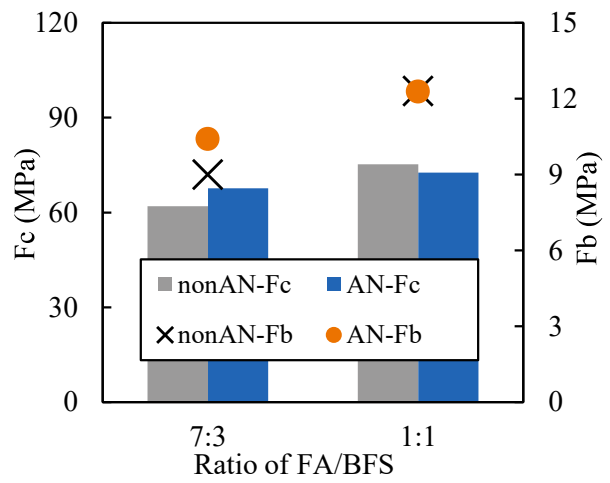
**Fig. 3.13** (a) shows the flexural and compressive strengths of series No.1 and No.3. We found that the AN surface treatment did not almost affect the strengths of BFS/FA blend-based GP mortar under heat-cured method. This is because the diffusion of the AN solution only reached the surface layer of the GP mortars.

**Fig. 3.12** (b) illustrates the air permeability of GP mortar specimens cured at 20 °C. Regardless of the curing method, the AN surface treatment significantly reduced the air permeability of the GP mortar specimens, indicating that modifying the surface with the AN solution can enhance the density of the internal structure. As discussed later, the AN treatment also contributed to a reduction in surface layer cracks in the GP mortar.

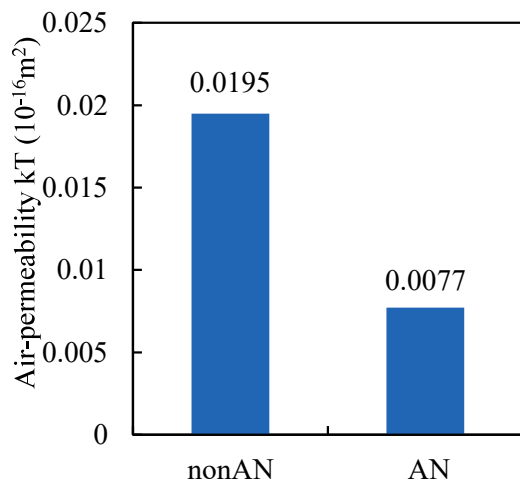
In contrast, the air permeability of 20 °C-cured specimens was lower than that of the 80 °C-cured specimens, aligning with findings from other studies[46,53]. The lower carbonation rate coefficient  $a$  for the 20 °C-cured specimens can be attributed to the presence of more capillary cracks, primarily under 0.01  $\mu\text{m}$ , compared to larger cracks found in heat-cured specimens[54]. These smaller cracks contribute to reduced air permeability, facilitating a denser microstructure in the ambient-cured GP mortar.



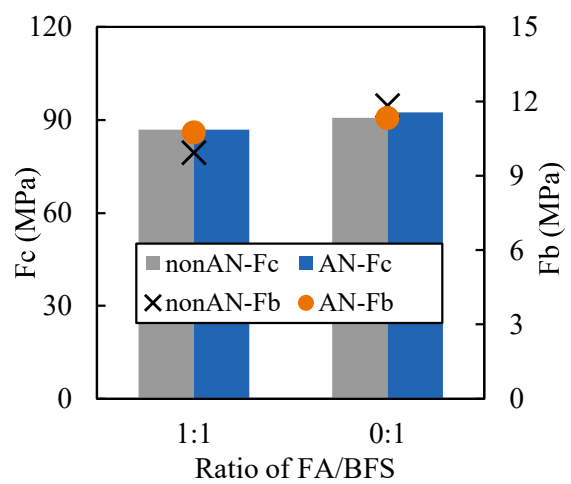
(a) Heat-cured GP mortars



(a) Heat-cured GP mortars



(b) Ambient-cured GP mortars



(b) Ambient-cured GP mortars

Fig. 3.12 Air-permeability of GP mortars with and without AN surface treatment

Fig. 3.13 Comparison of strengths of heat-cured GP mortars with and without AN surface treatment

**Fig. 3.13 (b)** displays the compressive and flexural strengths of ambient-cured GP mortars which FA/BFS were 1:1 and 0:1. The AN surface treatment had minimal impact on the strengths of the BFS/FA blend-based GP mortars at 20 °C, as the diffusion of the AN solution primarily affected only the surface layer.

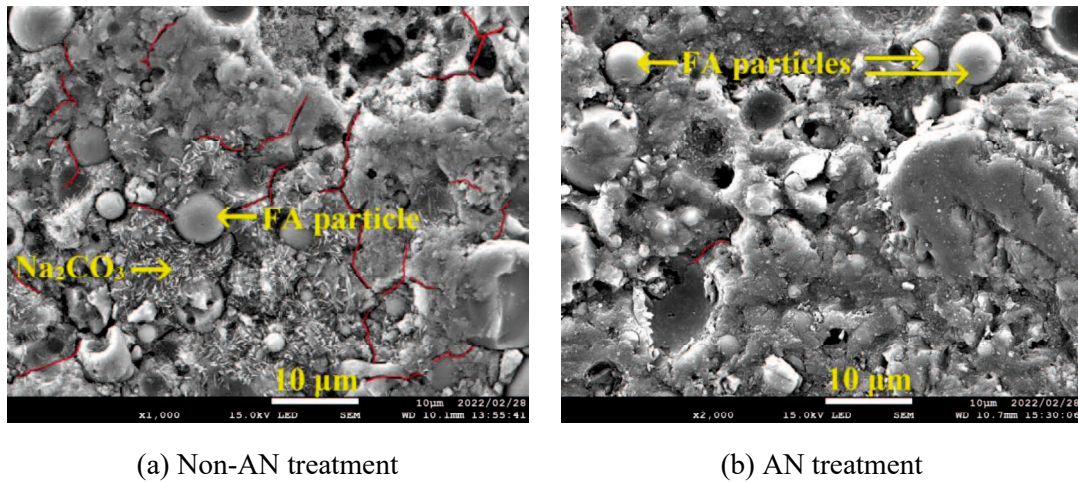


Fig. 3.14 SEM images of FA-based GP mortars.

Table 3.6 Comparison of average mole ratios of oxides of FA-based GP mortars with and without AN treatment

AN treatment	Na (%)	Mg (%)	Al (%)	Si (%)	Ca (%)	SiO <sub>2</sub> /Al <sub>2</sub> O <sub>3</sub>	SiO <sub>2</sub> /CaO
Non	6.23	0.60	5.19	14.15	1.76	5.45	8.04
Treated	3.67	0.44	6.35	12.40	1.22	3.90	10.16

### 3.4 Microstructure and Chemical Analysis of GP Mortars

#### 3.4.1 SEM-EDS analysis of surface-modified GP mortar

In the SEM analysis, in addition to the structural changes observed by SEM images, elemental analysis (EDS) was also performed to determine the changes in gel compositions. Since gel microstructure is significantly related to the SiO<sub>2</sub>/Al<sub>2</sub>O<sub>3</sub> ratio [44], we calculated the average mole ratio of SiO<sub>2</sub>/Al<sub>2</sub>O<sub>3</sub> for the whole analyzed area.

##### (1) FA-based GP mortar

**Fig. 3.14** (a) and (b) show the SEM results of FA-based GP mortar (series No. 2) with and without AN surface treatment after the accelerated carbonation test of 12 weeks. First, the AN surface-treated mortar was found to be denser than the mortar without the AN treatment, although the pores remained. In the former, almost no cracks are observed. The reduction in cracks may be due to the AN treatment, which reduced the drying shrinkage cracks caused by water evaporation. Although the AN-treated mortar became relatively dense, it still has a low resistance to carbonation because of the large number of tiny pores.

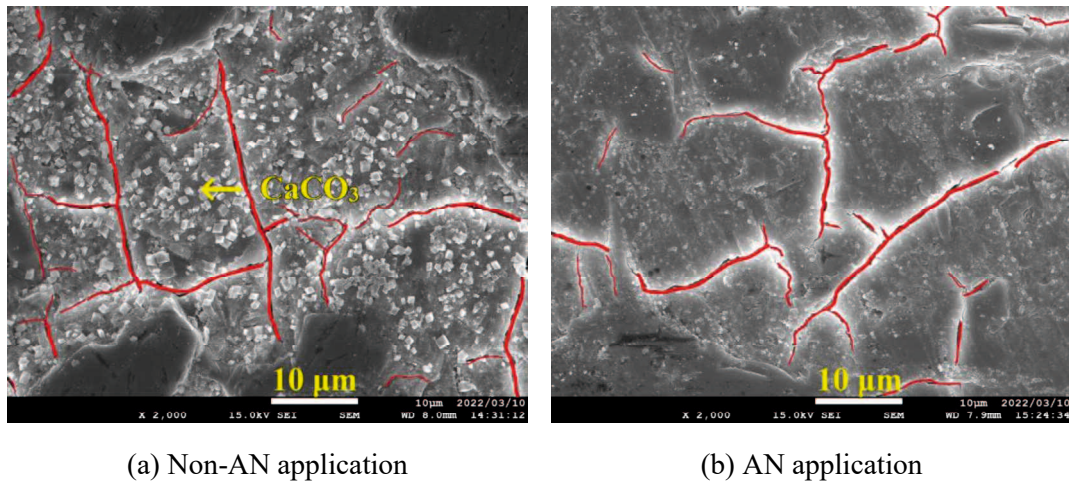


Fig. 3.15 SEM images of BFS-based GP mortars

Table 3.7 Comparison of average mole ratios of oxides of BFS-based GP mortars with and without AN treatment

AN treatment	Na (%)	Mg (%)	Al (%)	Si (%)	Ca (%)	SiO <sub>2</sub> /Al <sub>2</sub> O <sub>3</sub>	SiO <sub>2</sub> /CaO
Non-AN	6.49	1.53	2.78	7.87	8.57	5.66	0.91
AN	2.80	1.83	4.46	10.67	9.77	4.78	1.09

Fly ash particles with smooth surfaces can be found to remain in the two mortars. However, many fly ash particles in the AN-treated mortar were surrounded by dense gels or were corroded, which suggests that reaction products increased. During the accelerated carbonation test, the CO<sub>2</sub> reacted with the Na<sup>+</sup> remaining in the pores to form Na<sub>2</sub>CO<sub>3</sub> [45]. Since Na<sup>+</sup> is used to balance the Al<sup>3+</sup> charge of the Al(OH)<sub>4</sub> tetrahedra, an increase in N-A-S-H gels would reduce the residual Na<sup>+</sup> in the pores. Hence, we found there are many needle crystals in the FA-based GP mortar without the AN treatment, while needle crystals are rarely found in the mortar after AN surface treatment.

The microstructure of geopolymer is strongly influenced by the SiO<sub>2</sub>/Al<sub>2</sub>O<sub>3</sub> ratio, and geopolymer with a lower SiO<sub>2</sub>/Al<sub>2</sub>O<sub>3</sub> has a dense structure [46–50]. As shown in **Table 3.6**, the SiO<sub>2</sub>/Al<sub>2</sub>O<sub>3</sub> ratio of FA-based GP mortar decreased with the AN treatment. Thus, the AN-treated mortar has a denser microstructure than the mortar without the AN treatment, which also means higher carbonation resistance of GP materials.

#### (2) BFS-based GP mortar

**Fig. 3.15** shows the SEM images for the BFS-based GP mortars (series No. 4) without and with the AN treatment. The BFS-based GP mortars without the AN treatment had relatively dense microstructure. However, the AN treatment obviously reduced tiny cracks, resulting in a denser GP mortar. As stated above, the AN treatment decreases the cracks caused by dry shrinkage. In the GP

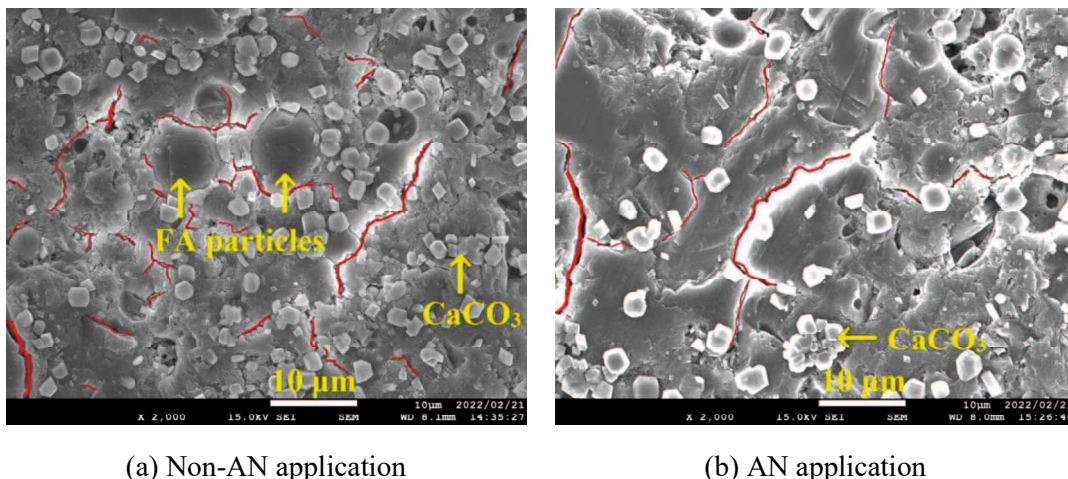


Fig. 3.16 SEM images of FA&BFS blend-based GP mortars

Table 3.8 Comparison of average mole ratios of oxides of FA&BFS blended-based GP mortars with and without AN treatment

AN application	Na (%)	Mg (%)	Al (%)	Si (%)	Ca (%)	SiO <sub>2</sub> /Al <sub>2</sub> O <sub>3</sub>	SiO <sub>2</sub> /CaO
Non-AN	2.30	0.84	3.92	13.16	4.68	6.71	2.81
AN	2.75	1.16	3.75	11.07	5.59	5.90	1.98

mortar without the AN treatment, many CaCO<sub>3</sub> crystals are found (see Fig. 3.15 (a)), while in the AN-treated mortar, CaCO<sub>3</sub> crystals are very few (see Fig. 3.15 (b)). The products of BFS-based GP are main C-A-S-H gels [55–57]. As the carbonation reaction proceeds, the C-A-S-H gel undergoes decalcification, and various calcium carbonate polymorphs are formed [58]. However, the AN treatment may strengthen the structure of the C-A-S-H gel due to the Al<sup>3+</sup> provided by the AN solution, making the C-A-S-H gel less susceptible to decalcification.

Duxson [47] reported that the denseness of geopolymer increases with the decrease in SiO<sub>2</sub>/Al<sub>2</sub>O<sub>3</sub> ratio. The abundant Al<sub>2</sub>O<sub>3</sub> provided by AN decreased the SiO<sub>2</sub>/Al<sub>2</sub>O<sub>3</sub> ratio, as shown in Table 3.7, contributing to the denser microstructure of AN-treated GP mortar and improved carbonation resistance, which was also reflected in the reduction of CaCO<sub>3</sub>. The above factors, including the reduction in cracks and strengthened C-A-S-H gel structure, collectively contributed to the carbonation resistance improvement of BFS-based GP mortars with AN treatment.

(3) FA&BFS-blended GP mortar

Fig. 3.16 shows the SEM images of FA&BFS-blended GP mortars (series No. 1) with and without AN surface treatment. Calcite is observed in the two mortars, but in the mortar with AN treatment, the calcite crystals are few, suggesting the reaction of CO<sub>2</sub> and Ca<sup>2+</sup> that originated from

decalcification of C-A-S-H gels was decreased because of AN treatment. Also, the mortar with the AN surface treatment had few fine cracks, compared to the mortar without the AN treatment. As explained before, AN treatment would reduce the cracks caused by dry shrinkage. Because the polycondensation of geopolymer is a dehydration reaction, consuming no water [59], large dry shrinkage may be resulted in a dense surface layer formed by AN surface treatment, reducing the escape of inside moisture, which contributed to the decrease of drying shrinkage cracks. Hence, the air permeability coefficient of AN-treated mortar was reduced, as shown in **Fig. 3.12**, and because of the decrease in drying shrinkage cracks, the carbonation was slowed down. Combining the decrease of the  $\text{SiO}_2/\text{Al}_2\text{O}_3$  ratio (see **Table 3.8**), we can conclude that the AN treatment increases the denseness of geopolymer and reduces the dry shrinkage and decalcification of geopolymer.

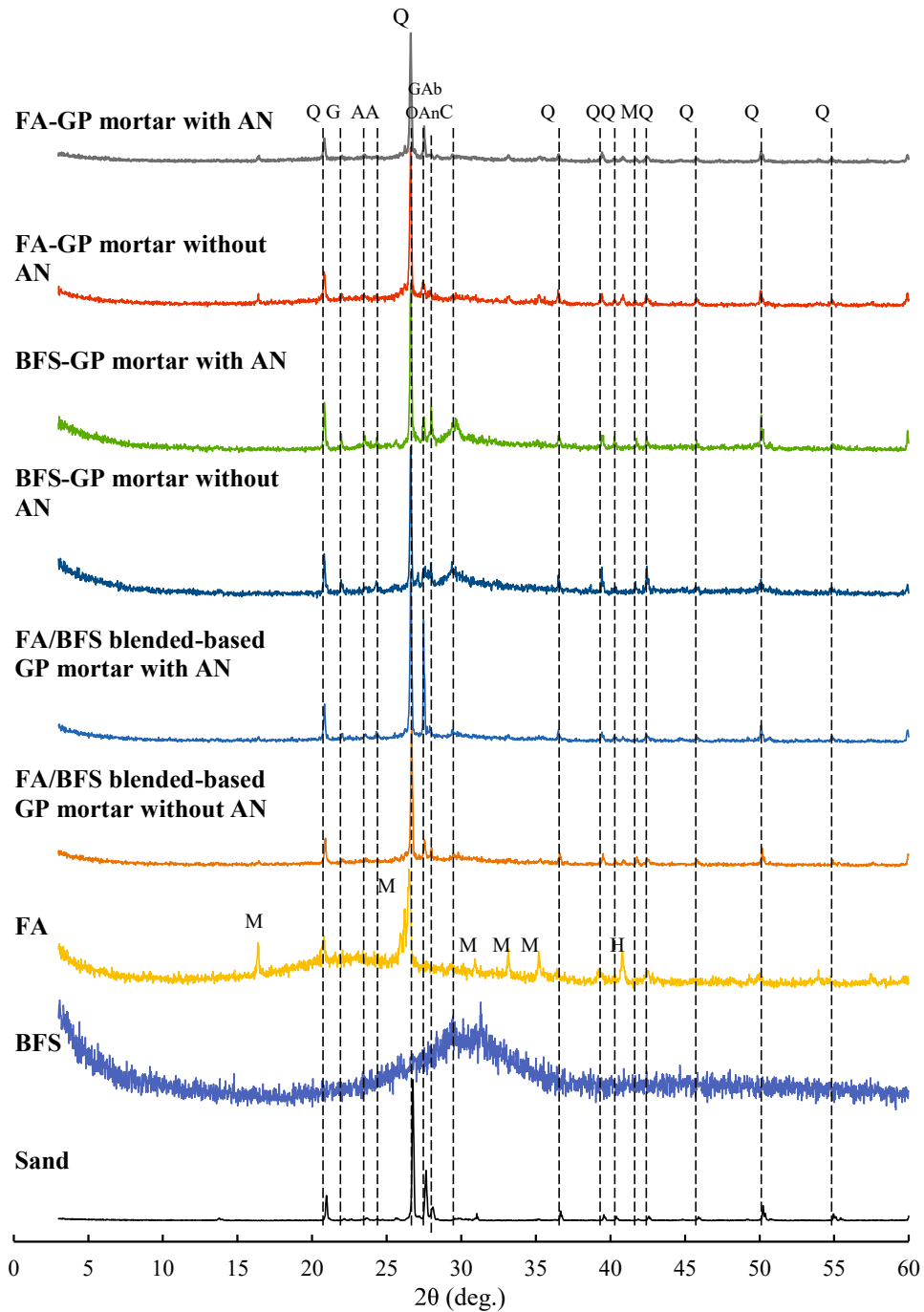
### ***3.4.2 XRD results of surface-modified GP mortar***

**Fig. 3.17** presents the X-ray diffraction (XRD) patterns of fly ash (FA)-based geopolymer (GP) mortars, comparing them with the XRD patterns of the raw materials, including FA and sea sand. In this study, all GP mortars were prepared using the same alkali activator solutions and fine aggregate, with FA serving as the sole precursor material. The XRD analysis reveals that raw FA primarily contains crystalline phases of quartz and mullite, while the sea sand used as aggregate—washed with tap water—contains quartz, mullite, and orthoclase.

Upon examining the FA-based GP mortars, it was observed that their crystal phases largely mirrored those of their raw materials, indicating that the AN (sodium aluminate) surface treatment did not generate any new crystalline products. However, a significant change in crystalline intensity was observed, particularly in the peak intensity of Na-gmelinite. This increase is likely attributed to the AN treatment, as the presence of sodium aluminate promotes the formation of Na-gmelinite, a phase also reported by Bae, et al.[51] to form in high-sodium environments within geopolymers.

Moreover,  $\text{Na}_2\text{CO}_3$  peaks were detected in the FA-based GP mortars treated with AN, which aligns with observations from SEM imaging, where  $\text{Na}_2\text{CO}_3$  deposits were visible. The increase in Na-gmelinite and the formation of  $\text{Na}_2\text{CO}_3$  due to the AN treatment likely play a critical role in modifying the microstructure of FA-based geopolymers. Specifically, these crystalline formations appear to reduce the pore size within the geopolymer matrix, thereby limiting the pathways for  $\text{CO}_2$  permeation. Consequently, this densification effect improves the carbonation resistance of the FA-based GP mortars by inhibiting  $\text{CO}_2$  diffusion, which is essential for enhancing the long-term durability of these materials in carbonation-prone environments.

The raw BFS primarily exhibited an amorphous structure with minimal crystalline phases, while the raw FA contained quartz and mullite. Sea sand, which was washed with tap water, showed crystalline phases of quartz, mullite, gismondine[60], and Na-gmelinite.



[Notes] Q: Quartz, M: Mullite, A: Albite, C: Calcite, G: Gypsum, Ab: Albite, An: Anorthite, S: Sodium carbonate, O: Orthoclase

Fig. 3.17 XRD pattern of FA/BFS-blended GP mortars

In the BFS-based GP mortars, the AN (sodium aluminate) treatment was found to increase the intensity of the gismondine peaks, suggesting that the treatment facilitated the formation of additional gismondine due to the higher availability of calcium (Ca) and aluminum (Al) in the BFS matrix. This finding aligns with prior studies indicating that Ca and Al-rich environments promote gismondine

crystallization. Additionally, notable calcite peaks were detected in the BFS-based specimens, consistent with observations from SEM analysis, which indicated the presence of calcite within the matrix.

For the FA/BFS blend-based GP mortars, the primary change observed with the AN treatment was a significant increase in the peak intensity of Na-gmelinite. Although Na-gmelinite is naturally present in the sea sand used as aggregate[61], the AN treatment, with its high NaAlO<sub>2</sub> content, likely contributed to the increased formation of Na-gmelinite within the GP matrix, as also reported by Bae, et al.[51] .

The enhanced formation of gismondine in BFS-based mortars and the intensified Na-gmelinite peaks in the FA/BFS blend-based mortars collectively indicate that the AN treatment aids in refining the microstructure of these GP materials. These crystalline modifications help reduce pore sizes within the geopolymer matrix, thereby lowering permeability and inhibiting CO<sub>2</sub> ingress, which is essential for improving carbonation resistance and enhancing the durability of BFS-based and FA/BFS blend-based GP mortars in carbonation-prone environments.

### 3.5 Conclusions

This study addressed the low carbonation resistance of geopolymer (GP) mortars, a critical challenge that cannot be effectively resolved through mixture design alone. By utilizing sodium aluminate (AN) aqueous solution as an inorganic surface modifier, the research demonstrated significant improvements in carbonation resistance for both heat-cured and ambient-cured GP mortars. The findings are summarized as follows:

(1) The AN surface modification substantially enhanced carbonation resistance in both heat-cured and ambient-cured GP mortars. For heat-cured specimens, the carbonation rate coefficient was reduced by approximately 70%, with undetectable carbonation depths over an 18-week accelerated test period in some cases. In contrast, for ambient-cured mortars, the carbonation rate coefficient decreased by over 30%, though the onset of carbonation was not delayed.

(2) The FA/BFS blend-based geopolymers exhibited the greatest improvement in carbonation resistance following AN treatment. Heat-cured specimens performed significantly better than ambient-cured ones, particularly when FA content was higher. Geopolymers using only BFS or FA as precursors showed comparatively lower improvements.

(3) In both curing conditions, the AN treatment improved the density of the surface layer by reducing surface cracks and promoting the formation of Na-gmelinite and gismondine. These phases reduced CO<sub>2</sub> permeability and mitigated shrinkage-induced cracking. However, the effects of AN treatment were limited to the surface layer and did not significantly impact mechanical strength in either heat-cured or ambient-cured mortars.

(4) For heat-cured GP mortars, a single application of a 40% AN solution was sufficient to achieve significant improvement in carbonation resistance. Sealed curing after treatment was unnecessary, simplifying the treatment process.

(5) For ambient-cured GP mortars, optimal AN treatment involved applying the 40% AN solution twice, starting at an early age of 3 days. Sealed curing after treatment was recommended to enhance carbonation resistance further, given the relatively lower performance of ambient-cured specimens compared to heat-cured ones.

(6) Heat-cured GP mortars benefited more from AN surface modification than ambient-cured ones due to their denser initial microstructure. However, the study demonstrated that AN treatment is a viable method for improving carbonation resistance across both curing methods, with particular effectiveness in FA/BFS blend-based geopolymers.

## References

- [1] L.K. Turner, F.G. Collins, Carbon dioxide equivalent (CO<sub>2</sub>-e) emissions: A comparison between geopolymer and OPC cement concrete, *Constr. Build. Mater.* 43 (2013) 125–130.
- [2] D.N. Huntzinger, T.D. Eatmon, A life-cycle assessment of Portland cement manufacturing: comparing the traditional process with alternative technologies, *J. Clean. Prod.* 17 (2009) 668–675.
- [3] P. Duxson, A. Fernández-Jiménez, J.L. Provis, G.C. Lukey, A. Palomo, J.S.J. van Deventer, Geopolymer technology: the current state of the art, *J. Mater. Sci.* 42 (2007) 2917–2933.
- [4] J. Davidovits, Geopolymers: inorganic polymeric new materials, *J. Therm. Anal. Calorim.* 37 (1991) 1633–1656.
- [5] C. Li, H. Sun, L. Li, A review: the comparison between alkali-activated slag (Si+ Ca) and metakaolin (Si+ Al) cements, *Cem. Concr. Res.* 40 (2010) 1341–1349.
- [6] K.A. Komnitsas, Potential of geopolymer technology towards green buildings and sustainable cities, *Procedia Eng.* 21 (2011) 1023–1032.
- [7] Z. Li, R. Kondoa, K. Ikeda, Development of Foamed Geopolymer with Addition of Municipal Solid Waste Incineration Fly Ash, *J. Adv. Concr. Technol.* 19 (2021) 830–846.
- [8] H. Zhang, L. Li, C. Yuan, Q. Wang, P.K. Sarker, X. Shi, Deterioration of ambient-cured and heat-cured fly ash geopolymer concrete by high temperature exposure and prediction of its residual compressive strength, *Constr. Build. Mater.* 262 (2020) 120924.
- [9] G. Kürklü, The effect of high temperature on the design of blast furnace slag and coarse fly ash-based geopolymer mortar, *Compos. Part B Eng.* 92 (2016) 9–18.
- [10] G.A. Khoury, Compressive strength of concrete at high temperatures: a reassessment, *Mag. Concr. Res.* 44 (1992) 291–309.
- [11] X. Fu, Q. Li, J. Zhai, G. Sheng, F. Li, The physical–chemical characterization of mechanically-treated CFBC fly ash, *Cem. Concr. Compos.* 30 (2008) 220–226.
- [12] B. Zhang, K.J.D. MacKenzie, I.W.M. Brown, Crystalline phase formation in metakaolinite geopolymers activated with NaOH and sodium silicate, *J. Mater. Sci.* 44 (2009) 4668–4676.
- [13] H. Xu, J.S.J. Van Deventer, Geopolymerisation of multiple minerals, *Miner. Eng.* 15 (2002) 1131–1139.
- [14] R. Pouhet, M. Cyr, Carbonation in the pore solution of metakaolin-based geopolymer, *Cem. Concr. Res.* 88 (2016) 227–235.
- [15] S. Li, Z. Li, T. Nagai, T. Okata, Neutralization resistance of fly ash and blast furnace slag based geopolymer concrete, *Proc. Jpn. Concr. Inst.* 39 (2017) 2023–2028.
- [16] Z. Li, S. Li, Effects of wetting and drying on alkalinity and strength of fly ash/slag-activated materials, *Constr. Build. Mater.* 254 (2020) 119–069.

- [17] S.A. Bernal, R. San Nicolas, R.J. Myers, R.M. de Gutiérrez, F. Puertas, J.S.J. van Deventer, J.L. Provis, MgO content of slag controls phase evolution and structural changes induced by accelerated carbonation in alkali-activated binders, *Cem. Concr. Res.* 57 (2014) 33–43.
- [18] M. Zhang, H. Xu, A.L. Phalé Zeze, X. Liu, M. Tao, Coating performance, durability and anti-corrosion mechanism of organic modified geopolymer composite for marine concrete protection, *Cem. Concr. Compos.* 129 (2022) 104495.
- [19] W. Yu, Z. Wenhua, W. Peipei, P. Yilin, Z. Yunsheng, Study on preparation and strengthening mechanism of new surface treatment agent of concrete at multi-scale, *Constr. Build. Mater.* 346 (2022) 128404.
- [20] L. Jiang, X. Xue, W. Zhang, J. Yang, H. Zhang, Y. Li, R. Zhang, Z. Zhang, L. Xu, J. Qu, J. Song, J. Qin, The investigation of factors affecting the water impermeability of inorganic sodium silicate-based concrete sealers, *Constr. Build. Mater.* 93 (2015) 729–736.
- [21] Z. Li, S. Li, Carbonation resistance of fly ash and blast furnace slag based geopolymer concrete, *Constr. Build. Mater.* 163 (2018) 668–680.
- [22] P. Nath, P.K. Sarker, V.B. Rangan, Early Age Properties of Low-calcium Fly Ash Geopolymer Concrete Suitable for Ambient Curing, *Procedia Eng.* 125 (2015) 601–607.
- [23] R. Xiao, Y. Ma, X. Jiang, M. Zhang, Y. Zhang, Y. Wang, B. Huang, Q. He, Strength, microstructure, efflorescence behavior and environmental impacts of waste glass geopolymers cured at ambient temperature, *J. Clean. Prod.* 252 (2020) 119610.
- [24] T. Xie, T. Ozbakkaloglu, Behavior of low-calcium fly and bottom ash-based geopolymer concrete cured at ambient temperature, *Ceram. Int.* 41 (2015) 5945–5958.
- [25] S. Kitasato, Z. Li, Experimental study on the properties of geopolymer concrete using fly ash and ground granulated blast furnace slag, part 14: effects of coating agent, *Summ. Tech. Pap. Annu. Meet. AIJ.* (2017) 751–752.
- [26] M.T. Marvila, A.R.G. Azevedo, G.C.G. Delaqua, B.C. Mendes, L.G. Pedroti, C.M.F. Vieira, Performance of geopolymer tiles in high temperature and saturation conditions, *Constr. Build. Mater.* 286 (2021) 122994.
- [27] S. Muthukrishnan, S. Ramakrishnan, J. Sanjayan, Effect of microwave heating on interlayer bonding and buildability of geopolymer 3D concrete printing, *Constr. Build. Mater.* 265 (2020) 120786.
- [28] M. Lahoti, S.F. Wijaya, K.H. Tan, E.-H. Yang, Tailoring sodium-based fly ash geopolymers with variegated thermal performance, *Cem. Concr. Compos.* 107 (2020) 103507.
- [29] J. Ye, W. Zhang, D. Shi, Effect of elevated temperature on the properties of geopolymer synthesized from calcined ore-dressing tailing of bauxite and ground-granulated blast furnace slag, *Constr. Build. Mater.* 69 (2014) 41–48.

- [30] J. Shi, B. Liu, S. Chu, Y. Zhang, Z. Di Zhang, K.D. Han, Recycling air-cooled blast furnace slag in fiber reinforced alkali-activated mortar, *Powder Technol.* 407 (2022) 117686.
- [31] C. Gunasekara, D.W. Law, S. Setunge, Long term permeation properties of different fly ash geopolymer concretes, *Constr. Build. Mater.* 124 (2016) 352–362.
- [32] K. Pasupathy, M. Berndt, A. Castel, J. Sanjayan, R. Pathmanathan, Carbonation of a blended slag-fly ash geopolymer concrete in field conditions after 8 years, *Constr. Build. Mater.* 125 (2016) 661–669.
- [33] S.A. Bernal, R. Mejía de Gutiérrez, J.L. Provis, Engineering and durability properties of concretes based on alkali-activated granulated blast furnace slag/metakaolin blends, *Constr. Build. Mater.* 33 (2012) 99–108.
- [34] Y. Luna Galiano, C. Fernández Pereira, M. Izquierdo, Contributions to the study of porosity in fly ash-based geopolymers. Relationship between degree of reaction, porosity and compressive strength, *Mater. Construcción.* 66 (2016).
- [35] J.L. Provis, R.J. Myers, C.E. White, V. Rose, J.S.J. Van Deventer, X-ray microtomography shows pore structure and tortuosity in alkali-activated binders, *Cem. Concr. Res.* 42 (2012) 855–864.
- [36] H. Cheng, K.-L. Lin, R. Cui, C.-L. Hwang, Y.-M. Chang, T.-W. Cheng, The effects of SiO<sub>2</sub>/Na<sub>2</sub>O molar ratio on the characteristics of alkali-activated waste catalyst–metakaolin based geopolymers, *Constr. Build. Mater.* 95 (2015) 710–720.
- [37] K. Ghosh, P. Ghosh, Effect of % Na<sub>2</sub>O and % SiO<sub>2</sub> on apparent porosity and sorptivity of fly ash based geopolymer, *IOSR J. Eng.* 2 (2012) 96–101.
- [38] R. Pouhet, M. Cyr, R. Bucher, Influence of the initial water content in flash calcined metakaolin-based geopolymer, *Constr. Build. Mater.* 201 (2019) 421–429.
- [39] C.E. White, J.L. Provis, T. Proffen, J.S.J. Van Deventer, The effects of temperature on the local structure of metakaolin-based geopolymer binder: A neutron pair distribution function investigation, *J. Am. Ceram. Soc.* 93 (2010) 3486–3492.
- [40] L. Tian, D. He, J. Zhao, H. Wang, Durability of geopolymers and geopolymer concretes: A review, *Rev. Adv. Mater. Sci.* 60 (2021) 1–14.
- [41] Z. Zhang, H. Wang, J.L. Provis, A. Reid, Efflorescence: a critical challenge for geopolymer applications?, in: *Concr. Inst. Aust. Bienn. Natl. Conf. 2013*, Concrete Institute of Australia, 2013: pp. 1–10.
- [42] O.A. Abdulkareem, M. Ramli, J.C. Matthews, Production of geopolymer mortar system containing high calcium biomass wood ash as a partial substitution to fly ash: An early age evaluation, *Compos. Part B Eng.* 174 (2019) 106941.

- [43] Y. Wang, J. Zhao, J. Chen, Effect of polydimethylsiloxane viscosity on silica fume-based geopolymer hybrid coating for flame-retarding plywood, *Constr. Build. Mater.* 239 (2020) 117814.
- [44] P. De Silva, K. Sagoe-Crenstil, V. Sirivivatnanon, Kinetics of geopolymerization: Role of Al<sub>2</sub>O<sub>3</sub> and SiO<sub>2</sub>, *Cem. Concr. Res.* 37 (2007) 512–518.
- [45] N. Sedira, J. Castro-Gomes, Microstructure Features of Ternary Alkali-activated Binder Based on Tungsten Mining Waste, Slag and Metakaolin, *KnE Eng.* 5 (2020).
- [46] Z. Kubba, G. Fahim Huseien, A.R.M. Sam, K.W. Shah, M.A. Asaad, M. Ismail, M.M. Tahir, J. Mirza, Impact of curing temperatures and alkaline activators on compressive strength and porosity of ternary blended geopolymer mortars, *Case Stud. Constr. Mater.* 9 (2018) e00205.
- [47] P. Duxson, J.L. Provis, G.C. Lukey, S.W. Mallicoat, W.M. Kriven, J.S.J. Van Deventer, Understanding the relationship between geopolymer composition, microstructure and mechanical properties, *Colloids Surfaces A Physicochem. Eng. Asp.* 269 (2005) 47–58.
- [48] M. Steveson, K. Sagoe-Crensil, Relationships between composition, structure and strength of inorganic polymers, *J. Mater. Sci.* 40 (2005) 2023–2036.
- [49] M. Rowles, B. O’connor, Chemical optimisation of the compressive strength of aluminosilicate geopolymers synthesised by sodium silicate activation of metakaolinite, *J. Mater. Chem.* 13 (2003) 1161–1165.
- [50] R.A. Fletcher, K.J.D. MacKenzie, C.L. Nicholson, S. Shimada, The composition range of aluminosilicate geopolymers, *J. Eur. Ceram. Soc.* 25 (2005) 1471–1477.
- [51] S.J. Bae, S. Park, H.K. Lee, Role of Al in the crystal growth of alkali-activated fly ash and slag under a hydrothermal condition, *Constr. Build. Mater.* 239 (2020) 117842.
- [52] T. Suwan, M. Fan, Influence of OPC replacement and manufacturing procedures on the properties of self-cured geopolymer, *Constr. Build. Mater.* 73 (2014) 551–561.
- [53] F.G.M. Aredes, T.M.B. Campos, J.P.B. Machado, K.K. Sakane, G.P. Thim, D.D. Brunelli, Effect of cure temperature on the formation of metakaolinite-based geopolymer, *Ceram. Int.* 41 (2015) 7302–7311.
- [54] P. Rovnanik, Effect of curing temperature on the development of hard structure of metakaolin-based geopolymer, *Constr. Build. Mater.* 24 (2010) 1176–1183.
- [55] Z. Li, R. Kondo, K. Ikeda, Recycling of waste Incineration bottom ash and heavy metal immobilization by geopolymer production, *J. Adv. Concr. Technol.* 19 (2021) 259–279.
- [56] A. D’Elia, D. Pinto, G. Eramo, R. Laviano, A. Palomo, A. Fernández-Jiménez, Effect of Alkali Concentration on the Activation of Carbonate-High Illite Clay, *Appl. Sci.* 10 (2020).
- [57] S. Zhao, M. Xia, L. Yu, X. Huang, B. Jiao, D. Li, Optimization for the preparation of composite geopolymer using response surface methodology and its application in lead-zinc tailings solidification, *Constr. Build. Mater.* 266 (2021) 120969.

- [58] A.E. Morandau, C.E. White, In situ X-ray pair distribution function analysis of accelerated carbonation of a synthetic calcium–silicate–hydrate gel, *J. Mater. Chem. A*. 3 (2015) 8597–8605.
- [59] H. Xu, J.S.J. Van Deventer, The geopolymerisation of alumino-silicate minerals, *Int. J. Miner. Process.* 59 (2000) 247–266.
- [60] J.E. Oh, J. Moon, S.-G. Oh, S.M. Clark, P.J.M. Monteiro, Microstructural and compositional change of NaOH-activated high calcium fly ash by incorporating Na-aluminate and co-existence of geopolymeric gel and C–S–H(I), *Cem. Concr. Res.* 42 (2012) 673–685.
- [61] W.S. Wise, The Na-rich zeolites from Boron, California, in: A. Gamba, C. Colella, S.B.T.-S. in S.S. and C. Coluccia (Eds.), *Oxide Based Mater.*, Elsevier, 2005: pp. 13–18.



## **Chapter 4 Geopolymer Materials Using Clinker Ash as Active Filler or Fine Aggregate**

### **4.1 Introduction**

### **4.2 Experimental Program**

### **4.3 Test Results and Discussion**

### **4.4 Microstructure and Chemical Analysis of GP Mortar with CA**

### **4.5 Conclusions**



# Chapter 4

## Geopolymer Materials Using Clinker Ash as Active Filler or Fine Aggregate

### 4.1 Introduction

After hundreds of years of development, the production of concrete has exceeded 10 billion tons globally every year[1] and this number is still rising. As the principal component material in concrete, the aggregate makes 70% of its volume[2,3]. However, because of the rapid growth of construction industry worldwide, natural resources such as river sand are being depleted at an alarming rate[4]. The prohibition on mining natural aggregates in certain areas and growing emphasis on environmental conservation are both exacerbating the scarcity of river sand. Consequently, the pursuit of sustainable alternative materials has become a pressing priority to curb the consumption of natural aggregates.

Meanwhile, numerous industrial wastes and by-products, including FA, BFS and CA are continuously being discharged, posing challenges to environmental issues. Among these, FA is commonly used as a precursor for GP, which has advantages on early strength development, chemical corrosion resistance, and fire resistance[5–11]. Because of these, GP is widely seen as having the potential to become the next generation of construction materials. The blast furnace slag, by-product of iron smelting, is usually added in FA-based geopolymer to raise its strength and makes room temperature curing possible[12]. Thus, recently FA and BFS are usually used in combination as precursors of GP.

Coal combustion in thermal power plants produces significant quantities of solid waste byproducts annually, including bottom ash constituting around 20% and fly ash making up approximately 80%[13]. Clinker ash is formed when bottom ash melts due to the high temperatures in the furnace and then solidifies into a glassy, granular material upon cooling. The CA consists of porous, irregularly shaped sand-like particles formed during the high-temperature combustion of coal around 1500 °C, followed by rapid cooling of the residual ash in water tanks beneath the boiler. As a byproduct of power generation, CA is primarily disposed of in landfills, where it is not effectively utilized and furthermore occupies valuable land resources. Due to the continuous urbanization, the management of municipal solid waste has become increasingly complicated in many countries due to the limited availability of landfill sites.

Steel reinforcement is commonly used in concrete structures to provide structural strength and durability. Concrete usually faces carbonation in natural environment, which reduces the alkaline environment and brings the risk of corrosion for steel bars in reinforced concrete. Hence, high carbonation resistance is important to ensure the durability of reinforced concrete structures. However, geopolymer materials generally exhibit lower carbonation resistance compared to the ordinary Portland cement concrete[14–17]. First, the residual sodium or potassium in GP pores are easier to react with  $\text{CO}_2$  than the  $\text{Ca}(\text{OH})_2$  in PC concrete. Moreover, the pores and cracks caused by water escape and drying shrinkage during the process of polymerisation have also become the internal channel of  $\text{CO}_2$ . Therefore, it is crucial to develop strategies for reducing the rate of carbonation[18,19]. Although heat curing can improve the carbonation resistance of FA-based GP concrete[14], it is still insufficient to reach the carbonation resistance level of ordinary concrete. LI, et al.[20] used sodium aluminate solution for surface treatment of heat curing GP materials with different mix proportions, achieving carbonation resistance that met and exceeded the level of ordinary concrete. However, the carbonation resistance of GP cured at room temperature still do not meet the expected performance.

Moreover, the porosity has a significant relationship with the durability and carbonation resistance of concrete. The carbonation depth and carbonation rate increased with growth of porosity of concrete[21]. As internal pore-rich materials, the utilization of CA for a partial or total replacement of sand as fine aggregate in mortar increased permeability coefficients and porosity[22–30]. An increase of 44% in carbonation depth of GP concrete, which half of the fine aggregates was substituted with CA, has been observed after 8 weeks' accelerated carbonation[31]. Rafat et al. found that the carbonation is not severe when the replacement of CA for sand is lower than 20%. However, once the replacing rate reaches 30 %, the depth of carbonation increases to a maximum of 55 % to that of which without CA for the same exposure period[32,33]. In summary, the utilization of CA will increase the risk of concrete carbonation.

The addition of slaked lime or cement to geopolymers can improve carbonation resistance, but it also substantially accelerates the setting time[34,35]. Some geopolymer formulations using volcanic pozzolans or blast furnace slag have exhibited good carbonation resistance[36], but this depends on factors like the reactivity and fineness of the pozzolan used[37]. Geopolymer concretes activated solely with sodium hydroxide or potassium hydroxide solutions have shown superior carbonation resistance compared to those using a blend of these hydroxides with sodium silicate[34]. However, the carbonation resistance achieved with just hydroxide activators still remains inadequate for many applications. Consequently, further research is needed to examine and improve the carbonation resistance of the industrial waste by-products incorporated GP materials.

This chapter explores the recycling of CA in concrete and mortar through geopolymer (GP) technology. We investigated the effects of replacing part of FA and sea sand with CA on the strength and carbonation resistance of FA&BFS-blended GP mortar and addressed the issue of low carbonation

resistance of GP mortar with fine aggregate replacements under ambient curing conditions using AN. We also examined the changes in the CA particles immersed in AS to elucidate the compatibility of CA with GP materials. The results indicated that CA particles reacted with AS, densifying and refining the interfacial transition zone (ITZ) between the GP matrix and CA particles. Although replacing FA with CA reduced the strength of GP concrete, substituting sand with up to 20% CA had minimal impact on the compressive and flexural strength of GP mortar. For GP materials using FA&BFS as a precursor, surface modification with AN greatly improved the carbonation resistance of GP materials with different AS and CA content after surface drying preparation. XRD analysis identified the components in CA, as well as the reaction products between the waste and AS. These results confirm the potential of CA as fine aggregates in geopolymer technology.

## 4.2 Experimental Program

### 4.2.1 Raw materials

The fly ash of JIS grade II, BFS of JIS 4000 class and crushed stone powder were used as active fillers of GP mortars, which properties are shown in **Table 4.1**, respectively. The metal oxide contents and density of sodium aluminate solution with a concentration of 40 wt.% are presented in **Table 4.1** as well. Sea sand, washed in advance with tap water, was used as fine aggregate of the GP mortars. CA were utilized as the replacement of partial fine aggregate for GP mortars, which physical properties are also shown in **Table 4.1**.

**Table 4.2** shows the results of X-ray fluorescence (XRF) analysis of the chemical compositions of the AFs and the substitutive aggregates. The CaO content in CA is comparatively less, similar to that of FA. The components of CA are mainly crystalline, which results in low activity in the alkaline solution.

**Fig. 4.1** shows the particle size distributions (PSD) of sea sand and CA. From this figure, we can see that the PSD of CA is close to that of sea sand the PSD curve mostly falls into the range of the standard PSD curve of fine aggregate (dotted line), which demonstrates the potential of CA as fine aggregate.

5 kinds of AS, named as AS01, AS21, AS31, AS41 and AS10, were used, which were 10 mole/L NH or a mixture with WG. The blending ratios were shown in **Table 4.3**. The WG was prepared by diluting JIS No.1 grade sodium silicate ( $\text{Na}_2\text{SiO}_3$ ) with distilled water by a volume ratio of 1:1.

### 4.2.2 Mix proportions of GP materials

The mix proportions of GP mortars used in this study are shown in **Table 4.4**. GP mortars were designed by adjusting the type of AS and the BFS blending ratio in AF. For all the mortar mixtures, the AS/AF ratio was 0.5, and the ratio of fine aggregates (S) to AF was 2.0 by mass.

In this study, GP concretes with different mix proportions were also investigated to confirm the

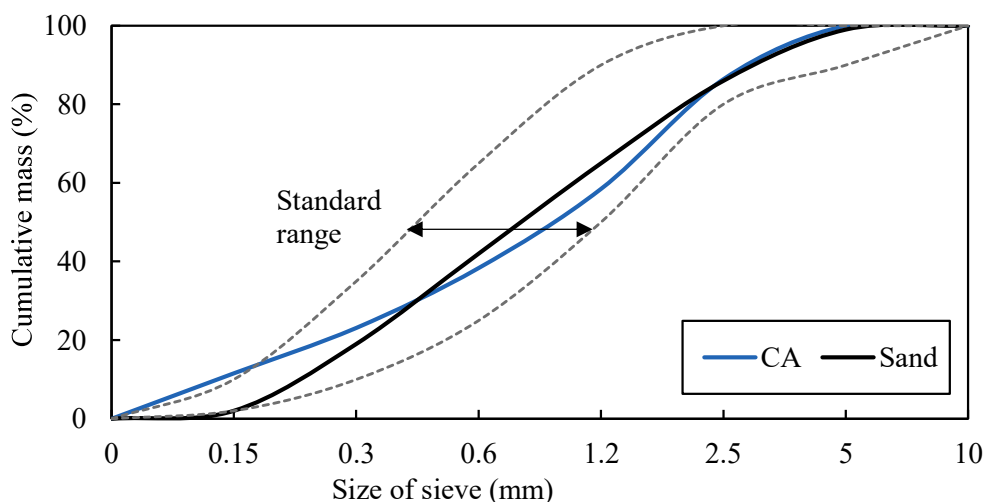


**Fig. 4.1** Particle size distribution curves of fine aggregates

influence of CA on fresh and mechanical properties, as summarized in Table 4.5.

### 4.2.3 Specimen preparation

A Hobart planetary mortar mixer was used to mix the GP mortars. The active fillers and fine aggregate (sea sand, CA) were first put into the mixer and mixed for 1 minute. Then, the AS was added and mixed for 2 min. to get GP mortar. Finally, coarse aggregate was added to the mortar and further mixed for 2 min to get GP concrete. After measuring the slump, fresh concrete was cast in the prismatic moulds with a size of 10×10×40 cm and the cylindrical moulds with diameter of 10 cm and height of 20 cm, and then vibrated for 20s by a rod vibrator. After the vibration, the outside of the mould was struck with a wood hammer.

The mixing procedure of GP mortar was the same as GP concrete except not adding coarse aggregate. The freshly mixed GP mortar was used to produce the prism specimens with a 4 cm side length of square section and 16 cm length, which were used for the strength test and the accelerated carbonation test. All the specimens were demoulded at 1 day age. The specimens were sealed with

Table 4.1 Physical properties of raw materials used

Raw material	Properties, etc.
FA	Specific density: 2.30 g/cm <sup>3</sup> , Blaine fineness: 4392 cm <sup>2</sup> /g
BFS	Specific density: 2.88 g/cm <sup>3</sup> , Blaine fineness: 4180 cm <sup>2</sup> /g
CA	Oven-dry density: 1.80 g/cm <sup>3</sup> , water absorption: 31.4%, F.M. 2.03
Sea sand (S)	Oven-dry density: 2.51 g/cm <sup>3</sup> , surface-dry density: 2.56 g/cm <sup>3</sup> , specific water absorption: 1.81%, solid content: 66.7%, F.M. 2.87
AN	Compositions: Na <sub>2</sub> O: 19%, Al <sub>2</sub> O <sub>3</sub> : 20%, molar ratio (Na <sub>2</sub> O/Al <sub>2</sub> O <sub>3</sub> ): 1.56, Specific gravity: 1.49 (40% concentration by mass)
NH	Specific gravity: 1.33, molar concentration: 10 mole/L
JIS No.1 sodium silicate	Compositions: Na <sub>2</sub> O: 17%, SiO <sub>2</sub> : 36%, molar ratio (SiO <sub>2</sub> /Na <sub>2</sub> O): 2.16, Specific gravity: 2.09

Table 4.2 Chemical compositions of raw materials (XRF analysis)

Raw material	Chemical compositions (% by mass)								
	SiO <sub>2</sub>	Al <sub>2</sub> O <sub>3</sub>	CaO	Fe <sub>2</sub> O <sub>3</sub>	MgO	Na <sub>2</sub> O	K <sub>2</sub> O	TiO <sub>2</sub>	Others
FA	59.10	23.91	3.48	7.37	1.06	1.07	1.68	1.27	1.06
BFS	34.67	14.46	43.13	0.34	5.50	0.25	0.25	0.55	0.85
CA	57.00	27.00	4.43	6.60	0.67	0.58	1.09	1.63	1.00

water-retention tape and then moved into the curing chamber with 20°C temperature and 60% relative humidity for 28 days in until reaching a 28-day age.

#### 4.2.4 Surface treatment

The specimens were sealed with water-retention tape, and then cured in the air at 20 °C, R.H. 60% for 28 days. For promoting the absorption of AN, specimens were dried in a drying oven of 20 °C for 7 days after the 28-day curing. Then, the surfaces of prismatic specimens were applied with AN solution every 6 hours for 4 times. Totally, four times of application were performed for each specimen. **Fig. 4.2** shows the appearance of the mortar specimen before and after the AN was applied. The subsequent accelerated carbonation tests of surface-modified GP mortars were carried out after 28-day re-curing.

Table 4.3 Components and densities of AS

AS	WG : NH (by volume)	Specific gravity	Mole ratio of SiO <sub>2</sub> /Na <sub>2</sub> O
AS10	1:0	1.378	2.100
AS41	4:1	1.374	1.396
AS31	3:1	1.372	1.255
AS21	2:1	1.370	1.045
AS01	0:1	1.333	0.000

Table 4.4 Mix proportions of GP mortars (by mass)

Series No.	AS	AS/AF	BFS: FA	Replacing ratio for sea sand	S/AF
CA (10)	AS10	0.5	3:7	0.20 (CA)	2.0
CA (41)	AS41				
CA (21)	AS21				
CA (01)	AS01				
CA (31)	AS31				
CA 10		0.10 (CA)			
CA 15		0.15 (CA)			
CA 20		0.20 (CA)			
CA 30		0.30 (CA)			
CA 40		0.40 (CA)			
CA 100		1.00 (CA)			

Table 4.5 Mix proportions of GP concretes mixed with CA

Role of CA	Series	Replaced material by CA	AS/AF (by mass)	AS sort	BFS/AF (by mass)	BFS sort	AF (kg/m <sup>3</sup> )	AS (kg/m <sup>3</sup> )	CA (kg/m <sup>3</sup> )	S (kg/m <sup>3</sup> )	RCA (kg/m <sup>3</sup> )
Active filler	C-FA-0	-	0.6	AS31	0.3	BFS3	440	264	-	654	1000
	C-FA-10	10% FA				0	396	264	44	654	
Fine aggregate in concrete	C-S-0	-	0.5	AS21		BFS4	420	210	-	721	
	C-S-10	10% Sand				0	420	210	70	634	
	C-S-20	20% Sand					420	210	137	550	
	C-S-30	30% Sand					420	210	202	471	

#### 4.2.5 Property test

After 28 days of curing, the strength test and the accelerated carbonation test were performed. It is noted that we did not examine the strengths of the GP mortars treated with AN solution because the AN only permeated into the surface layer of the GP mortar and thus would not have much effect on the strength of whole mortar.

For the accelerated carbonation test, the surfaces (two ends, top and bottom) of mortar specimens were sealed with an airtight sealing tape to ensure that CO<sub>2</sub> diffuses into the specimens only through the two side surfaces. Then, the sealed specimens were placed into a carbonation test chamber with

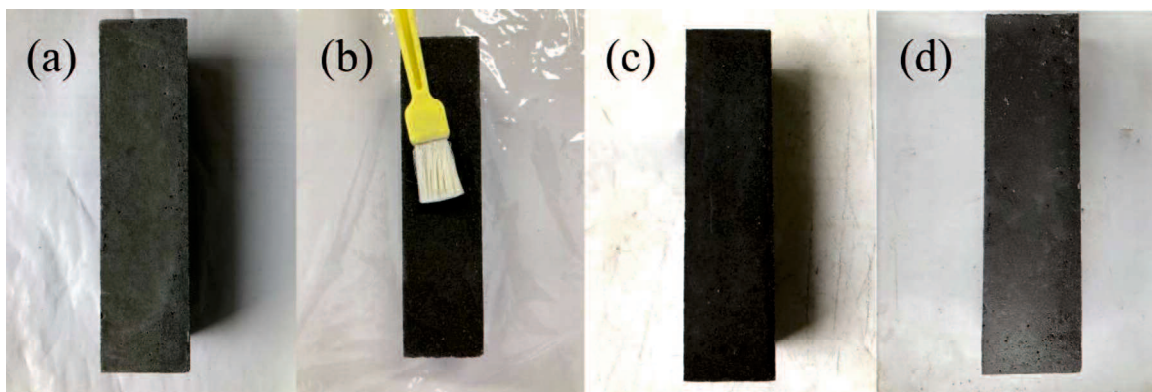


Fig. 4.2 The surfaces of CA-blended geopolymer mortar specimens (40×40×160mm): (a) before treatment, (b) AN surface treatment by brush, (c) right after AN treatment, and (d) AN-treated specimen before accelerated carbonation test

5% of CO<sub>2</sub> concentration, 20 °C, and R.H. 60%. At an interval of two weeks, the mortar specimen was cut at about 10 mm interval to measure carbonation depth. It should be noted that during the cutting, to ensure that the alkali matters were not washed away, spraying water was not used as a dust countermeasure.

The depth of the colourless region from the surface of the prism specimen was measured at 3 min. strictly after spraying the 1% phenolphthalein solution. The average value of six depths, three values on one side and 1 cm interval respectively, was recorded as carbonation depth. After the measurement of carbonation depth, the cut sections were sealed with airtight tape, and the remained GP mortar samples were returned to the CO<sub>2</sub> chamber to continue the carbonation test. The accelerated carbonation test lasted for a maximum of 16 weeks. Once the carbonation reached to the central of specimen, i.e. the carbonation depth was 20 mm, the test was stopped. Therefore, the max. detectable value of carbonation depth was 20mm.

### 4.3. Test Results and Discussion

#### 4.3.1 Fresh properties of GP materials with CA

The effect of CA as replacement of sand or FA in concrete mixtures on slumps of GP concretes and flow table test values of GP mortars are shown in **Fig. 4.3** and **Fig. 4.4**. We can conclude that when any type of the CA replaced part of fly ash, the slump of GP concrete decreased. When the CA replaced part of sea sand, the slump of GP concrete didn't decrease until the replacing ratio of the CA was larger than 20%. This means that the replacement of FA with CA will damage the fluidity of GP concrete. Similar to the use of recycled fine aggregate[40–42], the high water absorption and irregular shape of CA particles, compared to the spherical shape of FA particles, cause the decrease of fluidity of GP concretes with CA replacing partial FA.

However, replacing sea sand with the CA up to a ratio of 10% did not impair the fluidity of GP concrete. This resilience can be attributed to the adjustment of water content for CA. In contrast to the

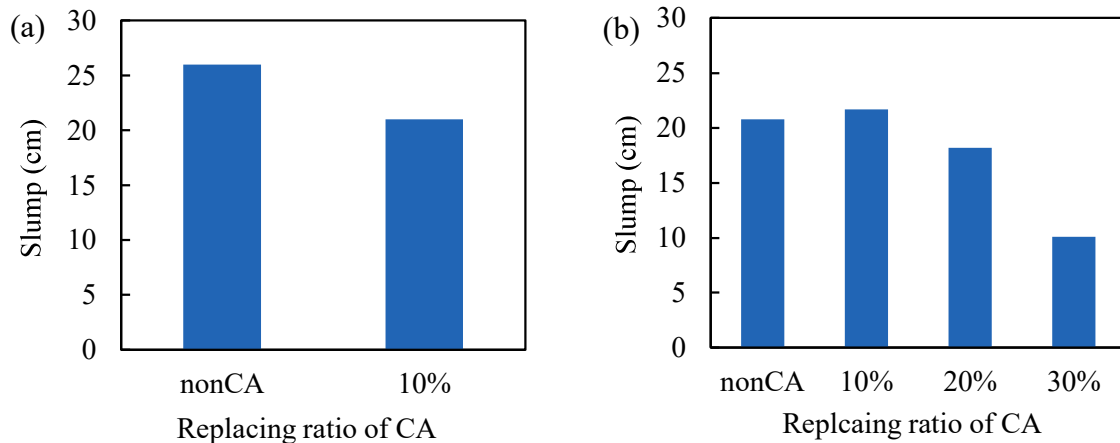


Fig. 4.3 Slump of fresh GP concrete: a) Replacing for FA; b) Replacing for sea sand

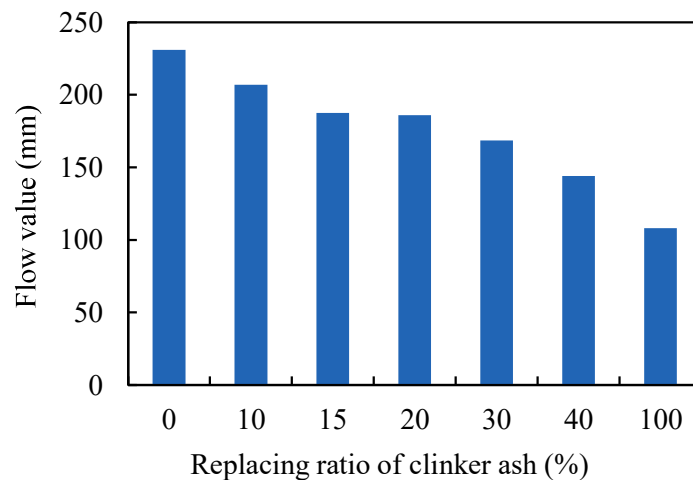


Fig. 4.4 Flow table test results of GP mortars

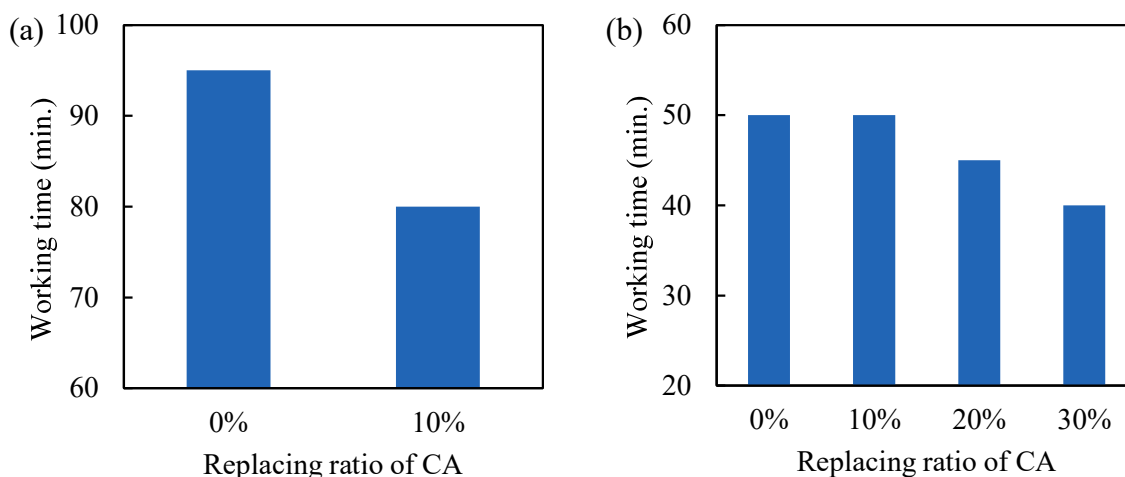


Fig. 4.5 Working times of GP concrete: a) Replacing for FA; b) Replacing for sea sand

use in an oven-dry state during FA replacement, CA was used in a saturated surface-dry state when replacing sea sand. Decline of fluidity was not observed until the substitution ratio exceeded 10%.

From **Fig. 4.4**, we can see that the table flow value decreased with the increase of replacing ratio of the CA. Combined with the results of GP concrete and mortar, we found that excessive CA addition in GP materials will lead to the decline of fluidity.

The working time of GP concretes are shown in **Fig. 4.5**. The working time of GP concrete decreased by 16% when the CA replaced 10% of the FA. However, when the replacing ratio of the CA was 10% as a substitute for the sea sand, the working time was not almost reduced. However, once the replacing ratios were 20% or 30%, the working time of GP concrete decreased greatly. In summary, a small replacing ratio (10%) of CA as a substitute for the sea sand did not shorten the working time of GP concrete, but as a substitute for FA, the utilization of CA decreased the working time of GP concrete.

### 4.3.2 Mechanical properties of GP materials with CA

#### (1) The effects on flexural strength

According to the mechanical experiments of heat and ambient-cured GP mortars with varying CA content (**Fig. 4.6**), the flexural strength (Fb) of GP mortars generally decreased with increasing clinker ash (CA) replacement ratios, regardless of whether the mortar was cured at 20°C or 80°C. However, the extent of the decrease varied with the curing method. For ambient-cured specimens, the maximum decrease in Fb was 49.4%, while heat-cured specimens experienced a slightly greater maximum decrease of 53.8%. This suggests that heat-curing may have a more pronounced impact on flexural strength reduction due to shrinkage and cracking effects that develop during the accelerated curing process.

Flexural strength is highly dependent on the mortar's ability to resist bending stresses, which are influenced by the quality of the interfacial transition zone (ITZ) between the CA particles and the GP

matrix. Due to CA's porosity and high water absorption, shrinkage can increase as water evaporates from the pores, leading to weaker ITZs and microcracks under stress. This effect is particularly prominent in heat-cured mortars, where drying shrinkage creates more ITZ-related cracks, further weakening flexural strength. Nevertheless, at a 30% CA replacement ratio, the reduction in Fb for ambient-cured mortars remained 23.8%, indicating that moderate CA additions have a limited effect on flexural properties and may still be viable for practical applications.

(2) *The effects on compressive strength*

The compressive strength of GP concretes with CA is shown in **Fig. 4.7**. It is found that when replacing FA, the compressive strength of GP concrete decreased. The factors responsible for the decrease in compressive strength of GP concrete with CA are considered as (1) lower reactivity of clinker ash for polymerization than FA, (2) even CA has the same reactive components to FA, but CA is coarser so that reactivity becomes low, and (3) the porosity of concrete was increased due to porous CA particles. On the other hand, when the CA replaced the sea sand, small replacing ratio (under 20%) led to an increase in the compressive strength of GP concrete. This suggests that CA has some reactivity in the polymerization reaction. However, when the replacing ratio of CA reached to 30%, the compressive strength of C7 was smaller than the normal GP concrete C-S-0, which means the negative effect of CA porosity on concrete strength exceeds the positive effect of its reactivity when added in large quantities.

From **Fig. 4.8** we can see that, the compressive strength ( $F_c$ ) of GP mortars also decreased with increasing CA replacement ratios, following a trend similar to that observed for flexural strength. The impact of CA was different under varying curing conditions. For ambient-cured specimens, the maximum decrease in ( $F_c$ ) was 65.3%, whereas heat-cured specimens showed a slightly lower

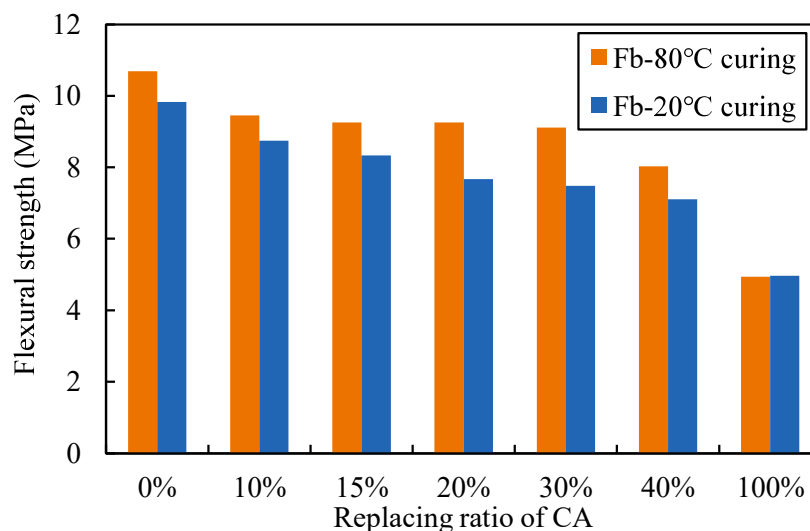


Fig. 4.6 Flexural strength of GP mortars with CA cured at 20 °C, and 80 °C

maximum decrease of 54.0%. This indicates that, while heat-curing facilitates the geopolymerization process, it can also induce microstructural issues that undermine the benefits of a dense matrix.

One notable observation was that the compressive strength of GP mortars with CA cured at 80°C for 8 hours was lower than that of mortars cured at ambient temperatures. This can be attributed to the formation of drying shrinkage cracks during heat-curing, where the high temperature accelerates water loss and creates microcracks within the GP matrix. Although specimens were wrapped in plastic film to limit water evaporation, the film was not fully effective in preventing shrinkage. Additionally, without coarse aggregates to mitigate shrinkage, the mortar matrix becomes more susceptible to crack formation.

The high water absorption of CA particles exacerbates shrinkage in heat-cured GP mortars. Water retained in the pores of CA particles evaporates as the mortar hardens, leading to increased shrinkage and further weakening the ITZ. The combination of CA's porosity and the potential for microcrack

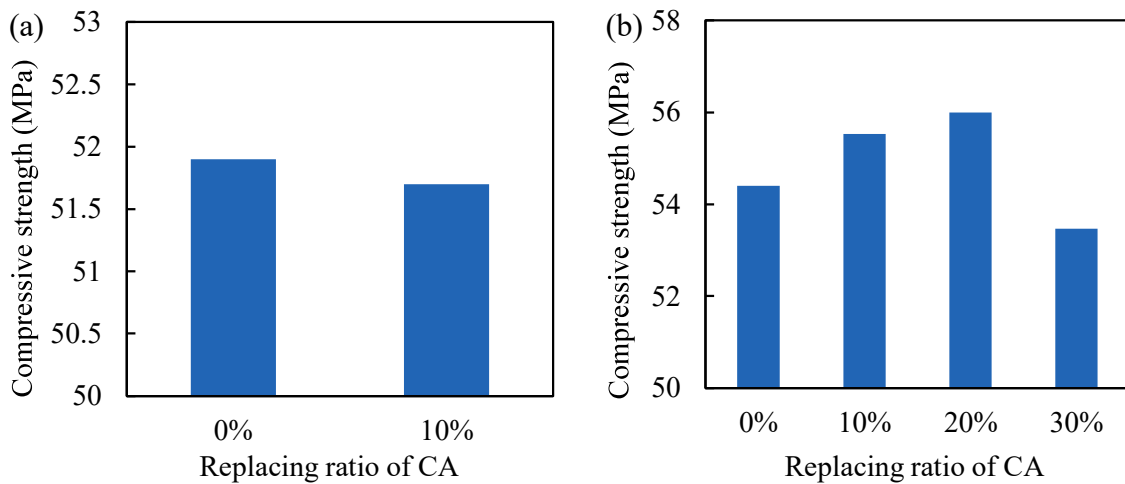


Fig. 4.7 Compressive strength of GP concrete: a) Replacing for FA; b) Replacing for sea sand

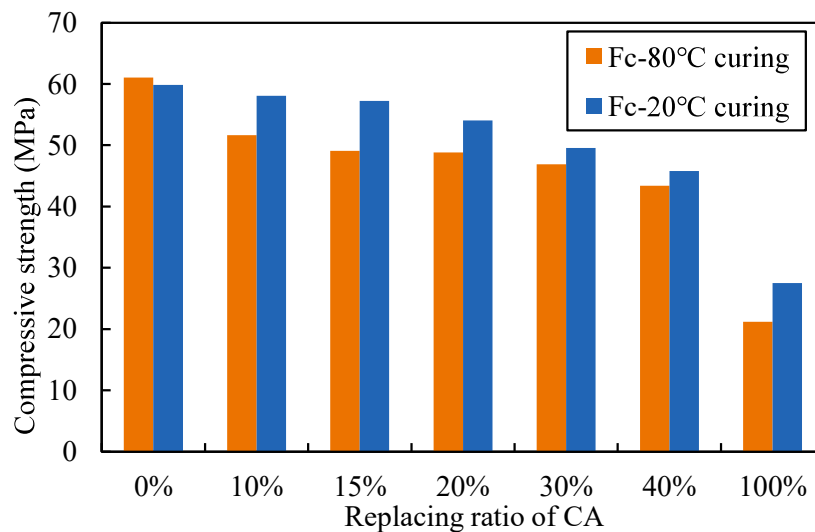


Fig. 4.8 Compressive strength of GP mortars with CA cured at 20 °C, and 80 °C

formation contributes to the strength reduction seen in heat-cured specimens. Previous studies, such as that by Paija et al. [43], have also highlighted that high-temperature curing can damage the microstructure of FA-based geopolymer, supporting these observations.

In summary, moderate CA additions (up to 15%) minimally impact both (Fb) and (Fc) in ambient-cured GP mortars. However, heat-curing, while beneficial for initial strength gain, can lead to issues with shrinkage-induced microcracks, particularly in the presence of CA particles with high porosity and water absorption. Further investigation into curing methods and CA replacement ratios can help balance these effects and improve the mechanical performance of GP mortars.

The replacement of FA with CA generally reduces compressive and flexural strength due to CA's lower reactivity, coarser particle size, and higher porosity. However, when CA partially replaces sand (up to 20%), it can enhance compressive strength due to its partial reactivity in the GP matrix. Beyond this threshold, the negative effects of increased porosity outweigh the positive effects of reactivity.

In summary, CA affected the mechanical properties of GP mortars differently. The impact depends on the specific replacement ratios, particle characteristics, and interactions within the GP matrix.

### ***4.3.3 Frost resistance of GP concrete with CA***

#### *(1) Relative dynamic modulus of elasticity*

The change in the relative dynamic modulus of elasticity with the freeze-thaw cycle is shown in **Fig. 4.9**. It is found that with the increase of freeze-thaw cycles, the relative dynamic modulus of elasticity of GP concrete decreased. The relative dynamic modulus of elasticity of GP concrete was still over 60% after 300 cycles when the CA was absent. But, when the cycle number was 150 cycles or 120 cycles, the relative dynamic modulus of elasticity of GP concretes using 10%, 20%, and 30% of CA was less than 60%. The greater the replacing ratio of the CA, the greater decrease in relative dynamic modulus of elasticity. Clinker ash particles with high water absorption and porosity increase weak points within concrete, leading to a decrease in stiffness and an increase in porosity of overall material, and therefore a reduction in the dynamic modulus of elasticity[44–47]. The water absorption of GP concrete using CA increases with the increase in the proportion of clinker ash replacing sand. During the freeze-thaw cycles, more water will freeze, creating greater internal expansion pressure. This results in more severe microstructural damage and crack development. Consequently, with the increase in the blending ratio of clinker ash, the reduction in the relative dynamic modulus of elasticity after the same number of freeze-thaw cycles became large.

If the requirement for frost resistance is that the relative dynamic modulus of elasticity after 150 cycles is not less than 60%, GP concrete can be mixed with CA instead of less than 10% natural sand. However, as general Portland cement concrete, the desirable frost resistance of GP concrete, which is that the relative dynamic modulus of elasticity after 300 cycles is not less than 60%, can be expected to be achieved by adding air entraining agent[48–51].

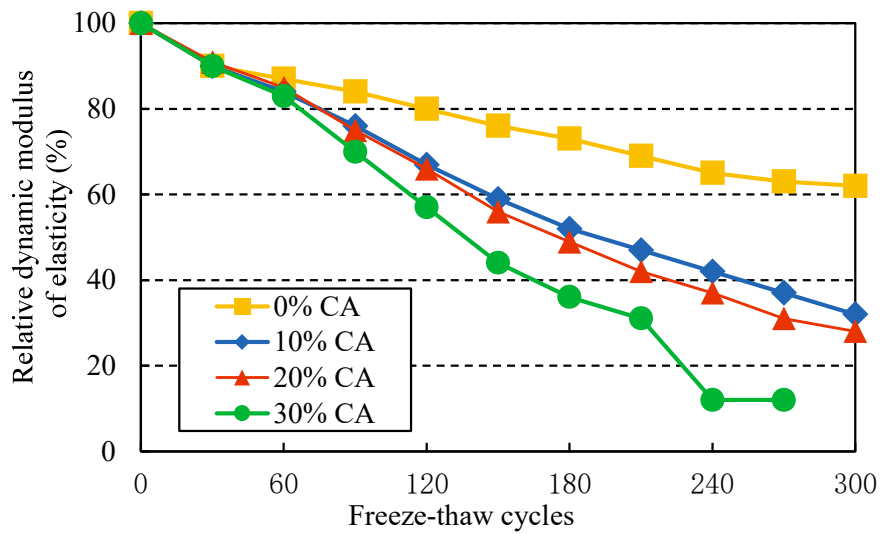


Fig. 4.9 Relationship between the number of freeze-thaw cycles and relative dynamic modulus of elasticity of GP concretes

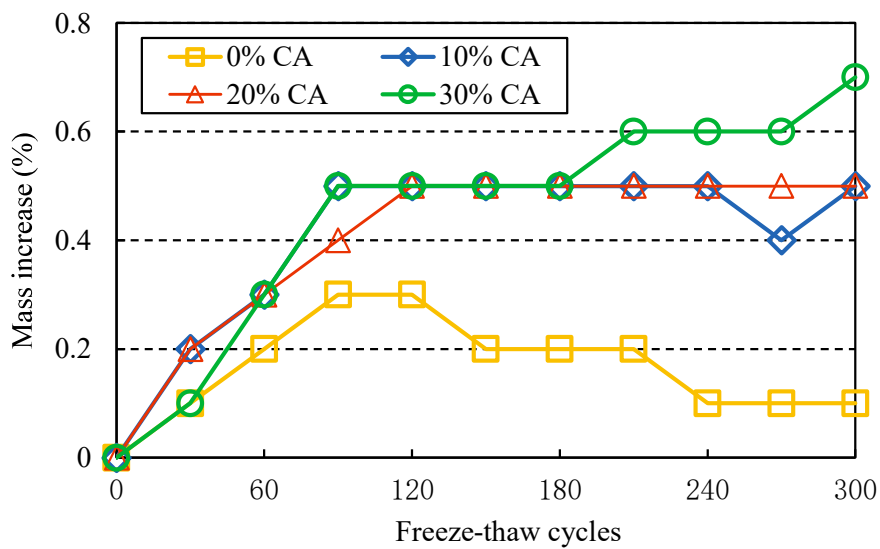


Fig. 4.10 Relationship between the number of freeze-thaw cycles and mass change of GP concretes

(2) Mass change

The relationship between the number of freezing-thawing cycles and the mass change is shown in Fig. 4.10. We can find that, the masses of GP concrete specimens with the CA were larger than the normal GP concrete after the same freezing-thawing cycles. Not like PC concrete, the mass of GP concrete increased with the freezing-thawing cycle. For the normal concrete C-S-0, the mass of the specimen first increased and then decreased after 120 cycles. For 10% and 20% replacing ratio of CA for sand, the mass first increased and then remained unchanged after 120 cycles. But for 30% replacing

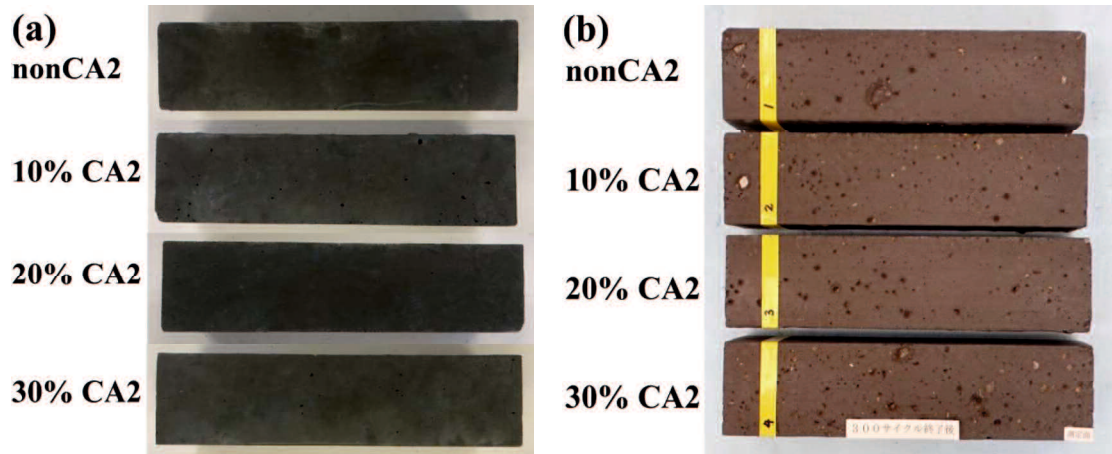


Fig. 4.11 Surfaces of GP concretes before and after the frost resistance test: a) Before 300 freeze-thaw cycles; b) After 300 freeze-thaw cycles

ratio, the mass of the specimen kept increasing throughout. It can be noticed that the concrete showed an increase trend in mass, and the trend of mass increase was more obvious with higher CA content. This is attributed to the penetration of water into the cracks and the pores in the specimens after the freezing–thawing. During the thawing phase, the water was absorbed by the specimen, and subsequent freezing could extend microcracks and pores, thereby facilitating further water absorption, but no spalling occurred on the surface of specimen in the early stage to reduce the mass. This led to the increase in mass of specimen[52–54]. The voids and pores of CA particles provided free expansion space for water when it freezes, thereby reducing the pressure induced by frost and therefore surface damage almost did not occur[55]. This is also why the mass of GP concrete with 30% CA had been continuously increasing. The subsequent mass reduction was attributed to the spalling of concrete caused by internal freezing pressure. Thus, we can divide the mass change into three stages: increase stage, steady stage, and decrease stage. With the increase of replacing ratio of CA, both the increase stage and steady stage became longer.

**Fig. 4.11** shows the 4 series of GP concrete specimens from C-S-0 to C-S-30 before and after experiencing 300 freezing-thawing cycles. Despite the large reduction in the relative dynamic elastic modulus, the surface deterioration was very slight. This is the reason why the mass of GP concrete did not decrease. The polymerization reaction of GP is a dehydrate (dewater) reaction, and the water channels produced by the dewater reduced the internal expansion pressure so that the surface spalling was very little, even invisible. Water absorption due to internal degradation is the reason for the mass increase of GP concrete specimen as stated above. The mass increase percentage of the normal concrete C-S-0 decreased after 120 cycles, indicating that it had less internal damage. The internal damage includes the dissolution of the remained alkali activator. That is, the percentage of mass

increase of GP concrete specimen depends on which dominates, the mass decrease due to surface spalling or the mass increase due to water absorption.

#### 4.3.4 The effectiveness of AN treatment on GP mortars with CA

The relationship between the carbonation depth and the elapsed time for different GP mortars are shown. The porous feature of CA may affect the carbonation resistance of GP mortar. In the following, we discuss the carbonation resistance of GP mortar using CA, and the effectiveness of the AN application under different conditions. In the legend of figures, “-AN” represents that the specimen’s surface was treated with the AN solution, whereas “-non AN” represents that the specimen’s surfaces were not treated.

The effects of AN treatment on the carbonation resistance of GP mortar with different mix proportions and with the different treatment conditions were discussed on the basis of regression analysis of carbonation depth - carbonation time relationship for different mortars and treatment conditions. As described later, due to the AN surface treatment, the carbonation depth of part of the specimens could be detected only after a period, so we used Eq. 4.1 for the regression analysis.

$$C_d = a \cdot \sqrt{\text{CO}_2\% / 5.0} \cdot \sqrt{t - b} \quad (4.1)$$

where  $C_d$  is carbonation depth (mm),  $t$  is carbonation period (week),  $\text{CO}_2\%$  represents  $\text{CO}_2$  concentration (%),  $a$  is proportional coefficient (mm/ $\sqrt{\text{week}}$ ), and  $b$  is elapsed time until the depth of carbonation can be detected, i.e., onset time of neutralization (week,  $\geq 0$ ).

In Eq. 4.1, the proportional coefficient  $a$  implies the rate of increase of the carbonation depth with elapsed time and therefore is called carbonation rate coefficient. The smaller the  $a$ , the higher the carbonation resistance of GP mortar. And the larger the  $b$ , the later the onset of carbonation, and therefore the higher the initial carbonation resistance.

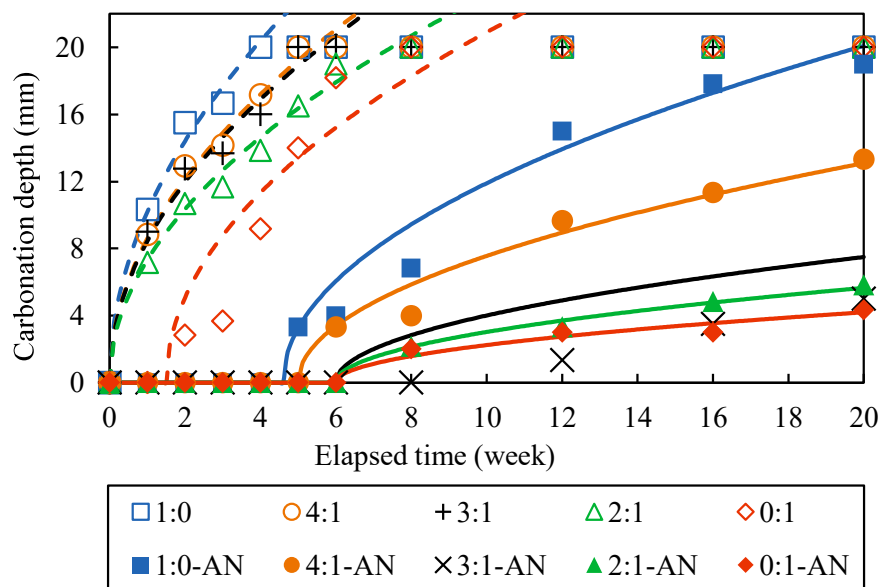
In Fig. 4.12 and Fig. 4.13, The tables under the figures are the carbonation rate coefficient  $a$  of the equations of relationships of carbonation depths with elapsed times of accelerated time of different GP mortars with and without AN treatment. In addition, the variations of coefficients of  $a$  are also listed in the right column in the table. With the comparison of the carbonation equations of GP mortars with different mix proportions before and after AN treatment, we can clearly observe the differences in the effectiveness of AN treatment on various GP mortars of mix proportions.

##### (1) Effects of alkali solution on the effectiveness of AN surface treatment

Fig. 4.12 illustrates the relationship between carbonation depth and elapsed time for GP mortars with different AS solutions and 20% CA. From this figure, it is obvious that GP specimens without AN surface treatment began to carbonate very early and rapidly, becoming fully carbonated within just 8 weeks. However, carbonation resistance was significantly improved with the AN surface treatment. The start of carbonation in the specimens treated with AN was delayed during the

accelerated carbonation test. Additionally, the carbonation rate was significantly reduced, indicating that AN surface treatment greatly enhanced the carbonation resistance of GP mortar.

An increased  $\text{SiO}_2/\text{Na}_2\text{O}$  molar ratio promotes the formation of N-A-S-H gels in GPs[38], enhancing carbonation resistance. The carbonation depths were significantly and negatively correlated with the blending ratio of NH in AS. An increase in NH decreased the  $\text{SiO}_2/\text{Na}_2\text{O}$  molar ratio and then reduced the apparent porosity of GP[39], resulting in a denser GP matrix and slower  $\text{CO}_2$  diffusion. Additionally, more residual  $\text{Na}^+$  present in the pores of GP is another factor contributing to the smaller carbonation depths in GP mortar specimens with a higher NH blending ratio. The high alkalinity of AN increased the alkalinity of pore solution of surface of GP mortars, which delayed the onset of carbonation. The continuous dissolution of silicate from the precursors, activated by the alkali, forms numerous free Si-O-Si tetrahedral monomers, contributing to the  $\text{SiO}_4$  and  $\text{AlO}_4$  linkage. Sodium aluminate solution provided an additional source of aluminum, which is crucial for the formation of



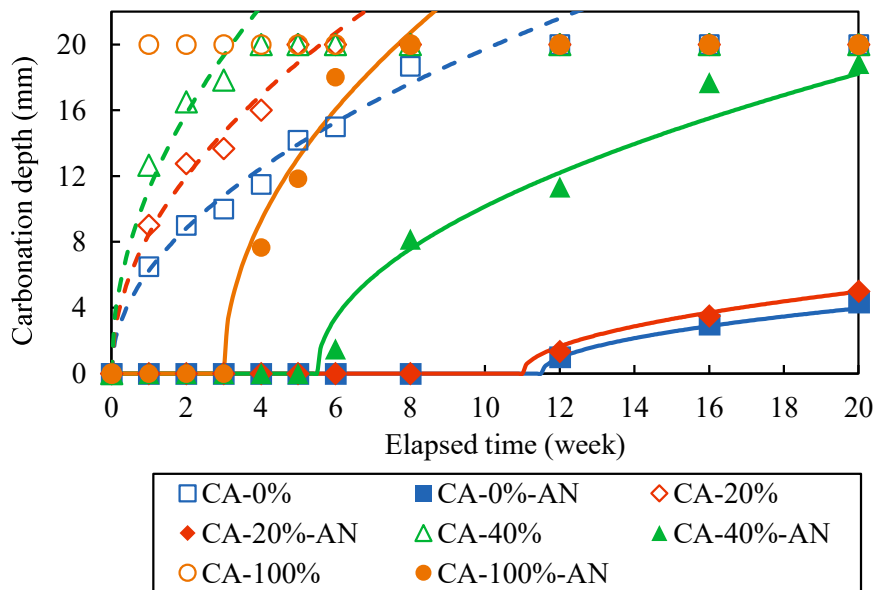
WG/ NH	$\text{SiO}_2/\text{Na}_2\text{O}$	Non-AN treatment	AN treatment	Decrease of a (%)
1:0	2.100	10.18	5.11	49.76
4:1	1.396	8.59	3.38	60.68
3:1	1.255	8.45	2.00	76.30
2:1	1.045	7.31	1.51	79.34
0:1	0.000	7.16	1.12	84.36

Fig. 4.12 Carbonation depths of GP mortars with 20% CA in place of sea sand but with different WG/NH ratios

aluminosilicate networks in geopolymers. These networks are more stable and less sensitive to carbonation compared to structures formed with lower aluminum content. The increased availability of aluminum due to sodium aluminate facilitates the formation of these stable structures, enhancing carbonation resistance. Research[40] demonstrated that the NH-dissolved fly ash and high  $\text{OH}^-/\text{Al}^{3+}$  ratio could ensure the domination of 6-coordinate aluminum in AN which formed fly ash-based geopolymers that are greater in strength to those activated with WG. In addition, significant amount of octahedral Al was produced in solution at high  $\text{OH}^-/\text{Al}^{3+}$  ratio. All above means a denser structure and explained why the improvement on carbonation resistance of GP mortars with AN increased with the NH blending ratio in AS.

(2) Effects of CA and AN surface treatment

Fig. 4.13 illustrates the carbonation depths of GP mortars containing different amounts of CA while using the same alkali-activator solution. As shown in Fig. 4.13, due to the porous nature of CA, the carbonation rate increased with higher replacing ratio of CA, indicating that an increase in CA replacement resulted the weakness in carbonation resistance of GP mortar. In addition, all specimens without AN treatment began to carbonate within the first week under accelerated carbonation



CA ratio	Non-AN treatment	AN treatment	Decrease of $a$ (%)	$b$ (week)
NonCA	6.23	1.36	78.14	11.5
20%	8.45	2.00	76.30	6
40%	11.14	4.78	57.04	5.5
100%	-	9.26	-	3

Fig. 4.13 Carbonation depths of GP mortars with different replacing ratios of CA

conditions, regardless of CA replacing ratio. However, with AN surface treatment, specimens containing 0%, 20%, 40%, and 100% CA showed no detectable sign of neutralization in 11.5, 11, 5.5, and 3 weeks, respectively, which means the use of AN delayed the onset of carbonation. Notably, the specimens with 100% CA replacement without AN treatment became fully carbonated within just one week. However, with AN surface treatment, it can remain uncarbonated for up to 3 weeks. Although the effectiveness of AN on the improvement for carbonation resistance of GP mortars is weakening with the increasing CA replacing rate, the reduction in the carbonation rate coefficient for GP mortar with 40% CA still reached 57 %.

Comparing the results of applying AN twice versus four times on the improvement of carbonation resistance of GP mortar, it is evident that four times of AN application can still significantly reduce the carbonation rate coefficient of GP mortar under accelerated carbonation conditions and greatly delay the onset of carbonation compared to AN application twice. Considering that the specimens were cured at 20 °C conditions resulting in high moisture content and few cracks, making it difficult for AN solution to permeate, we subjected them to normal temperature drying treatment to quickly evaporate the surface moisture. With further water loss, the moisture content reduced and the cracks grow[41] on the specimens' surface, making it easier for the AN solution to permeate. Under these conditions, even with four times of AN applications, compared to two applications, the carbonation resistance of GP mortar can still be greatly improved, especially in terms of delaying the onset of carbonation.

## 4.4 Microstructure and Chemical Analysis of GP Mortar with CA

### 4.4.1 SEM-EDS analysis of GP mortar with AN treatment

Fig. 4.14 shows the SEM images of the CA particle surfaces before and after immersed in the alkali activator solution AS31. As stated earlier, CA is a kind of light and porous material, there are a large number of pores on the surface layer and the inside of CA particles as shown in Fig. 4.14 (a). However, after the immersion in the AS31, obvious change in surface texture of CA particle can be found in Fig. 4.14 (b). This indicates that the CA has some reactivity with the AS31. Basically, CA is a crystalline substance, but may contain amorphous components similar to FA. In the presence of an alkali activator, the whole surface of CA particles was covered with a kind of newly generated products, which also explains what so many protrusions on the surface are and why the pores disappeared. Furthermore, compared with the chemical compositions of CA (shown in Table 4.2), the XRF test results of CA after the immersion in the AS31 shows a large variation in the content of different oxides.

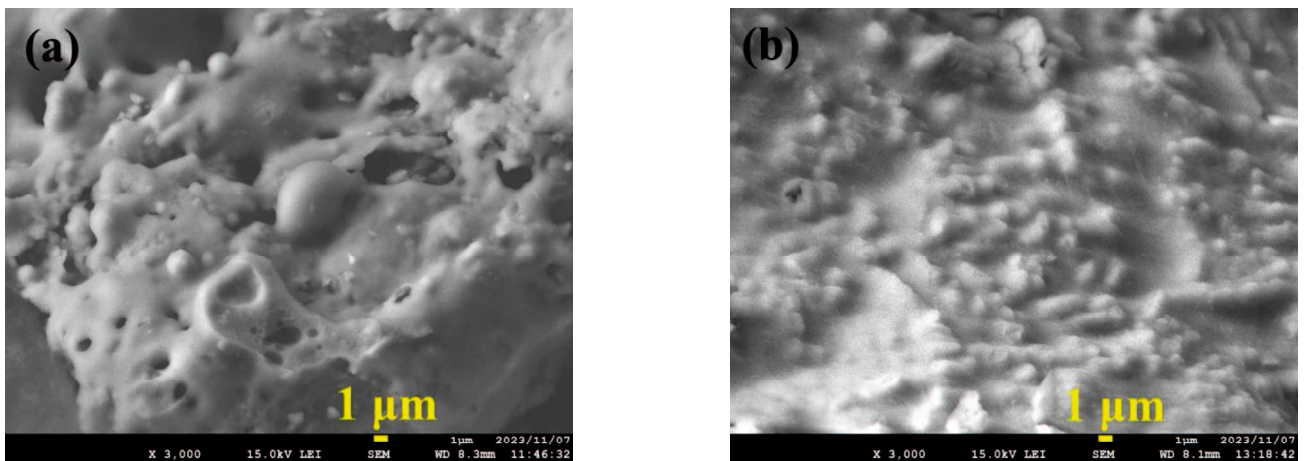


Fig. 4.14 Surface of CA particle before (a) and after (b) immersed with AS

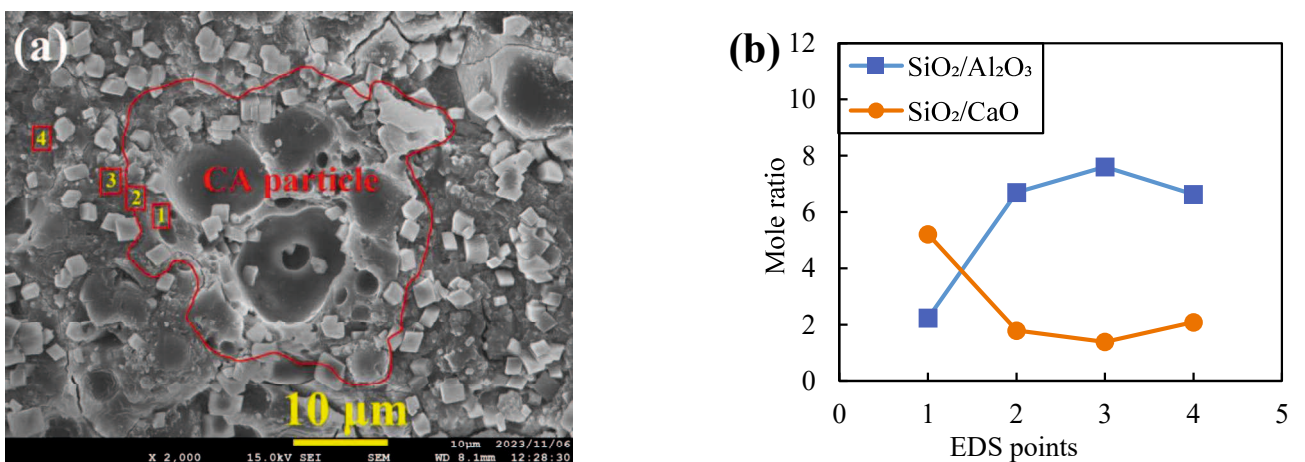


Fig. 4.15 CA particle bonded with GP matrix

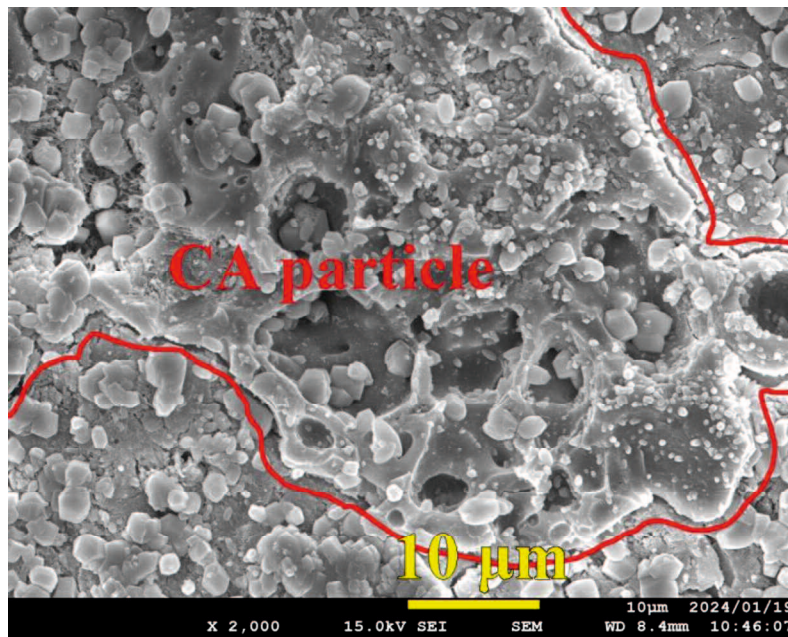


Fig. 4.16 The cracks between CA particle and OPC matrix

The reduction of aluminium oxide also indicates the occurrence of polymerization reaction. Considering compositions of the AS31, the sharp increase of sodium oxide was attributed to the polymerization reaction between the CAs and the AS31.

The effect of fine aggregate type on the morphology of mortar was analysed. Compared with sea sand particles, the CA particles have irregular shape and porous structure at a macroscopic level, which will increase interfacial contact and strengthen the connection between CA particles and GP matrix. From **Fig. 4.15** (a) we can find that the CA particles were well bonded by the GP matrix, and no particle interface is visible around the boundary of CA particle, which indicates that the CA particle has good affinity, and integrates with the GP matrix, compared with **Fig. 4.15** (a). The **Fig. 4.16** shows the obvious cracks between the CA particle and OPC paste matrix were found, which demonstrates that the compatibility between CA and GP matrix is better than which with the OPC matrix.

Moreover, the microstructure of geopolymer is strongly influenced by the  $\text{SiO}_2/\text{Al}_2\text{O}_3$  ratio, and geopolymer with a lower  $\text{SiO}_2/\text{Al}_2\text{O}_3$  has a dense structure [59,63–66]. **Fig. 4.15** (b) is the mole ratios of oxides of EDS points distributed around the CA particle. From this figure, we can find that the  $\text{SiO}_2/\text{Al}_2\text{O}_3$  ratio also shows a concomitant upward trend further away from the CA particle itself. The  $\text{SiO}_2/\text{Al}_2\text{O}_3$  ratio of Point 1, which is distributed at the ITZ of CA and GP matrix, is lower than Point 4 which distributed in the GP matrix completely. This also means a denser microstructure of the ITZ and a firm bond between CA particle and GP mortar. Therefore, the mechanical properties of GP mortar with CA are improved, compared to PC mortar using CA.

The porosity and high CaO content in CA can lower carbonation resistance in GP mortars, as  $\text{CO}_2$  can readily react with CaO to form  $\text{CaCO}_3$ , weakening the matrix over time. However, the SEM-EDS analysis shows that with optimized mix proportions and AN surface treatments, the durability of

CA-based GP mortar can be substantially enhanced. This treatment fills surface pores and improves the continuity of the aluminosilicate network, creating a more robust matrix that mitigates CO<sub>2</sub> diffusion.

In terms of mechanical performance, CA's rough and porous structure supports mechanical interlocking, which contributes to compressive strength. Yet, without surface treatments, the presence of microcracks around CA particles can reduce flexural strength, especially under repeated stress. Thus, for applications where durability and carbonation resistance are paramount, using AN-treated CA aggregates in GP mortar is recommended to achieve balanced structural performance and longevity.

In summary, the GP matrix might invade the surface pores of CA, and the surface layer of CA particles was involved in the GP hardening reaction that refines the CA particle and the ITZ.

#### **4.4.2 XRD analysis of GP mortar with Clinker Ash**

The X-ray Diffraction analysis of geopolymer mortar incorporating various waste by-products, including bottom ash aggregates, provides significant insights into the mineralogical composition of the materials before and after geopolymerization. As shown in **Fig. 4.17**, the XRD spectra highlight the differences in crystalline and amorphous phases present in sea sand, individual waste by-products, and final GP mortars. This analysis reveals the presence of common crystalline components, such as quartz and feldspars, as well as distinctive phases in specific waste materials, indicating the extent to which each component participates in or is altered by the GP formation process.

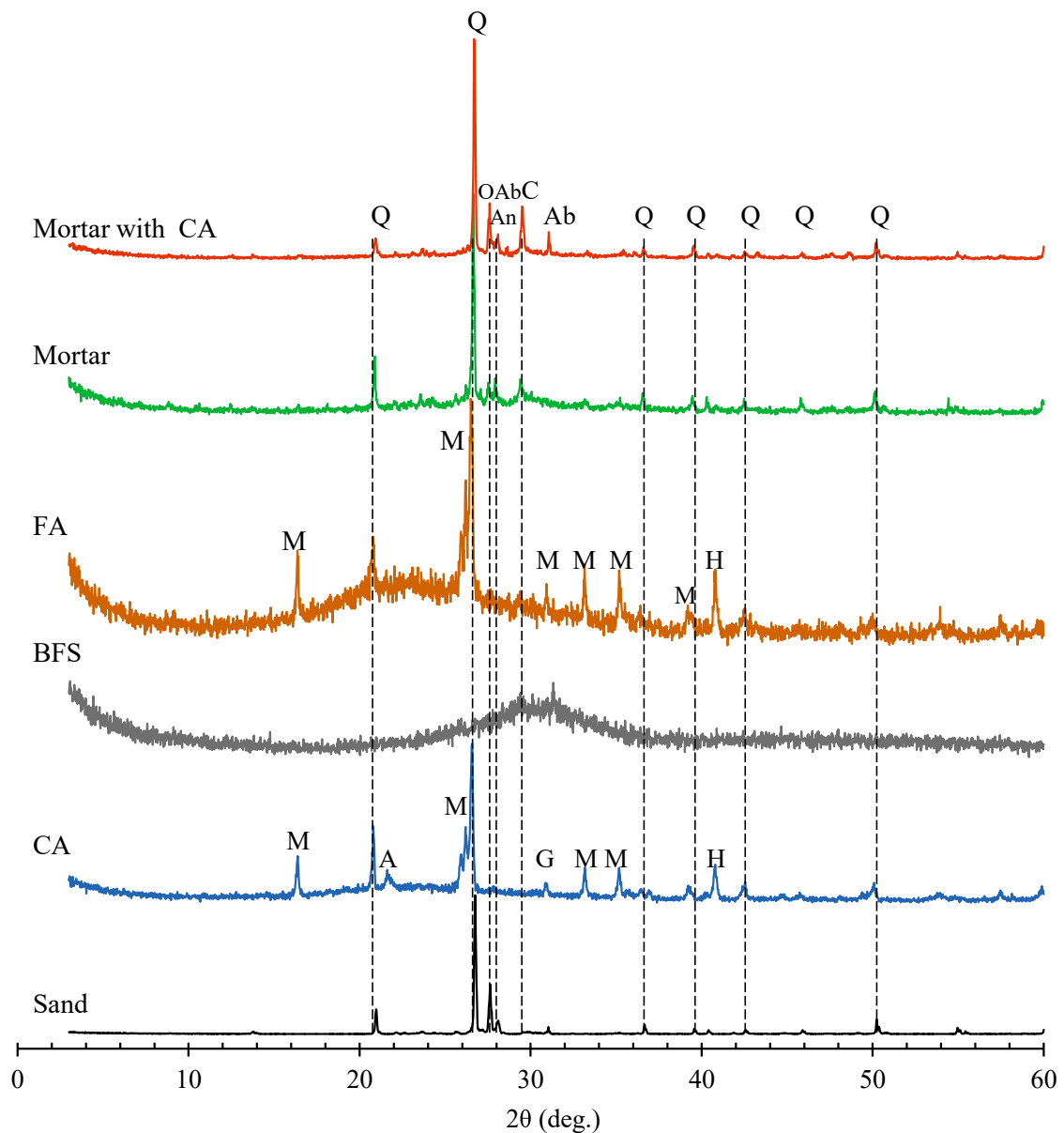
Quartz is consistently observed as the primary component in sea sand, bottom ash, and other waste by-products, acting as an inert filler that remains unreacted within the GP matrix. In addition to quartz, feldspar minerals, including orthoclase, albite, and anorthite, are detected in sea sand and waste by-products but remain largely unchanged within the GP matrix. These minerals do not participate in the polymerization reaction, functioning as stable, inert fillers that contribute to the structural matrix without significant alteration during the geopolymerization process.

A comparison of XRD spectra reveals notable distinctions between the components of CA. Each waste by-product displays unique mineral phases, reflecting their origin and previous chemical history. CA is characterized by a distinctive amorphous hump between 15° and 30°, indicating a higher proportion of amorphous aluminosilicate phases [42–44], which are reactive in the alkaline environment of GP mortars. Unlike other by-products, CA lacks feldspar but contains mullite, a durable, crystalline aluminosilicate phase that provides thermal stability and mechanical strength. During the GP formation process, the mullite in CA appears to dissolve or transform, as it is absent in the final GP mortar. This transformation suggests that mullite actively participates in the geopolymerization reaction, contributing aluminosilicate content to the GP matrix.

The XRD analysis highlights that specific phases in each waste by-product are actively consumed during geopolymerization, contributing essential chemical elements to the GP matrix. In CA, the

dissolution of mullite releases aluminosilicate species, enhancing the strength and thermal resistance of the GP mortar.

The results demonstrate that reactive phases in waste by-products enhance the structural integrity of the GP matrix. CA's amorphous aluminosilicate content contributes to the polymerization reaction, increasing the strength and cohesiveness of the GP mortar. However, the disappearance of reactive phases like gypsum, mullite, and hydrotalcite implies that these components are integral to the



[Notes] A: Anorthite, Ab: Albite, An: Anorthite, C: calcite, G: Gehlenite, H: Hematite, M: Mullite, O: Orthoclase, Q: Quartz

Fig. 4.17 XRD pattern of CA and GP mortars

geopolymerization process, releasing ions that enhance the binding capacity and durability of the GP matrix.

In summary, XRD analysis of GP mortar with bottom ash reveals that the inclusion of diverse waste by-products introduces a complex blend of reactive and inert phases, each contributing differently to the final material properties. Quartz and feldspar provide a stable framework, while CA offer reactive phases that actively participate in the formation of the geopolymer matrix, improving mechanical properties and durability. This analysis underscores the potential of tailored waste by-product compositions to optimize GP mortar performance for sustainable construction applications.

## 4.5 Conclusions

This study investigated the effects of partial or total replacement of sea sand with CA on the strength and carbonation resistance of GP mortar, and further examined the effectiveness of applying AN solution on the surface of the mortar to improve the carbonation resistance. The results obtained are as follows.

(1) When the replacement ratio of CA was less than 20%, the use of CA did not reduce obviously the strength of GP mortar.

(2) The application of AN can improve the carbonation resistance of GP using CA, not only delay the onset of neutralization, but also reduce the neutralization rate. The treatment of AN can change the ratio of  $\text{SiO}_2/\text{Al}_2\text{O}_3$  on the surface of the GP material and thus achieve the effect of densification.

(3) The neutralization rate is significantly negatively correlated with the blending ratio of NH in AS. And the greater the blending ratio of NH, the better the improvement of carbonation resistance of GP mortar using CA by the AN surface application. The AN treatment reduces carbonation depth by forming a denser surface layer that limits  $\text{CO}_2$  penetration. This makes surface treatments a valuable method for compensating for the increased porosity associated with CA and similar waste aggregates, enhancing the long-term durability of geopolymers.

(4) Although CA reduces carbonation resistance, the AN surface treatment can significantly improve the carbonation resistance of CA-blended GP. In fact, the carbonation resistance of AN-treated GP with CA was superior to that of GP without CA.

(5) The XRD analysis of GP mortar with CA reveals that the reactive phases, such as mullite in CA, actively participate in the geopolymerization process. The reactive components contribute essential elements (aluminosilicates, calcium) that strengthen and enhance the GP matrix's durability. CA's amorphous aluminosilicate content can improve structural integrity.

Overall, the stable and reactive phases of CA particles, support the development of a strong, durable GP mortar matrix and highlight the potential of specific waste compositions to optimize geopolymer performance in sustainable construction.

## References

- [1] C. Meyer, The greening of the concrete industry, *Cem. Concr. Compos.* 31 (2009) 601–605.
- [2] M.K. Dash, S.K. Patro, A.K. Rath, Sustainable use of industrial-waste as partial replacement of fine aggregate for preparation of concrete – A review, *Int. J. Sustain. Built Environ.* 5 (2016) 484–516.
- [3] K.S. Al-Jabri, M. Hisada, S.K. Al-Oraimi, A.H. Al-Saidy, Copper slag as sand replacement for high performance concrete, *Cem. Concr. Compos.* 31 (2009) 483–488.
- [4] A. Mardani-Aghabaglou, M. Tuyan, K. Ramyar, Mechanical and durability performance of concrete incorporating fine recycled concrete and glass aggregates, *Mater. Struct.* 48 (2015) 2629–2640.
- [5] Z. Li, R. Kondoa, K. Ikeda, Development of Foamed Geopolymer with Addition of Municipal Solid Waste Incineration Fly Ash, *J. Adv. Concr. Technol.* 19 (2021) 830–846.
- [6] P. Duxson, A. Fernández-Jiménez, J.L. Provis, G.C. Lukey, A. Palomo, J.S.J. van Deventer, Geopolymer technology: the current state of the art, *J. Mater. Sci.* 42 (2007) 2917–2933.
- [7] J. Davidovits, Geopolymers: inorganic polymeric new materials, *J. Therm. Anal. Calorim.* 37 (1991) 1633–1656.
- [8] C. Li, H. Sun, L. Li, A review: the comparison between alkali-activated slag (Si+ Ca) and metakaolin (Si+ Al) cements, *Cem. Concr. Res.* 40 (2010) 1341–1349.
- [9] K.A. Komnitsas, Potential of geopolymer technology towards green buildings and sustainable cities, *Procedia Eng.* 21 (2011) 1023–1032.
- [10] J. Davidovits, L. Buzzi, P. Rocher, D. Gimeno, C. Marini, S. Tocco, Geopolymeric cement based on low cost geologic materials. Results from the european research project geocistem, in: *Proc. 2nd Int. Conf. Geopolymer, 1999*: pp. 83–96.
- [11] Z. Li, K. Ikeda, Influencing Factors of Sulfuric Acid Resistance of Ca-Rich Alkali-Activated Materials, *Materials (Basel)*. 16 (2023) 2473.
- [12] J. Liu, G. Xie, Z. Wang, Z. Li, X. Fan, H. Jin, W. Zhang, F. Xing, L. Tang, Synthesis of geopolymer using municipal solid waste incineration fly ash and steel slag: Hydration properties and immobilization of heavy metals, *J. Environ. Manage.* 341 (2023) 118053.
- [13] M. Rafieizonooz, J. Mirza, M.R. Salim, M.W. Hussin, E. Khankhaje, Investigation of coal bottom ash and fly ash in concrete as replacement for sand and cement, *Constr. Build. Mater.* 116 (2016) 15–24.
- [14] Z. Li, S. Li, Carbonation resistance of fly ash and blast furnace slag based geopolymer concrete, *Constr. Build. Mater.* 163 (2018) 668–680.
- [15] B. Pandey, S.D. Kinrade, L.J.J. Catalan, Effects of carbonation on the leachability and compressive strength of cement-solidified and geopolymer-solidified synthetic metal wastes, *J.*

- Environ. Manage. 101 (2012) 59–67.
- [16] S.A. Bernal, J.L. Provis, D.G. Brice, A. Kilcullen, P. Duxson, J.S.J. van Deventer, Accelerated carbonation testing of alkali-activated binders significantly underestimates service life: The role of pore solution chemistry, *Cem. Concr. Res.* 42 (2012) 1317–1326.
- [17] K. Pasupathy, M. Berndt, A. Castel, J. Sanjayan, R. Pathmanathan, Carbonation of a blended slag-fly ash geopolymer concrete in field conditions after 8 years, *Constr. Build. Mater.* 125 (2016) 661–669.
- [18] J.S.J. Van Deventer, J.L. Provis, P. Duxson, Technical and commercial progress in the adoption of geopolymer cement, *Miner. Eng.* 29 (2012) 89–104.
- [19] P. Duxson, J.L. Provis, G.C. Lukey, J.S.J. Van Deventer, The role of inorganic polymer technology in the development of ‘green concrete,’ *Cem. Concr. Res.* 37 (2007) 1590–1597.
- [20] X. Li, Z. Li, Surface treatment of inorganic modifier for improving carbonation resistance of geopolymers, *Constr. Build. Mater.* 400 (2023) 132748.
- [21] J. Wang, H. Xu, D. Xu, P. Du, Z. Zhou, L. Yuan, X. Cheng, Accelerated carbonation of hardened cement pastes: Influence of porosity, *Constr. Build. Mater.* 225 (2019) 159–169.
- [22] S.K. Kirthika, S.K. Singh, Durability studies on recycled fine aggregate concrete, *Constr. Build. Mater.* 250 (2020) 118850.
- [23] R. Martínez-García, M.I. Sánchez de Rojas, P. Jagadesh, F. López-Gayarre, J.M. Morán-del-Pozo, A. Juan-Valdes, Effect of pores on the mechanical and durability properties on high strength recycled fine aggregate mortar, *Case Stud. Constr. Mater.* 16 (2022) e01050.
- [24] T.-P. Huynh, S.-H. Ngo, Waste incineration bottom ash as a fine aggregate in mortar: An assessment of engineering properties, durability, and microstructure, *J. Build. Eng.* 52 (2022) 104446.
- [25] E. Baite, A. Messan, K. Hannawi, F. Tsobnang, W. Prince, Physical and transfer properties of mortar containing coal bottom ash aggregates from Tefereyre (Niger), *Constr. Build. Mater.* 125 (2016) 919–926.
- [26] M. Singh, R. Siddique, Effect of coal bottom ash as partial replacement of sand on properties of concrete, *Resour. Conserv. Recycl.* 72 (2013) 20–32.
- [27] A. Cheng, Effect of incinerator bottom ash properties on mechanical and pore size of blended cement mortars, *Mater. Des.* 36 (2012) 859–864.
- [28] P. Shen, H. Zheng, J. Lu, C.S. Poon, Utilization of municipal solid waste incineration bottom ash (IBA) aggregates in high-strength pervious concrete, *Resour. Conserv. Recycl.* 174 (2021) 105736.
- [29] P. Shen, H. Zheng, D. Xuan, J.-X. Lu, C.S. Poon, Feasible use of municipal solid waste incineration bottom ash in ultra-high performance concrete, *Cem. Concr. Compos.* 114 (2020) 103814.

- [30] L. Berredjem, N. Arabi, L. Molez, Mechanical and durability properties of concrete based on recycled coarse and fine aggregates produced from demolished concrete, *Constr. Build. Mater.* 246 (2020) 118421.
- [31] M.M. Haque, N. Ankur, A. Meena, N. Singh, Carbonation and permeation behaviour of geopolymer concrete containing copper slag and coal ashes, *Dev. Built Environ.* 16 (2023) 100276.
- [32] R. Siddique, Design and development of self-compacting concrete made with coal bottom ash, *J. Sustain. Cem. Mater.* 4 (2015) 225–237.
- [33] R. Siddique, P. Aggarwal, Y. Aggarwal, Mechanical and durability properties of self-compacting concrete containing fly ash and bottom ash, *J. Sustain. Cem. Mater.* 1 (2012) 67–82.
- [34] K. Pasupathy, M. Berndt, A. Castel, J. Sanjayan, R. Pathmanathan, Carbonation of a blended slag-fly ash geopolymer concrete in field conditions after 8 years, *Constr. Build. Mater.* 125 (2016) 661–669.
- [35] G. Huang, Y. Ji, J. Li, Z. Hou, C. Jin, Use of slaked lime and Portland cement to improve the resistance of MSWI bottom ash-GBFS geopolymer concrete against carbonation, *Constr. Build. Mater.* 166 (2018) 290–300.
- [36] R.A. Robayo-Salazar, A.M. Aguirre-Guerrero, R. Mejía de Gutiérrez, Carbonation-induced corrosion of alkali-activated binary concrete based on natural volcanic pozzolan, *Constr. Build. Mater.* 232 (2020) 117189.
- [37] V. Charitha, G. Athira, A. Bahurudeen, S. Shekhar, Carbonation of alkali activated binders and comparison with the performance of ordinary Portland cement and blended cement binders, *J. Build. Eng.* 53 (2022) 104513.
- [38] H. Cheng, K.-L. Lin, R. Cui, C.-L. Hwang, Y.-M. Chang, T.-W. Cheng, The effects of SiO<sub>2</sub>/Na<sub>2</sub>O molar ratio on the characteristics of alkali-activated waste catalyst–metakaolin based geopolymers, *Constr. Build. Mater.* 95 (2015) 710–720.
- [39] K. Ghosh, P. Ghosh, Effect of % Na<sub>2</sub>O and % SiO<sub>2</sub> on apparent porosity and sorptivity of fly ash based geopolymer, *IOSR J. Eng.* 2 (2012) 96–101.
- [40] J.W. Phair, J.S.J. van Deventer, Characterization of Fly-Ash-Based Geopolymeric Binders Activated with Sodium Aluminate, *Ind. Eng. Chem. Res.* 41 (2002) 4242–4251.
- [41] M. Hoy, R. Rachan, S. Horpibulsuk, A. Arulrajah, M. Mirzababaei, Effect of wetting–drying cycles on compressive strength and microstructure of recycled asphalt pavement – Fly ash geopolymer, *Constr. Build. Mater.* 144 (2017) 624–634.
- [42] J.L. Provis, G.C. Lukey, J.S.J. van Deventer, Do Geopolymers Actually Contain Nanocrystalline Zeolites? A Reexamination of Existing Results, *Chem. Mater.* 17 (2005) 3075–3085.
- [43] C.K. Yip, G.C. Lukey, J.L. Provis, J.S.J. van Deventer, Effect of calcium silicate sources on geopolymerisation, *Cem. Concr. Res.* 38 (2008) 554–564.

- [44] Jgs. van Jaarsveld, J.S.J. Van Deventer, Effect of the alkali metal activator on the properties of fly ash-based geopolymers, *Ind. Eng. Chem. Res.* 38 (1999) 3932–3941.

## **Chapter 5 Conclusions and Future Works**

### **5.1 Conclusions**

### **5.2 Future Works**



# Chapter 5

## Conclusions and Future Works

### 5.1 Conclusions

This thesis systematically investigated the carbonation resistance, mechanical properties and structural feasibility of FA-based geopolymers CA under different curing conditions and proposed methods to improve the carbonation resistance. The research findings are concluded as follows:

Chapter 2 emphasizes the potential of coal ash, specifically fly ash and clinker ash, as precursors in geopolymer technology, which offers an eco-friendly alternative to Portland cement by repurposing industrial by-products. Coal combustion by-products like FA and CA provide substantial environmental benefits by reducing waste and alleviating the need for natural aggregates. FA-based geopolymers demonstrate considerable durability, thermal stability, and resistance to chemical degradation, although their carbonation resistance remains inferior to PC, especially in ambient curing. The chapter highlights the challenges of carbonation in FA-based GPs, especially when using highly porous aggregates such as CA, which facilitate CO<sub>2</sub> ingress. Overall, while FA and CA are promising materials, further research is necessary to optimize their use in geopolymer matrices to enhance carbonation resistance and ensure structural longevity in construction applications.

Chapters 3 explored the carbonation resistance of geopolymers formed from FA and BFS under different curing conditions. Heat-cured geopolymers, discussed in Chapter 3, benefit from enhanced geopolymerization that creates a dense microstructure, resulting in substantial early strength and improved durability. However, shrinkage cracks and internal pores make these materials vulnerable to carbonation. The addition of BFS to FA-based geopolymers under heat curing strengthens the matrix but increases carbonation risk due to residual alkalis. Applying an aqueous sodium aluminate (AN) treatment significantly reduces carbonation susceptibility, with reductions in carbonation depth of up to 70% in treated samples. The ambient-cured geopolymer materials developed a porous microstructure, making them more susceptible to carbonation. While AN treatments improve durability, their effectiveness is limited compared to heat-cured counterparts due to higher initial porosity. The research highlights that optimizing mix proportions and treatments is essential for enhancing carbonation resistance in ambient-cured FA/BFS geopolymers, ensuring their viability for sustainable construction applications.

Chapter 4 evaluated the performances of FA/BFS-based GP concretes and mortars using CA as precursor or fine aggregate. The properties including fluidity, setting time or working time, compressive and flexural strengths, and frost resistance were measured, and the effects of different blending ratio of CA were discussed. In addition, as a porous fine aggregate, the effect of CA blend on the carbonation resistance of GP mortar was also investigated. And the AN surface treatment experiments for the GP mortars with different alkali solutions and CA blending ratios were also conducted. The results indicate that the use of CA as a precursor of GP will reduce the strength of GP, but when CA is used as a fine aggregate in place of 20% or less of natural sand, the properties of GP mortar such as fluidity and strength will not be significantly reduced. Meanwhile, the improved AN surface treatment can significantly increase the carbonation resistance of CA-blended GP, which was superior to that of GP without CA. Moreover, the reactivity of CA, along with AN treatment, effectively densifies the surface of GP mortars and enhances the interfacial transition zone (ITZ) between CA particles and the GP matrix.

## 5.2 Future Works

1. Exploring Broader Applications of AN Surface Modification: The AN surface treatment effectively improved carbonation resistance in ambient-cured geopolymers. Future research should investigate its applicability across other geopolymer systems, particularly those using different precursors like metakaolin, and assess its potential to improve additional durability properties, such as frost resistance and chloride permeability.

2. Optimizing Curing Techniques: A hybrid curing process that combines ambient and heat curing could provide a balanced approach, enhancing the density and durability of GP matrices without requiring high energy input. Research into such techniques could offer solutions to improve carbonation resistance while remaining energy-efficient.

3. Incorporating Additional Industrial By-Products: Further investigation into aluminosilicate-rich by-products, such as volcanic ash or other slags, could diversify the waste materials used in GP formulations, potentially enhancing the binding properties and durability of the matrix while promoting environmental conservation.



## Paper List

### Published Papers in Journal etc.

1. Xuezhong LI, Zhuguo LI, Surface treatment of inorganic modifier for improving carbonation resistance of geopolymers, *Constr. Build. Mater.* 400 (2023) 132748, <https://doi.org/10.1016/j.conbuildmat.2023.132748> (SCI収録, IF: 7.4)
2. Xuezhong LI, Zhuguo LI, Study on Clinker ash recycling in geopolymer materials, *Journal of Material Cycles and Waste Management*, <https://doi.org/10.1007/s10163-024-02112-4> (SCI収録, IF: 2.7)
3. Xuezhong LI, Zhuguo LI, Properties of Geopolymer Materials with Clinker Ash, *コンクリート工学年次論文集*, Vol. 44, No. 1, pp. 1114-1119, 2022
4. Xuezhong LI, Zhuguo LI, Improvement of Carbonation Resistance of Geopolymer Material Using Bottom Ash as Fine Aggregate by Surface Modification, *コンクリート構造物の補修, 補強, アップグレード論文報告集*, Vol. 24, pp. 345-350, 2024

### Technical Papers

5. Xuezhong LI, Zhuguo LI, Daisuke SUGIHARA, Properties of Geopolymer Mortar With Clinker Ash, *日本建築学会中国支部研究報告集*, Vol.44, pp. 73-76, 2021
6. Xuezhong LI, Zhuguo LI, Study on Improvement of Carbonation Resistance of Geopolymer by Surface Modification, *日本建築学会 2022 年度大会 (中国) 学術講演梗概集*, Vol. 2022, pp. 1227-1228, 2022